NIST GCR 08-920

Multi-Parameter, Multiple Fuel Mixture Fraction Combustion Model for Fire Dynamics Simulator

Jason E. Floyd
Hughes Associates, Inc.
Fire Science & Engineering
3610 Commerce DR., #817
Baltimore, MD 21227

National Institute of
Standards and Technology
U.S. Department of Commerce

NIST GCR 08-920

Multi-Parameter, Multiple Fuel Mixture Fraction Combustion Model for Fire Dynamics Simulator

Prepared for
U.S. Department of Commerce
Building and Fire Research Laboratory
National Institute of Standards and Technology
Gaithersburg, MD 20899-8663

By
Jason E. Floyd
Hughes Associates, Inc.
3610 Commerce Dr., #817
Baltimore, MD 21227

Final Report
September 1, 2005–August 31, 2008

Issued November 2008

U.S. Department of Commerce
Carlos M. Gutierrez, Secretary

National Institute of Standards and Technology
Patrick D. Gallagher, Deputy Director

Notice

This report was prepared for the Building and Fire Research Laboratory of the National Institute of Standards and Technology under Grant Number 60NANB5D1205. The statement and conclusions contained in this report are those of the authors and do not necessarily reflect the views of the National Institute of Standards and Technology or the Building and Fire Research Laboratory.

Multi-Parameter, Multiple Fuel Mixture Fraction Combustion Model for Fire Dynamics Simulator

Final Report
Reporting Period September 1, 2005 through August 31, 2008

Grant # 60NANB5D1205

Submitted on November 24, 2008

Prepared for
Dr. Kevin B. McGrattan
Analysis and Prediction Group Leader

100 Bureau Dr, Stop 8663
Gaithersburg, MD 20899

Prepared by
Dr. Jason E. Floyd
Senior Engineer

3610 Commerce Dr., #817
Baltimore, MD 21227
Tel: (410) 767-8677
Fax: (410) 767-8688

TABLE OF CONTENTS

TABLE OF CONTENTS ii
LIST OF FIGURES iv
1.0 Summary 1
2.0 Overview of Work Performed During Annual Reporting Period 1
3.0 Software Coding Standard and Software Quality Assurance 1
3.1 Software Coding Standard 2
3.1.1 Update to Fortran 95 2
3.1.2 Coding Standard 3
3.2 Configuration Management 6
3.2.1 Revision Control 6
3.2.2 Source File Tagging 7
3.2.3 Automated Header Generation 7
3.3 Software Quality Assurance 7
4.0 Mixture Fraction Enhancements 8
4.1 Two Parameters, Single Step Reaction 9
4.2 Three parameters, Two Step Reaction 11
4.3 Mixture Fraction Space to Species Space 12
4.3.1 State Relationships 12
4.3.2 Thermophysical Properties 14
4.4 Radiative Absorption 15
5.0 Usability Enhancements 17
5.1 New/Modified Input Keywords 17
5.1.1 REAC 17
5.1.2 DUMP 18
5.1.3 DEVC/PROP 18
5.1.4 TABL 18
5.2 Sprinkler Spray Distributions 18
5.3 Detection 19
5.3.1 Beam Detectors 19
5.3.2 Aspiration Detectors 19
5.4 Control Systems 20
5.4.1 DEVC as controls 20
5.4.2 CTRL as controls 20
5.5 Colors 21
5.6 Time 22
5.7 Output Functionality 22
5.7.1 Output Statistics 22
5.7.2 Relative Humidity 22
5.7.3 Optical Depth 22
5.7.4 Radiative Flux 23
5.7.5 CSV Output Files Column Limit 23
5.7.6 Velocity Flux Quantities 23

5.8 Boundary Conditions 23
5.9 Maximum Droplets 24
5.10 Al_2O_3 24
6.0 Model Validation 25
6.1 Methane-Air Slot Burner 25
6.2 Burner Beneath a Small Hood 29
6.3 NIST RSE Tests 31
6.3.1 1994 NIST RSE Tests 31
6.3.2 2006 NIST RSE Tests 33
6.4 SNL Benchmark Testing 36
6.5 Helium Plume 38
6.6 Methane Fire 42
7.0 Support of NIST Fire Testing 44
7.1 Reduced Scale Enclosure Test Support 44
7.2 Full Scale Testing 47
8.0 User Support 48
8.1 Google Code 48
8.2 Discussion Forum 50
9.0 Ouput Compression 51
10.0 References 52
Appendix A – Issue Tracker Activity 55
Appendix B – Source Commits 59
Appendix C – Source Commits 65
Appendix D – Interflam 2007 Paper 66
Appendix E – Fire Safety Journal Paper 67
Appendix F – IAFSS Symposium Paper 68

LIST OF FIGURES

Figure 1: Oxygen Flammability Criteria 10
Figure 2: Flowchart of two-step combustion model 12
Figure 3: Comparison of RADCAL Computed Absorbtivities for Combined vs. Summed Individual Species 16
Figure 4: Error of RADCAL Computed Absorbtivities for Combined vs. Summed Individual Species 17
Figure 5: Predicted and measured temperature profiles over the half-width of a methane-air slot burner (x=0 is burner centerline, shaded region is burner lip) at two elevations above the burner. 26
Figure 6: Predicted and measured fuel (top) and oxygen (bottom) concentrations for a methane-air slot burner (x=0 is burner centerline, shaded region is burner lip) at two elevations above the burner. Note FDS shows zero O_2 inside the burner. 27
Figure 7: Predicted and measured carbon dioxide and carbon monoxide concentrations for a methane-air slot burner (x=0 is burner centerline, shaded region is burner lip) at two elevations above the burner. 28
Figure 8: Test Setup for Beyler Hood Experiments 29
Figure 9: Predicted and measured fuel, oxygen, carbon dioxide and carbon monoxide concentrations for 19 cm diameter propane fires in the Beyler hood apparatus. The burner distance above the hood lip for each test is shown in the insets. 30
Figure 10: CO_2 and CO predictions compared against measurements in a reduced scale enclosure (lines for predictions added as a visual aid). [16] is (Gottuk and Lattimer, 2002) 32
Figure 11: Lower (left) and Upper (right predictions compared against measurements in a reduced scale enclosure (lines for predictions added as a visual aid). [16] is (Gottuk and Lattimer, 2002) 33
Figure 12: Predicted and Measured CO_2 and CO concentrations in the front (solid symbols) and rear (open symbols) of the NIST RSE 34
Figure 13: Predicted and Measured upper (left) and lower (right) temperatures in the front (solid symbols) and rear (open symbols) of the NIST RSE 35
Figure 14: Drawing of Sandia FLAME Facility 37
Figure 15: Cut-away View of FDS model of FLAME Facility 38
Figure 16: Sandia Helium Benchmark Case Radial Velocity Profiles, FDS vs. Data 39
Figure 17: Sandia Helium Benchmark Case Vertical Velocity Profiles, FDS vs. Data 40
Figure 18: Sandia Helium Benchmark Case Helium Concentration Profiles, FDS vs. Data 41
Figure 19: Methane Benchmark Case Centerline Vertical Velocity, FDS vs. Data 42
Figure 20: Methane Benchmark Case Radial Velocity Profiles, FDS vs. Data 43
Figure 21: Methane Benchmark Case Vertical Velocity Profiles, FDS vs. Data 44
Figure 22: FDS v4 Predictions of Temperate and CO_2 in the RSE Doorway 45
Figure 23: RSE Test Data as Volume Fraction vs. Time 46
Figure 24: RSE Test Data in Mixture Fraction Space 46
Figure 25: Pre-test Predictions of Temperature as a Function of Fire Size in an ISO 9705 Compartment with a Standard Doorway (TR = rear and TF = front) 47

Figure 26: Pre-test Predictions of Oxygen Concentration as a Function of Fire Size in an ISO 9705 Compartment with a Standard Doorway 48
Figure 27: Screenshot of Issue Tracker 49
Figure 28: Screenshot of Downloads Page 50
Figure 29: Two-byte Real Numbers 52

1.0 Summary

This report summarizes work performed for the three year period funded by grant 60NANB5D1205.

2.0 Overview of Work Performed During Annual Reporting Period

Work performed during this reporting involved seven major task areas: implementation of modern software development practices along with a coding standard update, mixture fraction enhancements and related changes, addition of numerous enhancements improving the usability and flexibility of FDS for the practicing engineer, verification and validation testing, support of testing at NIST, user support via online bug tracking and discussion forums, and investigation of alternate methods of data output and storage. Details on each task area will be provided in sections 3.0 through 9.0.

3.0 Software Coding Standard and Software Quality Assurance

FDS development began in the 1980's. At the time FDS was little more than a research tool for investigating buoyant flows. The development team consisted of a small group of people within the Building and Fire Research Laboratory. Developers at the time did not envision that FDS would become the gold standard for fire modeling worldwide. Little attention was paid to issues of software quality assurance, formal software testing, and to the impact of coding practices and standards on future development. This approach continued through the release of FDS 4, at which point a number of factors were becoming clear:

- FDS development was no longer the exclusive domain of NIST. Primary developers were now at multiple locations, some outside the United States.
- Fire protection codes and standards related to performance based approaches to fire protection were becoming more mature and within some industries, such as nuclear, formal certification/accreditation processes were being developed and implemented.
- Over many years of development, FDS was becoming tangled with various features and submodels that were added without careful review of their impact on FDS flexibility or on future enhancements to FDS.
- The FDS user community was growing rapidly. Users were attempting to solve problems beyond those tested by the development team resulting in both requests for new capabilities as well as the discovery of bugs and model shortcomings. No formal process was in place to handle these requests or keep track of bug reports and the progress on them.

Given FDS's start as a research tool being developed by researchers at a National lab, the above issues are not surprising. However, with the focus of this grant on greatly expanding the capabilities of FDS, it was clear that changes were needed in how FDS was developed, tested, and maintained.

3.1 Software Coding Standard

3.1.1 Update to Fortran 95

FDS development began using Fortran 77. This placed a number of restrictions on the source code and requires the use of GOTO statements for exiting loops or performing complex condition branches. The current Fortran standard supported by the major compilers is Fortran 95 and many contain extensions to support the latest standard Fortran 2003. As each new Fortran standard is released, more features from early versions of Fortran are being eliminated (such as computed GOTO statements). Additionally newer versions of compilers typically perform the highest levels of optimization for source code that adheres closest to the latest Fortran standard. It was decided quickly that the first task would be a major overhaul of the FDS source code to update its coding standard.

Fortran 77 uses a fixed format for source code. This format has the first column in a file reserved for a comment indicator, columns one through five reserved for line numbers, column six reserved for a line continuation character, and columns seven through seventy-two for the source code. Additionally, variable names are limited to six characters and comments can occur solely on a separate line of code. The result of these format restrictions is that Fortran 77 source code is typically difficult to read, check, and debug. The variable name limits result in cryptic variable names and the line length limitations make it difficult to use indentation to indicate code structure. Fortran 77 also makes significant use of GOTO statements for execution control. GOTO statements make optimization difficult and they allow for the creation of poorly structured code.

The first task in performing the source code update was to convert all of the source code files from fixed format to free format. Free format source code allows the use of 132 columns for input with no need to reserve columns for line numbers or continuation characters. Comments are denoted by a "!" and can occur anywhere on a source code line (everything following the "!" will be considered a comment). Rather than using a character in the sixth column to indicate a line is a continuation of the previous line, the symbol "&" is used at the end of a line to indicate the following line is a continuation. With 132 columns it becomes reasonable to use indentation to indicate all levels of the source code structure. For example if each sublevel of the source code is indented by three characters:

```
DO K = 1, 10
   DO J = 1, 10
      DO I = 1, 10
         X = I + J + K
      END DO
   END DO
END DO
```

This makes the source much more readable and makes it easier to see where do loops and if-else blocks begin and end.

All source code files were updated to the free format standard and code structures using GOTO (including implied GOTO) statements were replaced with modern structures (DO WHILE loops, SELECT CASE structures, etc) where possible. The exception to eliminating GOTO statements were I/O error trapping routines and the pois.f90 file containing the Fishpak solver. The Fishpak solver was an existing code library and fully eliminating all GOTO statements would be time consuming and likely to introduce difficult to debug errors. I/O error trapping using GOTO statement is not desirable; however, they are acceptable since these errors result in a program halt. Additionally, indentation was applied to indicate the code structure.

3.1.2 Coding Standard

3.1.2.1 Explicit Typing

The Fortran language allows the user to denote explicitly the typing of numbers entered in the source code. For example 1._4 would explicitly indicate a four byte real number and 1._8 would explicitly indicate an eight byte real number. If one does not specify the type, a default type is assumed. If the number is being used in a statement with variables of higher precision, then the default typing can result in the potential for math errors. Part of the coding standard was to explicitly type all real numbers in the code.

3.1.2.2 Variable Naming

Fortran 77 had a limit of six characters for variables whereas Fortran 95 has a limit of 31 characters. A six character limit results in cryptic variable names. As part of the source code update, many cryptically named variables were given new, longer names to improve readability of the source code.

3.1.2.3 Loop/Branch Naming

Fortran 95 allows a developer to provide a descriptive name for a DO loop or an IF block. This name is applied at the beginning and end of the structure. For loops or blocks that extend past one screen of text or where there are complex nested structures, providing a descriptive name makes it easier to read the code. Descriptive names were added to many such structures in the FDS source code.

3.1.2.4 Tuning

A number of changes were made to improve execution speed. Consecutive IF blocks were converted to IF-ELSE or SELECT CASE structures. Branch statements evaluated using character strings were converted to use fixed integer parameters, a significantly faster comparison in terms of CPU cycles. For example rather than:

```
IF (THERMAL_BC_INDEX = 'ADIABATIC')
   ...
ELSE
   ...
ENDIF
```

The code was modified as follows:

```
INTEGER, PARAMETER::ADIABATIC = 1
...
SELECT CASE(THERMAL_BC_INDEX)
   CASE (ADIABATIC)
      ...
...
END SELECT
```

The end result of these changes plus the use of newer compilers was a 20^{+} % speedup in FDS v4. However, since the new combustion model requires tracking additional species, this speed gain is partially negated in FDS v5.

3.1.2.5 Source File Control

Additional changes were made to aid in compilation time during development. Currently the FDS source code consists of a number of source code files containing one or more modules. During recompilation any module dependent on a changed module must be recompiled. Source code files containing multiple unrelated modules are inefficient during recompilation as they often result in multiple dependencies that are not related to the specific code change. The source code file mods.f90 was one such file. It contained global variable definitions, math functions for interpolation and ramps, initialization routines for the radiation model, and other functions. Modifications to the imbedded functions would result in the need to recompile the entire source code. If multiple new approaches are being examined and debugged, this can become time consuming. These functions were therefore split out into new source code files.

A number of source code files were rearranged and/or broken up into multiple files in order to ease concurrent development. The goal was to have each source code file contain routines for a single aspect of the FDS computation (boundary conditions, combustion, radiation, etc.). The following source files underwent this process:

- func.f90 gathered together into one file the various functions for memory management, I/O management, math, and mixture fraction space to species space
- mass.f90 was divided into:
    - fire.f90: combustion
    - mass.f90: update of density, temperature, and species mass fractions
    - wall.f90: boundary conditions
- mods.f90 was divided into:
    - cons.f90: variable constants and global variables
    - devc.f90: device related variables
    - mesh.f90: mesh variables
    - prec.f90: precision declarations
    - types.f90: type structures
- radi.f90 was divided into:
    - irad.f90: initialization routines for radiation
    - radi.f90: radiation solver routines
- sprk.f90 and part.f90 were combined into part.f90

- vege.f90 was created for the development of submodels required for WUI research
- evac.f90 was created for the development of submodels required for egress modeling research

As a result of this, concurrent development of major phenomena (heat transfer and combustion for example) can occur with a greatly reduced risk of conflict.

3.1.2.6 Named Constants

Throughout the FDS source code specific subsections of the code were enabled or disabled during runtime through the use of IF or SELECT CASE blocks. In some cases there were string constants being used and in other cases integer values were being used. Both had their disadvantages. While a character string makes it clear what is being chosen, it is computationally expensive to evaluate a character string, so any runtime comparison using a string that occurred with a global loop becomes a significant cost. Comparison with an integer is cheap, but an expression such as:

```
IF (BOUNDARY_TYPE==1) THEN
```

makes it unclear what exactly is being done unless a comment is added to the source code which can act to reduce readability. The solution to both problems is to predefine integer constants. For example:

```
ADIABATIC=1
…
IF (BOUNDARY_TYPE==ADIABATIC) THEN
```

makes it clear what is being evaluated without adding clutter in the form of commenting.

3.1.2.7 Redundant Code

Over the two decades of development that culminated with FDS v4, many features were added to FDS. These features were often added without consideration for structure and operation of FDS as a whole. As a result, a number of algorithms were coded multiple times in different sections of the source code.

For example, FDS v4 had entirely separate routines for processing outputs for slice files, iso-surface files, boundary files, Plot3D files, and the point measurement file (&THCP). This had significant disadvantages. There was a sizeable amount of redundant code as each type of output had overlapping sets of quantities (for example Plot3D, slice, iso-surface, and &THCP all output heat release per unit volume). Adding a new parameter meant modifying multiple subroutines and historically this had not been done consistently resulting in not all possible output quantities being available for a given type of output file.

As part of the development of FDS v5, an effort was undertaken to remove these redundancies. In particular the following was done:

- In read.f90, rather than having each subroutine for reading the various types of outputs process the output quantities, a single routine was created to process the output quantities. This routine is called by each of the input file routines for outputs (&ISOF, &PL3D, &BNDF, &SLCF, &DEVC, and &PART). For outputs that are limited to specific ouput files (particle quantities for example), logical flags within the quantity processing routine will create error messages if a non-permissible output quantity is specified for a particular output file.
- Routines for processing the input file were simplified and generalized to support new functionality.
- Two routines were created to handle the generation of all the output quantities. The first routine handles all the gas phase output quantities and is called with a cell index and the desired quantity. The second routine handles all the boundary quantities and is called with a wall cell location and the desired quantity. Each type of output calls the appropriate routine for a single location (&DEVC) or a range of locations (&ISOF, &PL3D, &BNDF, &SLCF, integrated &DEVC). The advantage of this approach is once a new type of output quantity is added to either of the two routines, all types of output files can then use that quantity. Certain quantities (such as a beam detector) are restricted to &DEVC use only.
- Calls to the output processing routine were collected into a single subroutine, making it easier to manage the handling of outputs especially when running with multiple processors where MPI calls are needed to exchange data.
- Routines for handling particles and droplets were collected into serperate routines for insertion, transport, and, where required, heat and mass transfer.

3.2 Configuration Management

3.2.1 Revision Control

Prior versions of FDS had little formal source code control other than saving the source files for an official release. Having multiple people undertake simultaneous development and incorporating those changes was a laborious and error prone process. Also, there was no easy way to go back to an earlier version of the source code in the event that changes needed to be undone.

The resolution for this was to make use of a version control system. Early on in FDS v5 development, Component RCS was used for version control. While this package enabled revision control, it did not ease the process of collaboration over multiple sites. Bryan Klein (NIST BFRL) transtioned the revision control to the site SourceForge.net, which uses CVS for source code and documentation control. However, when FDS v5 entered beta testing, it became clear the SourceForge user interface was disliked by the user community. The FDS source was then migrated to GoogleCode which uses Subversion (SVN). With version control a centralized repository exists that contains the official versions of source code, documentation, or other items under version control (V&V files for example). Each developer maintains a set of these files on their local machine. Version control software allows each developer to commit changes to the repository and determine if there are any updates made by other developers that must be brought down to the local machine. The specifics of each commit are stored by the repository. This

allows a user to determine what changes were made when, by whom, and to recover any prior version of the software. When an official release is made, the specific version of files for that release can be tagged with the release identifier (e.g. 5.0). This makes it easy to quickly recover prior released versions of the software as well.

3.2.2 Source File Tagging

All source code files are under revision control using Subversion. Statements were added to each source file to assist in this process. In each source file a series of character parameter strings are defined. For example the strings in main.f90 are:

```
CHARACTER(255), PARAMETER :: mainid='$Id: main.f90 2462 2008-10-08 14:18:42Z
mcgratta $'
CHARACTER(255), PARAMETER :: mainrev='$Revision: 2462 $'
CHARACTER(255), PARAMETER :: maindate='$Date: 2008-10-08 10:18:42 -0400 (Wed,
08 Oct 2008) $'
```

The string contains the name of the source file, the version of the file (this reflects only the source file version and not the overall release version number), the date and time of the file version, and the person who checked the file in to the archive. Upon compiling, these strings will be stored in the executable file. The user is then capable of searching the executable file, for example, for strings beginning with `$Id:`. This will result in a list of all source files compiled and their version. Within the SVN archive any specific version of a source file can be extracted and differences between versions can be determined.

3.2.3 Automated Header Generation

At the start of an FDS simulation FDS writes header information to the Smokeview output file, FDS output file, and the FDS log file. This header information contains the version of FDS used to perform that simulation. While each release is tagged with a specific version number (e.g. 5.0.1), there may be many commits of source code to the SVN repository before a new version is released with an incremented version number. Thus, if a developer or a user who performs their own compilation discovers an error, the version number written to the output files may not be sufficient to identify the specific set of source code files used. Rather one would need to know the SVN revision number of the most recently committed source file.

Using the source file tagging discussed in the previous sections a series of subroutines were created, one per source file, which parses the $Id in each file and extracts from it the SVN revision number. Each of these subroutines is called at the start of an FDS run and the largest (and hence most recent) revision number is determined. This number is written along with the FDS version number to the output header information. A user can now identify specifically the source code used for a particular compilation of FDS when reporting an error.

3.3 Software Quality Assurance

With a complex piece of engineering software such as FDS, it is not uncommon to introduce an error during the process of fixing a bug or adding a new feature. Coding standards as discussed in 3.1.2 reduce but do not eliminate the occurrence of errors. Many errors can be discovered by

the use of a suite of verification cases with high coverage (coverage is the fraction of executable lines exercised by the test suite) of the source code. Running the verification suite prior to each release provides an opportunity to discover bugs likely to be encountered by the typical user. The author has contributed a number of test cases to suite.

4.0 Mixture Fraction Enhancements

The primary goal of this grant effort was to enhance the current mixture fraction model to add increased capabilities, especially those of extinction, CO production, and soot formation. The mixture fraction model in FDS v4 was a single parameter, *Z*, mixture fraction model (Floyd, et al., 2003). The model tracked a single scalar variable which represents the amount of mass that was originally fuel, Eqn 1. At any point in the computational domain, a set of state relationships provides a mapping from *Z* to specific mass fractions of species.

$$Z = \frac{sY_F - \left(Y_{O_2} - Y_{O_2}^{\infty}\right)}{sY_F^I - Y_{O_2}^{\infty}} = Y_F + \frac{Y_{H_2O}M_{H_2}}{M_{H_2O}} + \frac{Y_{CO_2}M_C}{M_{CO_2}} + \ldots \tag{1}$$

With only a single parameter, no information regarding the completeness of the combustion reaction is stored. The impact of this is twofold. First, as a fire becomes vitiated the single parameter mixture fraction will not result in a change in the ratio of CO to CO_2 production. The FDS v4 user could choose only one ratio for the computation. Second, if conditions are reached for extinction, the heat release in a grid cell can be set to zero, but Z will still represent combustion products according to the state relationships. For many fire protection problems such as validating a smoke control system design or determining likely sprinkler activation times, the single parameter mixture fraction is sufficient as the fire scenarios of interest are well ventilated. For other fire protection problems such as extinction due to water mist systems, the single parameter mixture fraction is not sufficient.

To overcome the limitations of the current single parameter, mixture fraction model, additional information was required to be able to account for CO formation and extinction. Since it was desired to minimize the complexity of a new combustion model and to ensure its applicability to simulations with large grid sizes, the simplest possible CO formation and extinction mechanism was used. The following two-step combustion was assumed (Westbrook and Dryer, 1981):

$$\text{Step 1: } F + O_2 \rightarrow CO + \text{Other Products} \tag{2}$$

$$\text{Step 2: } CO + \frac{1}{2}O_2 \rightarrow CO_2 \tag{3}$$

In the first step fuel and oxygen react to form carbon monoxide and other combustion products. If extinction occurs, then unreacted fuel, *F*, and oxygen, O_2, will also be present. In the second step carbon monoxide reacts with oxygen to form carbon dioxide. This simple two-step reaction allows for both extinction and for CO formation and destruction. Note that at this time no assumptions on reaction rates have been applied.

To implement the two reaction approach in a mixture fraction model there must be a scalar quantity that denotes the amount of fuel that is present, a second scalar quantity to denote extinction, and a third quantity to denote the CO/CO_2 production ratio. Additionally, these scalar quantities need to be conserved, they must allow for a numerically stable combustion model to be implemented, and they must uniquely define a set of species mass fractions.

Conservation can be guaranteed by deriving the new mixture fraction parameters from the existing species transport equations. That is, by taking linear combinations of the transport equations for fuel (both virgin and unburned), carbon monoxide, and carbon dioxide, transport equations for mixture fraction quantities can be developed. The species transport equations are:

$$\frac{\mathrm{D}Y_F}{\mathrm{D}t} = \nabla \cdot D\rho\nabla Y_F + \dot{m}'''_{F,1}, \tag{4}$$

$$\frac{\mathrm{D}Y_{CO}}{\mathrm{D}t} = \nabla \cdot D\rho\nabla Y_{CO} + \dot{m}'''_{CO,1} + \dot{m}'''_{CO,2}, \text{ and} \tag{5}$$

$$\frac{\mathrm{D}Y_{CO_2}}{\mathrm{D}t} = \nabla \cdot D\rho\nabla Y_{CO_2} + \dot{m}'''_{CO_2,2}. \tag{6}$$

In FDS v5, two versions of the multiple parameter mixture fraction were developed. The first approach uses two mixture fraction parameters and single step reaction. The second approach uses a three parameter mixture fraction and the two step reaction identified above.

Additional details on the development of this new approach can be found in (Floyd and McGrattan, 2007) and (Floyd and McGrattanm, 2008a and 2008b), copies of which are provided in Appendices D through F.

4.1 Two Parameters, Single Step Reaction

With two parameters, the combustion model takes unburned fuel and converts it to burned fuel. In each grid cell containing fuel and oxygen, the model decides whether or not to allow combustion to take place. If combustion is allowed, then as much combustion as allowed by the more limiting of the two species is allowed to occur. This is then limited by a maximum allowable heat release per unit volume which is based on nominal heat release rates per unit area of a flame. Oxidation of fuel means that Z_1 becomes Z_2. In this scheme, the two steps shown in Equations 2 and 3 are combined in to a single step where fuel plus oxygen forms CO_2 plus other products.

At each time step of the calculation the individual species mass fractions of fuel and oxygen are extracted from the mixture fraction variables. Then, an empirical criterion is used to decide whether oxidation of fuel to CO_2 and other products can occur. If the temperature and oxygen mass fraction of a given cell and that of its neighbors are too low to support combustion for the fuel-oxygen reaction, (the black region of Figure 1 where Step 1 refers to the single step

reaction) or if the temperature and fuel mass fraction of a given cell and that of its neighbors are too low to support combustion (figure would be similar to that of oxygen), then combustion cannot occur. The neighboring cells represent either the fuel or oxidizer stream of classical diffusion flame theory. The local flammability criterion is based on the critical adiabatic flame temperature, as described by Beyler (2002), and a simplified thermodynamic analysis by Mowrer (2002). The criterion determines if the energy released by consuming the maximum possible amount of fuel or oxygen can raise the local temperature above the critical flame temperature. If so, then combustion is allowed. Because large scale fire simulations usually have grid cell sizes far greater than the flame width, it is not appropriate to use a detailed kinetics model as the flame temperature and local strain rate are not available. Currently, the default value of lower flammability limit for fuel is set to zero meaning that only oxygen determines whether or not combustion occurs

If the local environment is assumed to support combustion, then combustion just depletes either fuel or oxygen, releasing the corresponding amount of energy into the grid cell, up to an empirically-based maximum value. This maximum value is based on two assumptions. First, that a flame sheet can generate no more than 200 kW/m^2 of energy (Linteris, 2003); second, that the numerical grid is resolved enough such that any grid cell is cut by only one flame sheet.

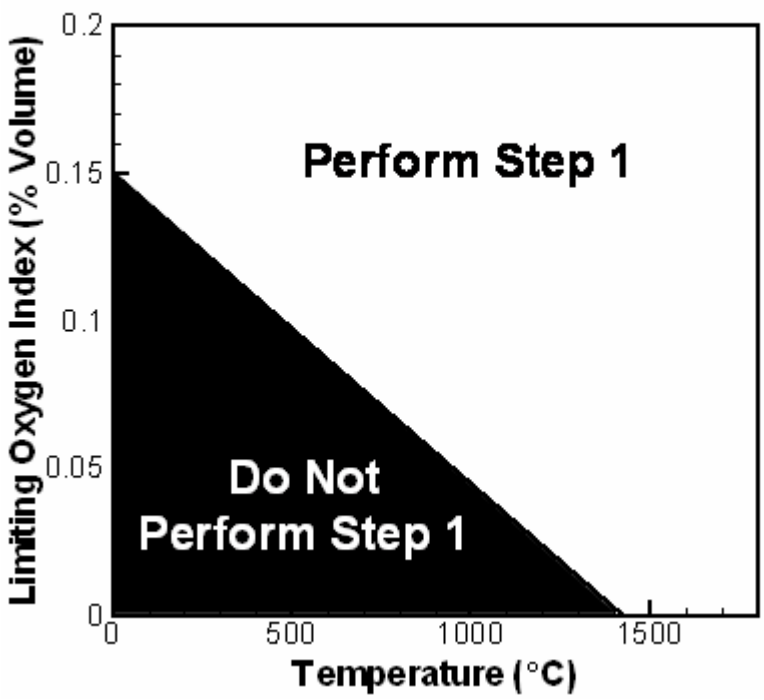

Figure 1: Oxygen Flammability Criteria

The limitation of this simple extinction model is that it presumes that ignition will always occur if the fuel and oxidizer streams have suitable concentrations and temperatures. In other words, for any particular grid cell, an adequate oxygen and fuel supply in any of its neighboring cells

automatically triggers the reaction to occur. This means that the model may over-predict the burning rate, and, thus, over-predict exhaust product concentrations in scenarios where fuel rich gases meet ambient air along an interface oriented in any direction.

4.2 Three parameters, Two Step Reaction

With three parameters, the combustion model takes unburned fuel and converts it to carbon monoxide plus other products and then takes the carbon monoxide and converts it to carbon dioxide. For Step 1, oxidation of the fuel to carbon monoxide, the same process is applied as was done for the two-parameter mixture fraction. If the local environment is assumed to support combustion, then combustion just depletes either fuel or oxygen, releasing the corresponding amount of energy into the grid cell, up to an empirically-based maximum value. Oxidation of fuel to CO means that Z_1 becomes Z_2.

Step 2 of the reaction, the oxidation of CO, is determined by one of two methods depending on the outcome of Step 1. The first method presumes that if Step 1 results in any heat production in a given grid cell, then a flame (and flame temperatures) are present and the conversion of CO is "fast." For this case the maximum possible CO conversion is assumed, again limited by the upper bound on the local volumetric heat release rate. If no heat is produced in Step 1 (i.e. the white region of Figure 1), it is presumed that a flame is not present and, therefore, the existing temperature is an accurate representation of the conditions in the cell. A finite rate computation (Westbrook and Dryer, 1981) is then performed to determine the rate of CO oxidation. Oxidation of CO means that Z_2 becomes Z_3.

The two step process is illustrated in the flowchart shown in Figure 2. Full details on the two step model operation can be found in (Floyd and McGrattan, 2008a), a copy of which is provided in Appendix E.

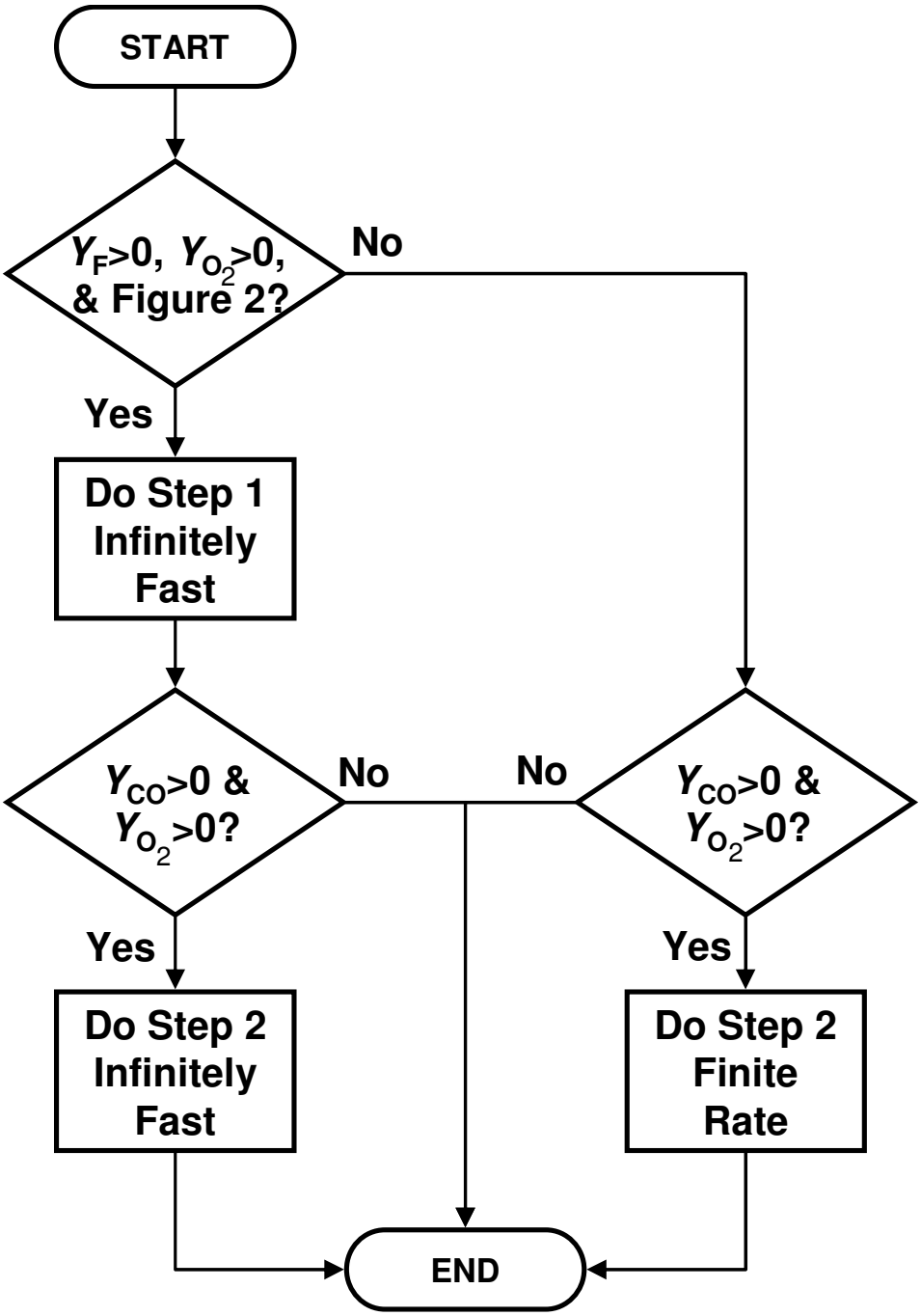

Figure 2: Flowchart of two-step combustion model

4.3 Mixture Fraction Space to Species Space

4.3.1 State Relationships

The extraction of species mass fraction from the three parameter mixture fraction is presented in this section. The two parameter approach follows in a similar manner and full details can be found in the FDS Technical Guide.

Recovering the species mass fractions from the mixture fraction variables is relatively easy and computationally efficient. To derive the necessary formulae, first consider Eqs. 2 and 3 written completely in terms of all the species:

$$C_xH_yO_zN_aM_b + \nu_{O_2}O_2 \rightarrow \nu_{H_2O}H_2O + (\nu'_{CO} + \nu_{CO})CO + \nu_S soot + \nu_{N_2}N_2 + \nu_M M \tag{7}$$

$$\nu'_{CO}\left(CO + \frac{1}{2}O_2 \rightarrow CO_2\right) \tag{8}$$

The parentheses in Eq. (8 are there to indicate that the two reactions sum to the complete combustion reaction for the fuel. Note that CO has two stoichiometric coefficients where ν'_{CO} applies to the CO that can be converted to CO_2 and ν_{CO} applies to the CO that exists post-flame. The combustion model to be discussed later in this paper is not capable of predicting the small levels of CO that still exist in well ventilated fires; hence, the need to preserve this empirical value. M is a species that representing that portion of the fuel that is not C, H, O, or N.

Next, some additional quantities are defined. The fuel stream may be specified as diluted given by Y_F^I, the mass fraction of fuel in the fuel stream. The diluent is presumed to be nitrogen with a mass fraction of $Y_{N_2}^I = 1 - Y_F^I$. The ambient mass fractions of oxygen, $Y_{O_2}^\infty$, and nitrogen, $Y_{N_2}^\infty = 1 - Y_{O_2}^\infty$, are also specified. Accounting for fuel dilution and the atom fraction of hydrogen in the soot, X_H, the mixture fraction parameters are given as:

$$Z_1 = \frac{Y_F}{Y_F^I}, \tag{9}$$

$$Z_2 = \frac{W_F}{W_{CO}\left(x - (1 - X_H)\nu_S\right)} \frac{Y_{CO}}{Y_F^I}, \text{ and} \tag{10}$$

$$Z_3 = \frac{W_F}{W_{CO2}\left(x - (1 - X_H)\nu_S\right)} \frac{Y_{CO2}}{Y_F^I}. \tag{11}$$

The mass fractions of the species are then given by:

$$\begin{bmatrix} 0 & Y_F^I & 0 & 0 \\ Y_{N_2}^\infty & Y_{N_2}^I & \frac{\nu_{N_2} W_{N_2}}{W_F} Y_F^I & \frac{\nu_{N_2} W_{N_2}}{W_F} Y_F^I \\ Y_{O_2}^\infty & 0 & -\frac{\nu'_{O_2} W_{O_2}}{W_F} Y_F^I & -\frac{\nu_{O_2} W_{O_2}}{W_F} Y_F^I \\ 0 & 0 & \frac{(\nu'_{CO} + \nu_{CO}) W_{CO}}{W_F} Y_F^I & 0 \\ 0 & 0 & 0 & \frac{\nu_{CO_2} W_{CO_2}}{W_F} Y_F^I \\ 0 & 0 & \frac{\nu_{H_2O} W_{H_2O}}{W_F} Y_F^I & \frac{\nu_{H_2O} W_{H_2O}}{W_F} Y_F^I \\ 0 & 0 & \frac{\nu_S W_S}{W_F} Y_F^I & \frac{\nu_S W_S}{W_F} Y_F^I \\ 0 & 0 & \frac{\nu_M W_M}{W_F} Y_F^I & \frac{\nu_M W_M}{W_F} Y_F^I \end{bmatrix} \times \begin{bmatrix} 1 - Z_1 - -Z_2 - -Z_3 \\ Z_1 \\ Z_2 \\ Z_3 \end{bmatrix} = \begin{bmatrix} Y_F \\ Y_{N_2} \\ Y_{O_2} \\ Y_{CO} \\ Y_{CO_2} \\ Y_{H_2O} \\ Y_S \\ Y_M \end{bmatrix}. \tag{12}$$

The stoichiometric coefficients are given by:

$$\begin{aligned} \nu_{N_2} &= \frac{a}{2} & \nu_{H_2O} &= \frac{y}{2} - X_H \nu_S \\ \nu'_{O_2} &= \frac{\nu'_{CO} + \nu_{H_2O} - z}{2} & \nu'_{CO} &= x - \nu_{CO} - (1 - X_H)\nu_S \\ \nu_{O_2} &= \nu_{CO_2} + \frac{\nu_{H_2O} - z}{2} & \nu_{CO} &= \frac{W_F}{W_{CO}} y_{CO} \\ \nu_{CO_2} &= x - (1 - X_H)\nu_S & \nu_S &= \frac{W_F}{W_S} y_S \\ \nu_M &= b & W_S &= X_H W_H + (1 - X_H) W_C \end{aligned} \tag{13}$$

where y_{CO} and y_S are the user specified post-flame yields of CO and soot and a, b, x, and y are from the specification of the fuel molecule in Eq. (13). In short, the individual gas species mass fractions are just linear combinations of the three mixture fraction variables, and the solution of transport equations for the three mixture fraction variables rather than the eight species reduces the computational expense of the entire simulation by roughly 30 %.

4.3.2 Thermophysical Properties

In addition to needing the actual species mass fractions, other properties must also be determined from the mixture fraction parameters. These include the average molecular weight, the specific heat, the conductivity, the diffusivity, and the viscosity. For all but the average molecular weight, the desired parameter, given as G in the equation that follows, is computed as follows:

$$G = \sum_i G_i Y_i \,, \tag{14}$$

where G_i is the value of G for species i (this may be temperature dependent) and Y_i is the mass fraction of species i. Since the species mass fractions are linear combinations of the mixture fraction parameters, G can also be computed directly from the mixture fraction without having to first compute the individual mass fractions. This is shown in the equation below where G_∞ is the value of G in the ambient. The vector for G is precomputed by multiplying each row in the matrix shown in Eqn 12 by the value of G_i for that row.

$$G = G_\infty + \vec{G}_Z \cdot \vec{Z} \tag{15}$$

The average molecular weight, $\overline{W}$, of a mixture of gasses, however, is given by:

$$\overline{W} = \frac{1}{\sum_i \frac{Y_i}{W_i}} . \tag{16}$$

The equivalent expression in mixture fraction space is

$$\overline{W} = \frac{Y_{Z,\infty} + \vec{Y}_Z \cdot \vec{Z}}{W_\infty + \vec{W}_Z \cdot \vec{Z}} , \tag{17}$$

where the W terms are as the G terms in Eqn. 15 and the Y_Z terms are obtained by expanding the matrix multiplication in Eqn. 13 into a single row and collecting the constant and Z terms together.

4.4 Radiative Absorption

In FDS v4 the mixture fraction model used RADCAL (Grosshandler, 1993) to precompute and array of absorbtivities, denoted by Kappa, as a function of Z and temperature. In the event that water vapor from droplets was present, it was not included in the absorbtivity, although the droplets were. In finite rate mode, the user can specify a constant absorbtivity for the entire domain, but there was no method to compute it for the specific species and temperature present in the computation. Potentially, one could compute a new look up table with a degree of freedom for temperature and each mixture fraction and finite rate species present. This approach, however, quickly requires a very large array with a correspondingly large number of precomputations using RADCAL.

An alternative approach was postulated that involves computing a separate table for each mixture fraction and finite rates species as a function of temperature. The absorbtivity would then be computed by a weighted sum. It is recognized that this approach will not account for band overlaps in the species; however, the range or errors in this approach was unknown. 10,000 random sets of species states representing a plausible set of combustion products were generated. Random temperatures and pathlengths were also generated. RADCAL was run once for the combined set of species and separately for each species. The sum of the separate species computations was then compared against the combined computation. The result of this exercise

is shown below in Figure 3 with the error shown in Figure 4. Analysis of the results in the figure show that 96 % of the results for FDS v5 are within 80 % of the RADCAL results and 70 % are within 5 %. The outliers are primarily at very low values of Kappa (little radiation is either produced or absorbed with low Kappa). This suggests that while some reduction in accuracy of the radiation solver may occur, that it will be tolerable given the other uncertainties in the code.

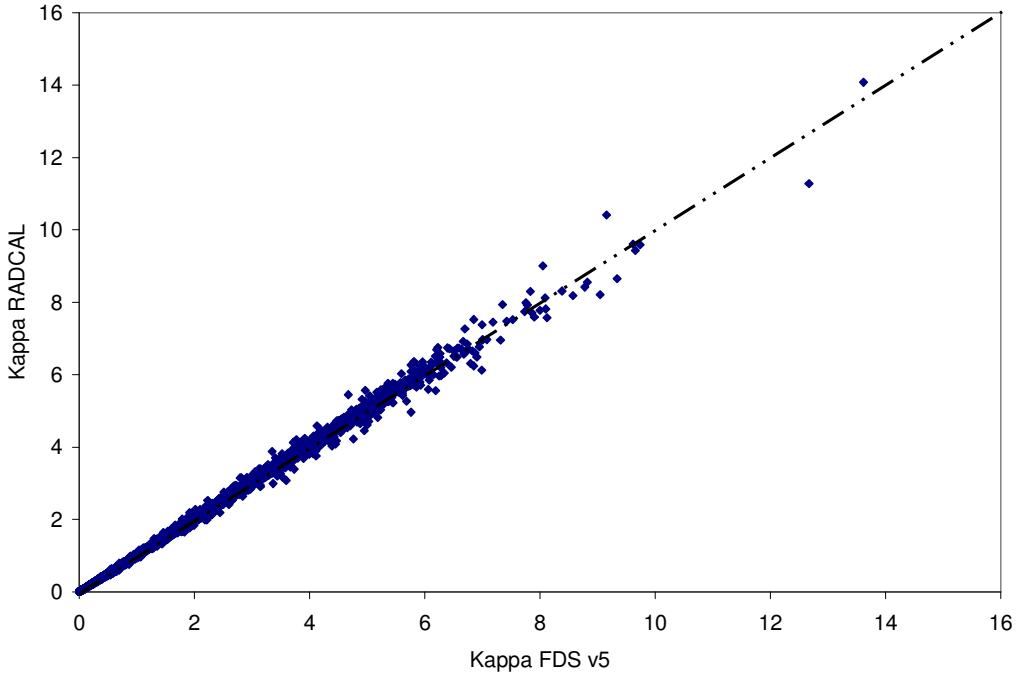

Figure 3: Comparison of RADCAL Computed Absorbtivities for Combined vs. Summed Individual Species

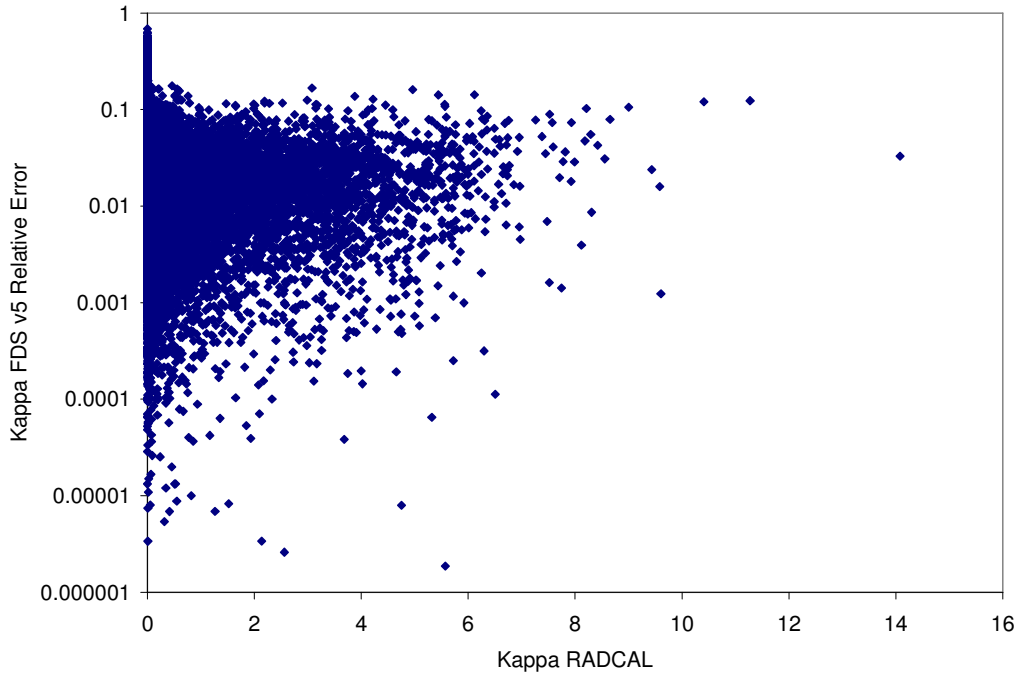

Figure 4: Error of RADCAL Computed Absorbtivities for Combined vs. Summed Individual Species

Based on this assessment a new radiation initialization routine was developed. This routine precomputes lookup tables mixture fraction species and for the absorbing species in RADCAL if they are explicitly specified as a species. These precomputed values are then used to generate a weighted sum in the radiation solver. This approach allows all absorbing species to participate even in finite rate mode.

5.0 Usability Enhancements

5.1 New/Modified Input Keywords

5.1.1 REAC

Users typically make use of a wide variety of data sources for FDS inputs. For some fuels one may have a heat of combustion based on the assumption of complete combustion, but desire to specify a soot and/or carbon monoxide yield. In this case the appropriate action is to reduce the ideal heat of combustion to account for the products of incomplete combustion. The user can now specify the parameter IDEAL on the REAC line, and if it is true, FDS will automatically reduce the heat of combustion to account for products of incomplete combustion.

Specification of the fuel when using the mixture fraction has also changed. Rather than having the user specify the stoichiometric coefficients, the user now specifies the fuel chemistry and the stoichiometric coefficients are computed. This removes the confusion that existed over how to specify the coefficients when soot or CO yields were also specified.

Minor changes have also been made to the finite rate inputs. Previously the user specified the reactants and products in terms of their stoichiometric coefficients. It was presumed that the exponents in Arrhenius rate calculation were equivalent to the stoichiometric coefficients. Users now specify the exponents separately from the coefficients.

5.1.2 DUMP

A new namelist entry, &DUMP, was created that gathers together all of the output options that had previously been distributed over many different namelist entries. With these parameters gathered in one place it is easier to ensure consistent treatment as the further development occurs.

5.1.3 DEVC/PROP

FDS v4 had a number of namelist quantities for inputting various types of detection devices (&SMOD, &HEAT), output quantities (&THCP), and suppression devices (&SPRK). It quickly became clear that to expand the capabilities of FDS under this framework would require creating additional namelist groups and the associated logic for processing them. Instead, the input file was simplified to two sets of namelist entries: &DEVC (DEViCe) and &PROP (PROPerty). The &DEVC namelist entry allow the user to specify a location (area or volume for some quanitities) and a type of device. This type could be a code computed quantity such as temperature or density or it could represent a sprinkler or detection device. For some types of devices such as sprinklers a user will typically have many locations with each location behaving in the same manner. For these types of devices the &PROP namelist group was created. With the &PROP input the user can define the characteristics of a spot smoke detector and then refer to that property with a number of &DEVC inputs.

5.1.4 TABL

A new namelist entry was created called &TABL. This input quantity is intended to provide a generic method to provide multidimensional tabular input. The format for the namelist quantity is:

&TABL ID=’name of table’, TABLE_DATA= X(1),X(2),…X(N) /

where the ID is referred to by other inputs and TABLE_DATA contains a row of data for that TABL. Multiple lines with the same ID would constitute a single table. The number of TABLE_DATA entries would be dependent upon the use of the table. In this manner one routine can read in data for an arbitrary TABL format which can be processed separately by each TABL user.

5.2 Sprinkler Spray Distributions

FDS v4 allowed the user to input a sprinkler spray pattern by specifying an array of mass fluxes and velocities. A unit sphere centered around the sprinkler nozzle was divided into a number of equal solid angles, based on a user provided number of azimuthal and longitudinal segments, and mass fluxes and velocities were specified for each segment. This approach had its

disadvantages. The resulting inputs were not easily readable. For many nozzles, large portions of the unit sphere have no droplet flux. Multiport nozzles were difficult to specify. Lastly, the method required a separate input file to contain the sprinkler data which is less desirable from a QA point of view where one would wish all the inputs to be self-contained in one file.

The new input method makes use of the TABL entry discussed previously. For a spray pattern the format is:

&TABL ID='name of spray pattern', TABLE_DATA= LAT1, LAT2, LON1, LON2, VELOCITY, FRACTION /

Where LAT1 and LAT2 are the beginning and ending of an azimuthal segment of the unit sphere, LON1 and LON2 are the beginning and ending of a longitudinal segment of the unit sphere, VELOCITY is the droplet velocity in the solid angle, and FRACTION is the fraction of the nozzle flowrate that passes through that solid angle. Only non-zero segments of the unit sphere are specified. The input data is processed by creating a vector structurewith elements equal to the number of rows in the table. Each vector element is provided with the cumulative mass fraction for that row in the table. In the droplet insertion routine, a random number is generated which is then located within the vector. The vector element bounding that random number gives the row in the table from which two additional random numbers pick an insertion location within the segment described by the table row.

5.3 Detection

5.3.1 Beam Detectors

A new device type was added to simulate a beam detector. The user specifies the end points of the beam's path. The algorithm then determines the grid cells along the path and the distance the beam travels through each of the cells. It computes the total obscuration by integrating the differential obscuration along each cell in the beam's path:

$$\%obs = 100 \times \left(1 - e^{-\kappa \sum_i \rho_{s,i} \Delta x_i}\right) \ldots \tag{18}$$

where i is a cell along the path κ is the extinction coefficient in m^2/kg, $\rho_{s,i}$ is the soot density in cell i, and Δx_i is the distance the beam travels in cell i.

5.3.2 Aspiration Detectors

A new device type was added to simulate an aspiration smoke detection system. The user specifies a series of sampling locations, the sampling flowrates at each location, and the time it takes the sample to travel from each location to the detector. The user can specify an additional flowrate to represent portions of the system not being modeled (e.g. sampling locations that exist in the prototype but are not part of the computational domain for the model). The algorithm determines the longest transport time and uses 1 % of that as an integration time interval. An array of sampling location vs. time interval is continuously updated with a running average of the

soot density at each sampling location. After each integration time interval has passed, the array is right shifted. The detector output is determined by computing a flowrate weighted soot density using the appropriately time-shifted soot data from the array. The output is the obscuration in %/m.

5.4 Control Systems

FDS v4 had a limited ability to control the activation of sprinklers, the creation and removal of obstacles, and the opening and closing of vents. These were limited to time, a smoke detector, or a heat detector. Each method of control had its own inputs and its own block of code. This had two main disadvantages. The control functions were being evaluated in multiple regions within the source code. Each type of function had its own set of inputs. Many user's have requested the ability to perform these actions for a variety of input conditions. To add these new features was not trivial as it meant creating new namelist quantities and new subroutines. Additionally since control functions were being evaluated in multiple regions of the code, there was the possibility of conflict between subroutines.

In FDS v5 the entire approach to using control functions was completely rewritten. Two methods are provided to the user to control the code behavior. Any &DEVC can be used to open and close a vent, add and remove an obstacle, or turn on and off a sprinkler nozzle. Additional capabilities are provided by a new namelist entry, &CTRL (ConTRoL), which allows for more complex behavior.

5.4.1 DEVC as controls

For any &DEVC input the user can specify an ID, a unique name for the &DEVC; a SETPOINT, the value at which the &DEVC changes state; an INITIAL_VALUE, the logical state of the &DEVC at the start of the run; the TRIP_DIRECTION, whether the &DEVC changes state as it increases or decreases past the SETPOINT; and whether or not the &DEVC will LATCH, change state only once. Inputs for &OBST, &HOLE, &VENT, and &DEVC can use the namelist entry DEVC_ID to refer an ID on a &DEVC input. The state of the &DEVC will then control the behavior of the item referring to it. For example the following two lines will create a 1 m^3 obstacle that will disappear after 10 s:

```
&OBST XB=0,1,0,1,0,1, DEVC_ID='TIMER'/
&DEVC ID='TIMER', QUANTITY='TIME', SETPOINT=10. ,INITIAL_STATE=.TRUE./
```

Any quantity that FDS can output can now be used to control the code execution.

5.4.2 CTRL as controls

There are times when more complex behavior is desired. For example one may wish a smoke control system to activate only after two detectors have alarmed. Behaviors such as this can be handled with the new namelist quantity &CTRL. Each &CTRL is provide with a unique ID, the inputs to the function via the array INPUT_ID (requires that IDs for &DEVC and &CTRL be jointly unique), the INITIAL_STATE of the function (false unless specified otherwise), and details related to the type of function. The available functions are:

- ALL: all inputs must be true for the function to change state
- ANY: a single input must be true for the function to change state
- ONLY: an exact number of inputs must be true for the function to change state
- AT_LEAST: greater than or equal to an exact number of inputs must be true for the function to change state
- TIME_DELAY: the control function changes state a given number of seconds after the input becomes true
- CUSTOM: the numerical value of a &DEVC is used to determine the state of a control function by having the user specify a &RAMP with the &DEVC quantity as the independent variable and the control function state as the dependent (negative number is keep INITIAL_STATE and positive number is change INITIAL_STATE)
- DEADBAND: the numerical value of a &DEVC is used along with two SETPOINT values and the ON_BOUND. If ON_BOUND is LOWER the &CTRL function will be true if the &DEVC has dropped below the lower SETPOINT and will become false when it crosses back over the upper SETPOINT and vice versa if the ON_BOUND is UPPER. Those are a thermostat in heating and cooling mode, respectively.
- KILL: if the input is true, code execution will be terminated
- RESTART: if the input is true a restart file will be written

Consider as an example a pre-action sprinkler system. In this system, the normally dry sprinkler pipes are flooded when a detection event occurs. For this example, the detection event is when two of four smoke detectors alarm. It takes 30 s to flood the piping network. The nozzle is a &DEVC named 'NOZZLE 1' controlled by the &CTRL named 'nozzle trigger'. The nozzle activates when both detection ('smokey') **and** the time delay ('delay') have occurred.

```
&DEVC XYZ=1,1,3, PROP_ID='Acme Smoker', ID='SD_1' /
&DEVC XYZ=1,4,3, PROP_ID='Acme Smoker', ID='SD_2' /
&DEVC XYZ=4,1,3, PROP_ID='Acme Smoker', ID='SD_3' /
&DEVC XYZ=4,4,3, PROP_ID='Acme Smoker', ID='SD_4' /
&DEVC XYZ=2,2,3, PROP_ID='Acme Nozzle', QUANTITY='CONTROL', ID='NOZZLE 1',
CTRL_ID='nozzle trigger' /
&CTRL ID='nozzle trigger', FUNCTION_TYPE='ALL', INPUT_ID='smokey','delay' /
&CTRL ID='delay', FUNCTION_TYPE='TIME_DELAY', INPUT_ID='smokey', DELAY=30. /
&CTRL ID='smokey', FUNCTION_TYPE='AT_LEAST', N=2,
INPUT_ID='SD_1','SD_2','SD_3','SD_4' /
```

5.5 Colors

FDS v4 allowed the user to specify the color of an obstacle or vent by either specifying an RGB triplet of real numbers from 0 to 1 or by specifying one of a handful of COLOR keywords. While this worked it had two minor disadvantages. Most current graphics programs use integer values for RGB (from 0 to 255) which requires the user to do the integer to real normalization. The available COLOR keywords were the primary and secondary color palette which is also the palette used for slice and Plot3D files. This meant that obstacles and vents could get lost when viewing those output files. The input processing was changed to have the RGB values be input

as integers and a list of over 500 COLOR keywords was added (based on the X11 colors). A small subset of the COLOR keywords with color swatches were placed in the User's Guide and the entire list is made available on the FDS web page. Making it easier to specify a real world pallete for the Smokeview aids the understanding of the visualization by providing better visual cues.

5.6 Time

To make it easier to match FDS runs to experimental data two minor changes were made to the source code. The first change allows the user to specify a start time other than 0 s. Thus in an experiment with two minutes of background data with a fire starting at 120 s, the user can input T_START = 120. and not have to adjust the output files for plotting alongside the experimental data. A second change allows the user to specify a TIME_SHRINK_FACTOR. When this is specified all time-dependent &RAMP inputs and all time based inputs have this factor applied as well as to the specific heat of materials. This in some sense "accelerates" FDS, and for some experiments allows one to match temperature trends over time with a greatly reduced computational time.

5.7 Output Functionality

5.7.1 Output Statistics

`&DEVC` outputs had been provided with functionality to perform operations on areas volumes such as integration, determine maximum value, and determine minimum value. Additional operations were added to determine either the volume weighted or mass weighted average for an area or volume within a single computational mesh.

5.7.2 Relative Humidity

A new output `QUANTITY` called `RELATIVE HUMIDITY` was created. This device will output the relative humidity at a location.

5.7.3 Optical Depth

The solution of the 1D radiative transport equation for a purely absorbing region with a constant absorptivity is

$$I = I_0 e^{-\kappa L}, \tag{19}$$

where I is intensity, L is a pathlength, and κ is the absorptivity in units of m^{-1}. If one were to plot measured data for the above equation to determine κ, plotting the natural log of the equation would result in a straight line fit to determine κ. Historically, such data has been processed not with the natural log, but rather with $\log_{10}$. As a result the determined κ will differ by a factor of 2.3 (the natural log of 10). This approach results in what is typically referred to in fire protection engineering as the optical depth. A new `QUANTITY` called `OPTICAL DEPTH` was added to FDS to

perform this computation rather than requiring users to divide the `QUANTITY OPTICAL DENSITY` by 2.3.

5.7.4 Radiative Flux

FDS has long had the capability to output the radiative flux to a surface within a model. This was an easy task as this was computed and stored within the radiation transport routine. A number of users had requested to ability to do this without having to specify a solid surface. Generally, the interest was in determining what flux a person might be exposed to if they were present in a particular location. The optimization of the memory requirements for the radiation routine is such that the individual angular components of the radiative field are not stored in gas phase cells, only at solid boundaries. A new `&DEVC QUANTITY` called `RADIATIVE_FLUX_GAS` was created to perform this operation. If such a device is present, during each update of an angle within the radiative transport routine, the flux for that angle is stored for the location of each `RADIATIVE_FLUX_GAS` device. The algorithm assumes that the device sees 2π steradians (i.e. it sees a hemisphere) along a user defined `ORIENTATION`. Thus, unlike the surface measurement, the `RADIATIVE_FLUX_GAS` is not restricted to sightlines along the major coordinates axes of the computational domain.

5.7.5 CSV Output Files Column Limit

FDS currently outputs a number of comma separated value (CSV) files. The majority of FDS users examine these files using Microsoft Excel. Excel has a limit of 255 columns for importing a CSV file. To read in a file with more columns, the user must select a subset of columns to eliminate. To aid the FDS user, logic was added to the dump routines that checks to see if the number of outputs in a given CSV file will exceed 255 columns. If it does, then multiple files are written. For example if a user requests 100 THCP outputs, then FDS will write an output file called fileid_tc.csv. If instead there were 260 TCHP outputs, then FDS would write two output files called fileid_1_tc.csv and fileid_2_tc.csv. Based on user feedback, the keywords `DEVC_COLUMN_LIMIT` and `CTRL_COLUMN_LIMIT` were added to enable the user the dictate the maximum number of columns in an output file. Further enhancements are planned but not yet added to enable the user to group outputs into predetermined files.

5.7.6 Velocity Flux Quantities

FDS tracks velocities at cell edges and other parameters at cell centers. Computing fluxes requires either averaging velocities to get cell center values or averaging the flux parameter to get cell edge values. The existing flux routines in FDS v4 did not do this consistently. These were fixed.

5.8 Boundary Conditions

FDS v4 contained a mass flux boundary condition for inserting a mass flux of a particular species into the domain. It did not contain the ability to remove a fixed mass flux from the domain. The algorithm for the inlet mass flux was modified to allow for its use as a total outlet mass flux (e.g. removes all species proportionate to their mass fraction at the vent).

5.9 Maximum Droplets

To prevent out of memory errors, FDS limits the maximum number of droplets that are permitted in a simulation. In a case with droplets, a type array for droplets contains the information on droplet position, velocity, temperature, etc. With each droplet insertion, this array is reallocated up to the point where the maximum number of droplets is reached and further droplet insertions are prohibited until existing droplets are killed by evaporation, leaving the domain, or reaching a user defined lifetime.

Originally, the approach taken did nothing to ensure that droplets could be inserted. If the number of droplets was at its maximum and it was time to insert more droplets, none would be inserted. Thus, if a calculation was not killing droplets at a fast enough rate, few if any droplets would be inserted. This resulted in poor spray dynamics as nozzles became intermittent rather than continuous. The solution was to modify the permissible drop lifetime. Prior to each call the droplet killing routine, a droplet lifetime was computed that used the current droplet insertion rate, current droplet count, and insertion interval. For example if there is a maximum of 100 droplets allowed, there is currently 10 droplets, and 10 droplets per second are being inserted, then an effective lifetime of 9 seconds can be computed. If at any droplet insertion interval, sufficient droplets have not been killed to allow for the full insertion of 10 droplets per second, then droplets older then 9 seconds would be culled until enough memory was available for the next insertion. In this manner spray nozzles will remain continuous with their user defined spray characteristics.

5.10 Al_2O_3

A new logical keyword was added to the `&MISC` inputs called `AL2O`. When set to .TRUE., it replaces the RADCAL computed absorptivity for soot with a computation for the absorptivity of small particles of Al_2O_3. The particles are assumed to be in the Rayleigh limit (as is done for soot particles), but the constant valued index of refraction for soot is replaced with a temperature dependent index of refraction for Al_2O_3:

```
IF (AL2O3) THEN
   IF (RCT(1) > 2570._EB) THEN
      FF_FAC = 0.017_EB
   ELSEIF (RCT(1) < 500._EB) THEN
      FF_FAC = 5.E-6_EB
   ELSE
      FF_FAC = 0.00073_EB
   ENDIF
ELSE
   FF_FAC = 8.9_EB
ENDIF
```

Using this keyword enables an FDS user to compute the radiative emissions from rocket exhaust plumes.

6.0 Model Validation

During the development and testing of the new mutli parameter mixture fraction approach, a number of validation test cases were created. The test cases were selected to exercise both the DNS and LES modes of operation. Additionally the interest was in using test cases that were well documented in terms of geometry, boundary conditions, measurement uncertainty, and the availability of the experimental data.

6.1 Methane-Air Slot Burner

The goal of this analysis was to demonstrate the validity of the new two-step approach and to demonstrate that it is an improvement over the prior single-step approach used in FDS v4. The Wolfhard-Parker slot burner consists of an 8 mm wide central slot flowing fuel surrounded by two 16 mm wide slots flowing dry air. Velocity and species profiles for a methane test for various heights above the burner are archived on the BFRL web page (Smyth, 1996 and 1999). The experimental errors were reported as 5 % for temperature and 10 % - 20 % for the major species (Norton, et al., 1993). A DNS simulation was run of the slot burner using both FDS v4 and FDS v5 (with a CO yield of 0) with the new two step combustion model.

A three dimensional simulation was performed for one quarter of the slot burner with a uniform 0.5 mm numerical grid. This grid was selected using a grid study of 0.25 mm, 0.5 mm, and 1.0 mm. The 0.5 mm and 0.25 mm grid had no change in flame position and differences in the peak temperature, peak velocity, and CO and CO2 gas concentrations were less then 10 %. Because the flow field was laminar, symmetry boundary conditions could be assumed along the burner's vertical centerline. The computational domain was 32 mm by 32 mm by 48 mm with 393,000 grid cells. A two dimensional simulation was also performed, but the results were less accurate because radiative losses along the plane of symmetry are not possible in a 2D computation. The 3D simulation was run for 4 s of physical time, requiring 104 hours of CPU time on a 2.4 GHz Intel processor for FDS v5 with the last second of results averaged. While this might sound like a very costly calculation, it is typical of direct numerical simulation. While DNS is typically not practical for fire protection engineering applications, it is a useful approach for evaluating the new combustion methodology.

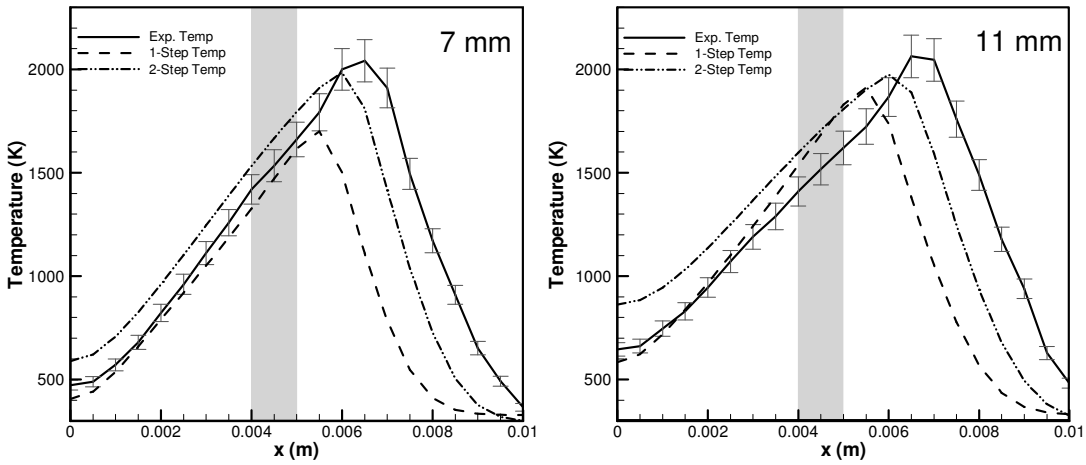

Figure 5: Predicted and measured temperature profiles over the half-width of a methane-air slot burner (x=0 is burner centerline, shaded region is burner lip) at two elevations above the burner.

Figure 5 shows predicted and measured temperature for the single-step (FDS v4) and two-step (FDS v5) reaction schemes, plotted as a function of the distance from the burner centerline at a height of 7 mm and 11 mm above the burner. The measurement uncertainty is indicated by the vertical bars. Both versions of FDS predict a narrower and cooler flame than measured, but the two-step predictions lie closer to the data and the peak temperature is within the measurement uncertainty. If the two-step profiles were expanded to the measured flame width the two-step profile would match the experimental data within the measurement uncertainty everywhere except in a narrow band about the centerline. These results are not surprising as the first reaction step is infinitely fast. Thus, combustion occurs at the grid cell immediately above the lip of the burner. In reality, the cold fuel and air streams do not react infinitely fast and some oxygen penetrates the flame at the base, seen in Figure 6 below. This lower amount of combustion in the experiment at the burner lip results in cooler gasses being entrained into the core of the flame with a resulting drop in the centerline temperature. The single-step version predicted lower temperatures throughout the flame and this was likely a result of the single parameter model not capturing the appropriate heat release distribution vertically over the burner.

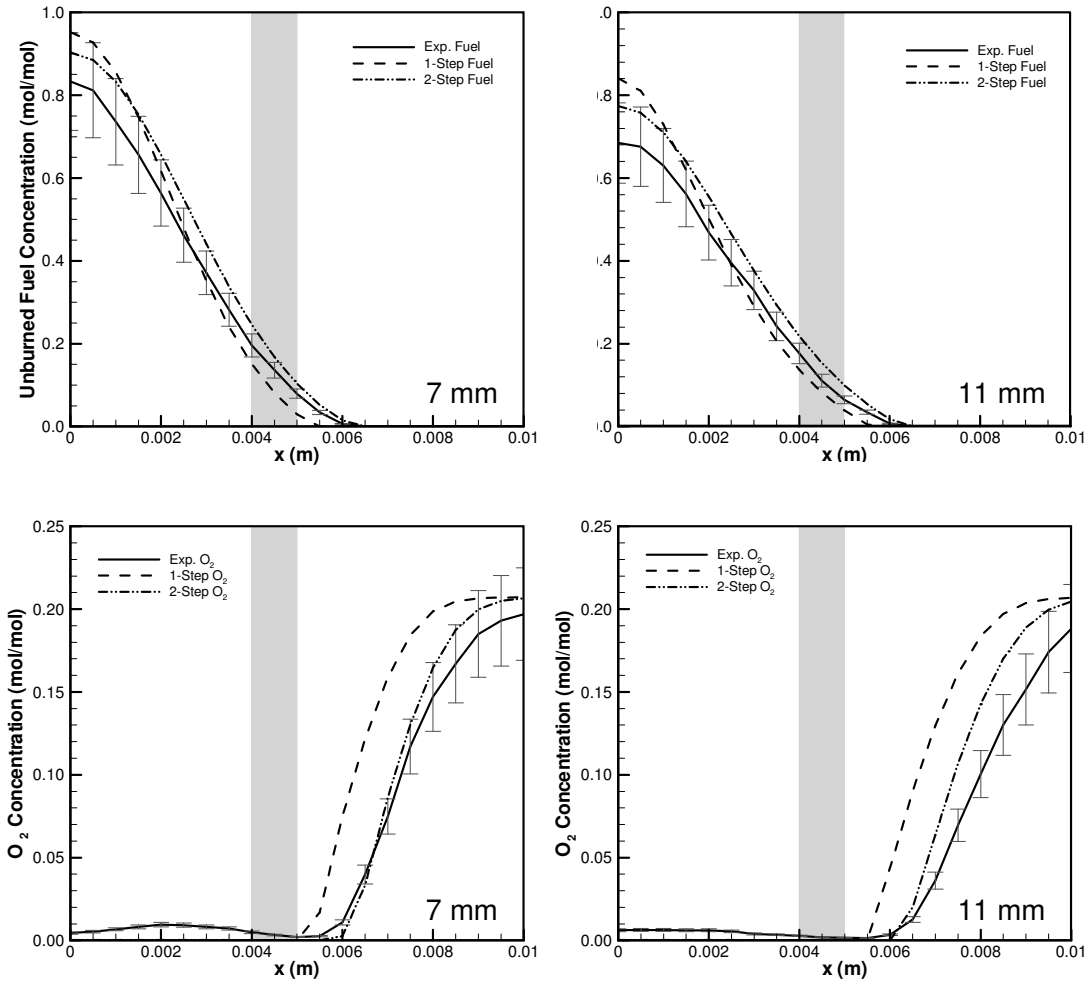

Figure 6: Predicted and measured fuel (top) and oxygen (bottom) concentrations for a methane-air slot burner (x=0 is burner centerline, shaded region is burner lip) at two elevations above the burner. Note FDS shows zero O_2 inside the burner.

Figure 6 shows predicted and measured fuel and oxygen profiles for the single and two-step reaction schemes, plotted as a function of the distance from the burner centerline at a height of 7 mm and 11 mm above the burner. The two-step predictions for fuel and for oxygen outside the flame at 7 mm are within the measurement uncertainty. The single-step method does not perform as well within only a few locations lying within the measurement uncertainty. Neither reaction scheme captures the small amount of oxygen within the flame as the fast primary reaction step in both methods is not allowing oxygen to peneatrate the flame sheet.

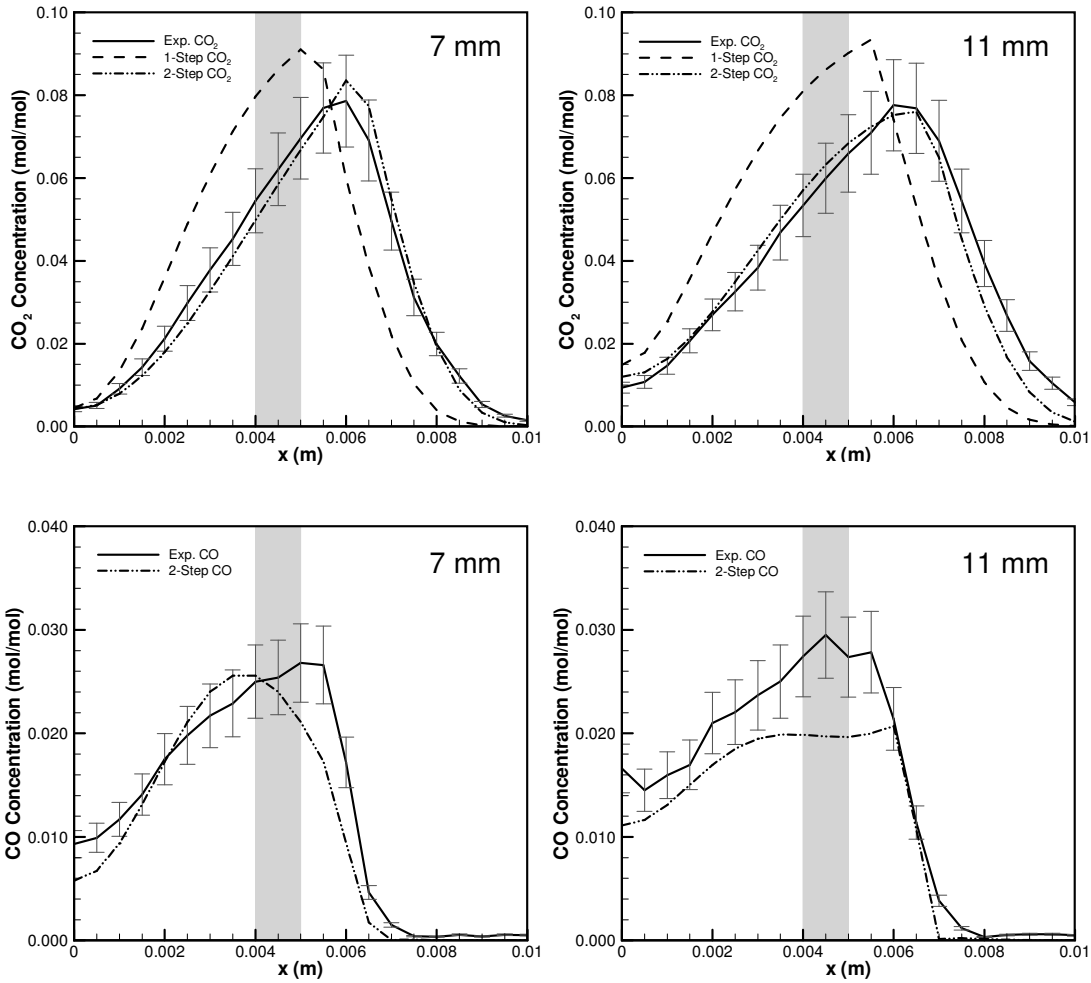

Figure 7: Predicted and measured carbon dioxide and carbon monoxide concentrations for a methane-air slot burner (x=0 is burner centerline, shaded region is burner lip) at two elevations above the burner.

Figure 7 shows predicted and measured carbon dioxide and carbon monoxide profiles for the single and two-step reaction schemes, plotted as a function of the distance from the burner centerline at a height of 7 mm and 11 mm above the burner. For almost all locations the two-step schemes predictions for carbon dioxide are within the measurement uncertainty. The single-step scheme is over predicting the carbon dioxide concentrations. The single-step method is not capable of predicting the formation and destruction of carbon monoxide, so no comparison can be made for that quantity. The two-step scheme predicts a profile within the measurement uncertainty inside the flame at the 7 mm elevation and slightly below the measurement uncertainty at the 11 mm elevation. This is a marked improvement in capability over that present in FDS v4 and demonstrates the basic validity of the method.

Some of the remaining error in the FDS v5 predictions could likely be improved with the addition of more species and reactions (such as OH or H_2). However, in large scale simulations these species would not be resolvable.

6.2 Burner Beneath a Small Hood

Beyler (1986) performed a large number of experiments involving a variety of fuels, fire sizes, burner diameters, and burner distances beneath a hood. The hood consisted of concentric cylinders separated by a gap that allowed combustion products to be removed uniformly from the hood perimeter, see Figure 8. The exhaust gasses where then analyzed to determine species concentrations. The burner could be raised and lowered with respect to the bottom edge of the hood.

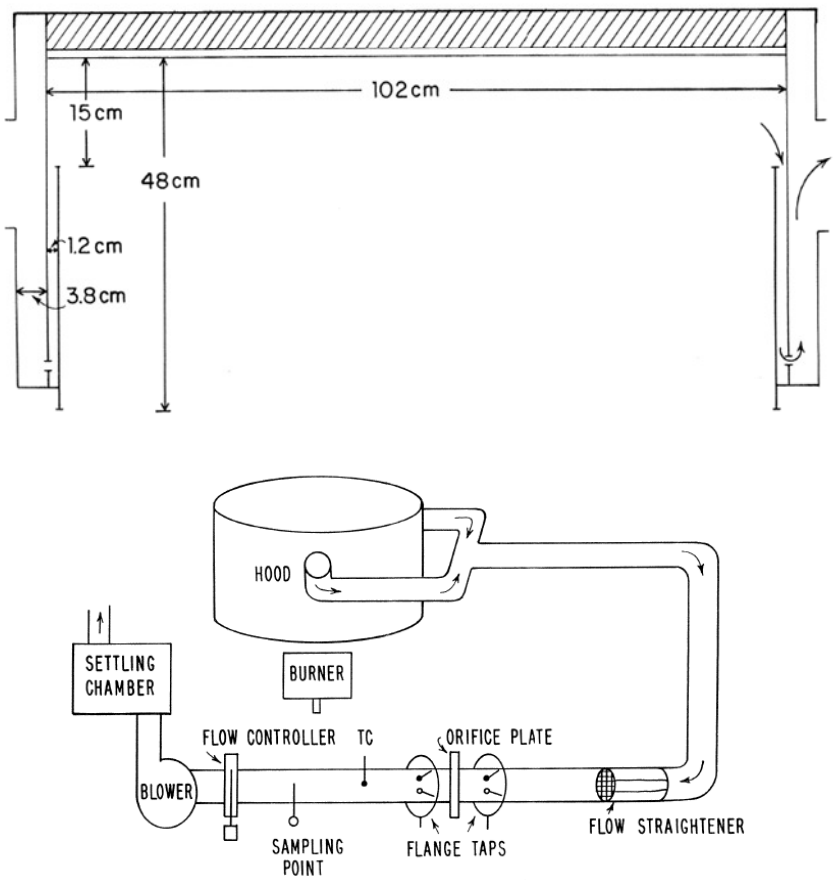

Figure 8: Test Setup for Beyler Hood Experiments

FDS simulations using the two step combustion model were run for 12 of the propane tests using a 19 cm round burner. The cylindrical hood was modeled in FDS as an equivalent area box while preserving the height. A 1.4 cm grid was used. A lower fuel flammability limit of 3.3 % was set for the simulations (Beyler, 2002).

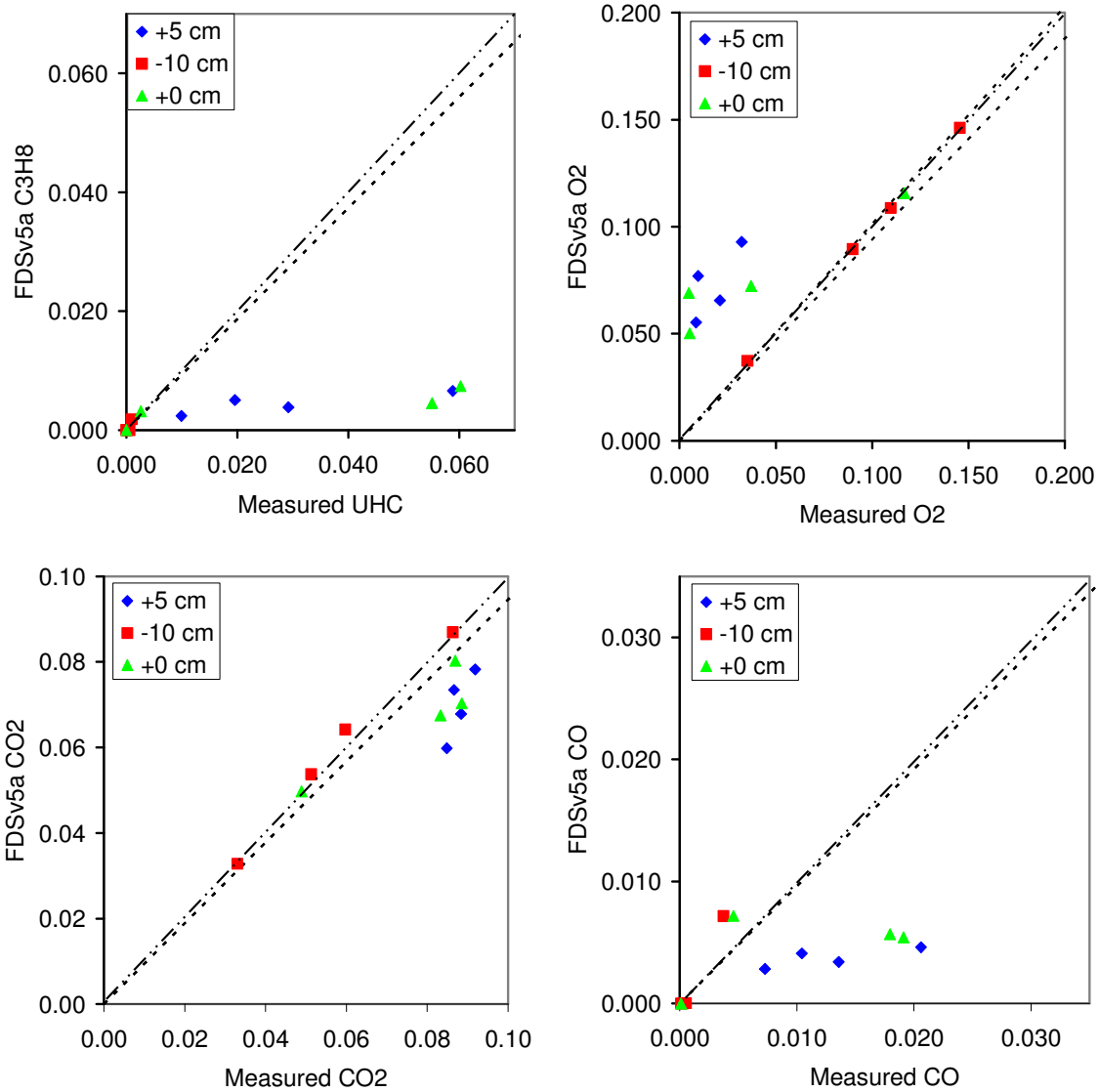

Figure 9: Predicted and measured fuel, oxygen, carbon dioxide and carbon monoxide concentrations for 19 cm diameter propane fires in the Beyler hood apparatus. The burner distance above the hood lip for each test is shown in the insets.

Figure 9 above shows predicted and measured fuel, oxygen, carbon dioxide, and carbon monoxide concentrations. The datapoints are color coded by the distance of the top of the burner from the lip of the hood with a negative number being below the lip. The -10 cm cases are well ventilated and FDS predictions match the measured data. This level of performance is expected. The +0 cm and +5 cm tests transition from well to poorly ventilated as the size of the fire increases. As the degree of underventilation increases, the performance of FDS decreases. FDS is predicting too little unburned fuel and carbon monoxide and too much oxygen in the hood. The root cause appears to be the assumptions of the first reaction step. Unburned fuel and oxygen meet at the layer interface of the hood and by the assumptions in Figure 1, combustion occurs. This energy release at the bottom of the layer results in an updraft and the entrainment of oxygen into the layer. As a result fuel and carbon monoxide are consumed at the layer interface

and entrained oxygen penentrates into the layer. Modeling this type of stratified environment will require changing the conditions under which the first reaction step is allowed to take place. This would suggest a user would need to be careful when modeling elevated fires in a space (may obtain layer burning when it wouldn't occur) and for backdraft / reflash scenarios.

6.3 NIST RSE Tests

6.3.1 1994 NIST RSE Tests

The NIST Reduced Scale Enclosure (RSE) was a 40 % scaled version of the ISO 9705 compartment. It measured 0.98 m wide by 1.46 m deep by 0.98 m tall, with a door centered on the small face that measured 0.48 m wide by 0.81 m tall. A 15 cm diameter natural gas burner was positioned in the center of the compartment. The burner was on a stand so that its top was 15 cm above the floor. Species measurements were made inside the upper layer of the compartment at the front near the door and near the rear (Bryner, Johnsson, and Pitts, 1994). Heat release rate uncertainties were reported as 8.6 %, and CO and CO_2 concentration measurements had reported uncertainties of 0.24 %.

FDS was used to simulate eight fires at fixed HRRs in the compartment: 50 kW, 75 kW, 150 kW, 200 kW, 300 kW, 400 kW, 500 kW, and 600 kW. The tests were modeled using properties of a typical natural gas supplied to the test facility (Bundy, et al., 2007). The simulation included the compartment interior along with a 0.6 m deep region outside the door that was modeled using a 2.4 cm grid resolution for a total of 240,000 grid cells. The grid study used the 500 kW fire with grid sizes of 1.9 cm, 2.4 cm, and 3.5 cm as well as a study using the 2.4 cm grid with a 50 % lower CFL limit (i.e. reduced the time steps by a factor of two). Between the 1.9 cm and the 2.4 cm grids as well as the reduced time step there was no significant change in the location and magnitude of the heat release rate contours and discernable differences in upper layer temperatures and CO and CO_2 concentrations were less then 10 %. The wall boundary condition used a reduced material density for the compartment lining. This was done so that the computation would reach steady state in less time. Each fire size was simulated for 300 s which for the new approach took approximately 45 hours on a 2.4 GHz processor.

Simulations were performed with both the single and two-step reaction schemes. While the one-step reaction scheme does not predict CO formation, it does allow the specification of a fixed post flame CO yield. Setting an increased CO yield to account for a higher equivalence ratio would be a typical practice for an engineer using the one-step model; therefore the correlation in Eq. 20 (Gottuk and Lattimer, 2002) was used to set the CO yield for each simulation with the equivalence ratio, ϕ, determined using Eq. 21.

$$Y_{\mathrm{CO}} = \frac{0.19}{180}\tan^{-1}\left(10\left(\phi - 0.8\right)\right) + 0.095\,. \tag{20}$$

$$\phi = \frac{\dot{m}_{burner} \dfrac{\nu_{O_2} W_{O_2}}{W_F}}{\dfrac{Y_{O_2}^{\infty}}{2} A_{door} \sqrt{H_{door}}} . \tag{21}$$

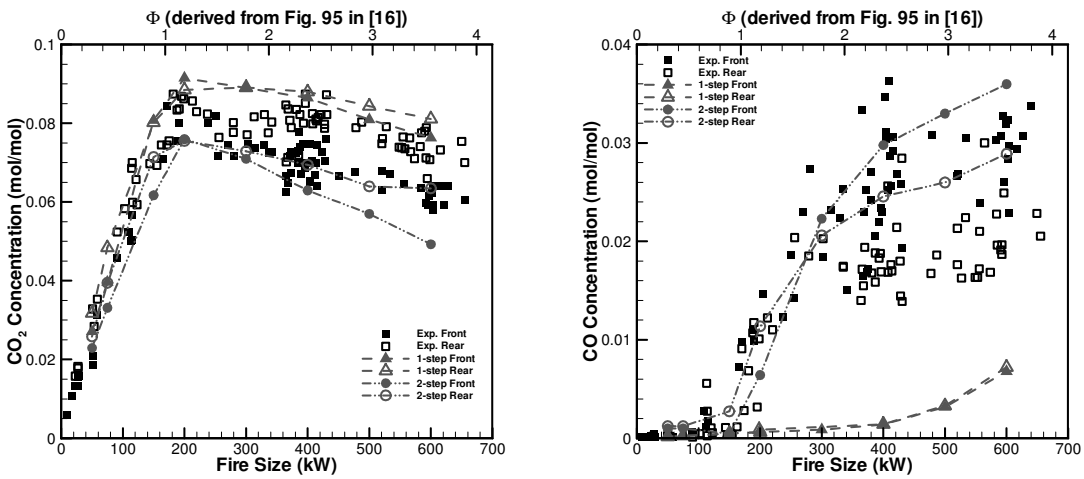

Figure 10: CO_2 and CO predictions compared against measurements in a reduced scale enclosure (lines for predictions added as a visual aid). [16] is (Gottuk and Lattimer, 2002)

The predicted and measured CO and CO_2 concentrations at the front and rear locations are shown in Figure 10. The measured data represents points taken at multiple times during multiple experiments (where HRR was varied over time). The equivalence ratios in the figure are based upon the computed mass flow rates derived from temperature measurements made during the tests; they differ from the presumed equivalence ratios used to set the CO yield for the one-step model. Both reaction schemes capture the general trends seen in the CO_2 data. The one-step scheme over-predicted the concentrations while the two-step scheme under-predicted them. Moreover, the two-step scheme over-predicted the CO concentrations, but the amount of over-prediction was consistent with the amount of under-prediction in CO_2. The one-step scheme, using an equivalence ratio correlation for CO yield, could not replicate the measured values at the two specific locations inside the compartment. Not surprisingly, the under-prediction of CO by the one-step scheme was consistent with its over-prediction of CO_2.

At 600 kW, the two-step predictions of CO_2 at the front and rear locations were 4.9 % and 6.3 % respectively vs. the 6.1 % and 7.1 % in the data. For CO the corresponding results were 3.6 % and 2.9 % vs. 2.9 % and 2.1 %. Note, however, that the absolute front and rear under-prediction in CO_2 of 1.2 % and 0.8 % was similar to the 0.7 % and 0.8 % over-prediction of CO. This implies that a significant contributor to the model error was likely the infinitely fast chemistry assumption of the first reaction combined with the sequential vs. simultaneous reaction steps.

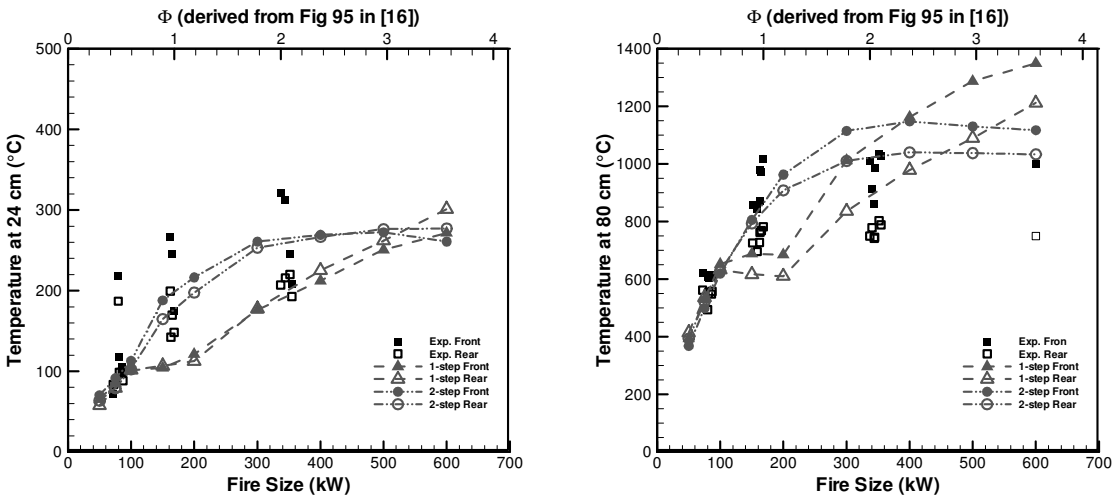

Figure 11: Lower (left) and Upper (right predictions compared against measurements in a reduced scale enclosure (lines for predictions added as a visual aid). [16] is (Gottuk and Lattimer, 2002)

The predicted and measured lower and upper temperatures are shown in Figure 11. The two-step predictions show a similar trend to the data (reaching plateau at higher equivalence ratios) that is not seen in the single-step predictions. Both approaches over predict the upper layer temperatures; however, the degree of over prediction is much less for the two-step scheme.

6.3.2 2006 NIST RSE Tests

In 2006, the Building and Fire Research Laboratory undertook a series of 17 fire tests involving a wide range of fuels in a reduced scale enclosure (Bundy, et al., 2007). Seventeen tests involving seven different fuels (including solid, liquid, and gas) were conducted. The tests occurred in a 0.95 m wide x 1.42 m deep x 0.98 m tall compartment with a 0.48 m wide x 0.81 m tall door centered on one of the 0.95 m walls. The floor of the compartment was 0.19 m above the floor of the test facility. The compartment was lined with a ceramic fiber insulating board. The fires were centered on the floor of the compartment. Measurements included temperature, species, velocity, heat flux, and heat release rate. Measurement uncertainties were generated for specific time intervals for each measurement point for each test. The reported uncertainties are solely for the measurement process (i.e. the reported uncertainty in temperature does not include a contribution due to the uncertainty in the measured fire size). Fuels included natural gas (NG), heptanes (Hep), ethanol (Etnl), polystyrene (PS), methanol (Mtnl), and toluene (Tln).

A validation study of FDS v5 was performed that examined 18 measured quantities in 11 tests. These were: 8 gas measurements (O_2, CO_2, CO, and unburned hydrocarbons made in the front and rear of the compartment above the top of the door), 4 aspirated thermocouples (two locations in the front and rear of the compartment: the upper third and lower third of the compartment), 4 bi-directional probe velocities in the centerline of the doorway, and 2 total heat fluxes on the compartment floor (in front of and behind the burner). During each test, averages of the data

were taken over time periods when the heat release rate was quasi-steady state. This process resulted in a total of 36 data points distributed over the 11 tests

For each test, the compartment plus a small region outside the door and above the compartment was modeled. The external region was modeled so that an open pressure boundary condition would not be present at the compartment door. The computational domain was 0.95 m x 2.44 m x 1.50 m and was gridded with a single computational mesh of 40 x 100 x 72 (288,000) cells. A grid study was performed using test #6.5 with approximately 1/2 and 2 times the number of nodes to establish that the grid was adequate. The burner pictured represents the pan for containing the spray fire. The spheres are locations of measurement devices used during the testing.

In creating the inputs for each simulation, there is some uncertainty to the input data which will impact the FDS predictions being compared with the data. Uncertainties in the fuel flow rate specified in the input file will have an impact on the species production as will uncertainties in the wall thermal properties (which change the compartment temperature and hence can impact the oxidation of CO to CO_2). Other input data such as fuel type and compartment geometry have little associated uncertainty. Thus, in addition to the eleven RSE tests, the maximum fire size observed in tests #6.5 (methane with low soot production) and #7 (heptane with higher soot production) was used to run a series of sensitivity calculations where thermal conductivity of the walls was varied by 10 % and where the fire size was varied by the test determined uncertainty. Each calculation was run state using a constant power large fire and small fire. The change in the predicted quantities was then used to compute FDS uncertainties. These uncertainties were then used when plotting FDS predictions by selecting the closest corresponding uncertainty (i.e. for a large fire with a sooting fuel, the large fire heptane uncertainties were applied to the FDS results). Other uncertainties exist, such as the impact of not including the hood flow and the various flow baffles that existed around the sides of the compartment during the test.

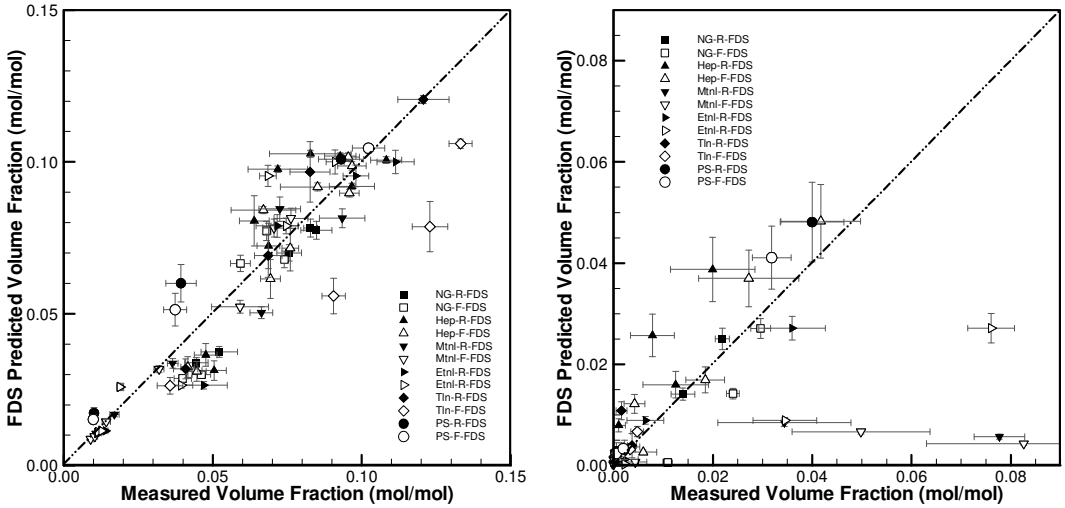

Figure 12: Predicted and Measured CO_2 and CO concentrations in the front (solid symbols) and rear (open symbols) of the NIST RSE

FDS predictions of the CO_2 volume fraction, Figure 12, were within the uncertainty for 36 % of the dataset. With the exception of the rear location of the toluene data, those points that were not within the uncertainty were generally close to being so, and if all sources of FDS uncertainty were accounted for then agreement would be likely. There is a slight trend towards under-prediction of the CO_2 levels. This may result from the current combustion model which treats the reaction as two separate steps and as a result may create locations where O_2 is fully consumed making CO when if parallel reactions were occurring some would be consumed by simultaneous oxidation of CO. The root mean square of the relative difference between CO_2 prediction and measurement was 19 %.

CO predictions, Figure 12, were in agreement for 40 % of the dataset. This is essentially the same performance as for CO_2. The worst predictions are for the oxygenated fuels (methanol and ethanol). These fuels can form CO without the consumption of O_2 from the air, which is a phenomena not accounted for in the current combustion model. Ignoring those data points, there is a trendency to over-predict the CO. Given the CO_2 performance, this is expected for the same reason as for the under-prediction of CO_2.

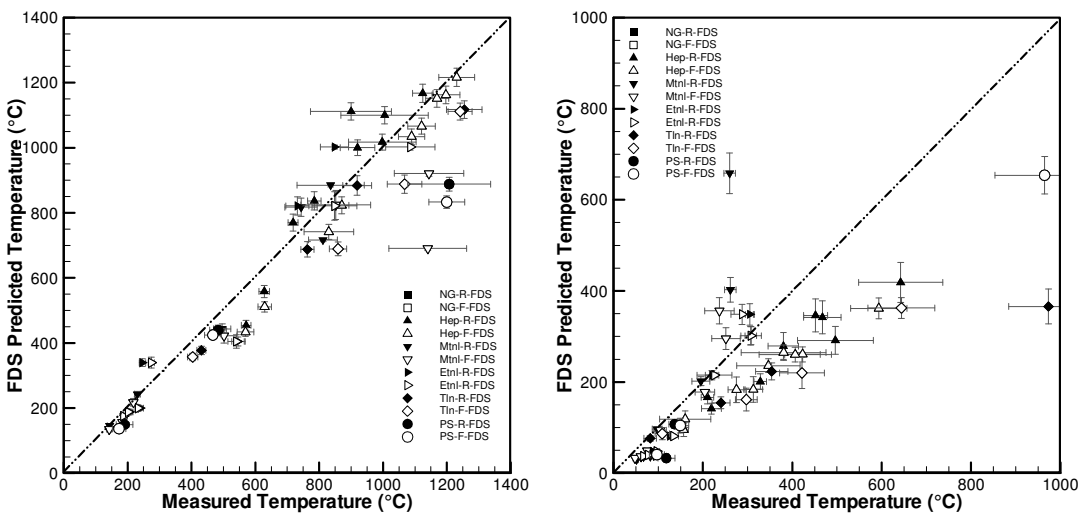

Figure 13: Predicted and Measured upper (left) and lower (right) temperatures in the front (solid symbols) and rear (open symbols) of the NIST RSE

Figure 13 shows the quantities of upper and lower temperature which respectively agree within uncertainty for 28 % and 17 % of the data points. The rms relative difference for the upper measurements is only 10 % with a maximum difference of 32 % (for the previously discussed largest methanol spray fire). For the smaller fire sizes, the upper temperature predictions are generally low compared to the data. This trend is not as evident for the larger fire sizes. For the lower points the rms relative difference is 18 % with a maximum difference of 75 % also for the methanol spray fire. Lower temperature predictions are biased low in comparison to the measurements.

With the exception of the alcohol tests, FDS correctly predicted the trends in various gas species and matched the measurements within uncertainty for approximately half the data set. It can be seen that the current implementation of the two-step combustion model is over predicting CO,

under predicting CO_2, and under predicting unburned fuel. The assumption that the first step is infinitely fast combined with performing the two steps sequentially rather than allowing for some simultaneous reaction is a likely contributor to this.

Temperature predictions by FDS did not match the data within uncertainty as well as other parameters. However, in the upper layer while only 28 % of the predictions were within uncertainty, the average relative difference was only 10 %.

The new two step combustion model has been shown capable of reproducing the conditions within the reduced scale enclosure over a range of fuels and fire sizes

6.4 SNL Benchmark Testing

In May 2005, Sandia National Laboratory hosted a fire model validation symposium. As part of this symposium a series of three benchmark cases were provided to attendees. Submitted results from simulating the benchmark cases were presented at the symposium. Each of the cases results from tests in the FLAME facility at Sandia (Blanchat, 2001). The cases were a helium plume (O'Hern, et al., 2004), a methane fire (Tieszen, et al., 2002), and a JP-8 fire (Murphy and Shaddix, 2004). The helium and methane benchmark cases were simulated using FDS v5.

The FLAME facility is a rectangular chamber with a pyramidal top and a chimney, see Figure 14. The chamber is 6 m wide with the burner 2.45 m above the floor and the top of the pyramid 4.56 m above the burner. The chamber contains a pedestal topped by a flat plate where gaseous or liquid fuel fires can occur. The bottom of the facility contains an annulus of uniform air inflow. The inflow rate can be adjusted to roughly equal the expected air entrainment of the fire in an open or unconfined configuration. A cylindrical shield wall extends from the base of the facility to slightly above the fuel pedestal. This aids in keeping the inflow radially uniform by isolating it from the corners of facility. For the helium plume and methane fire, PLIF (laser fluorescence) and PIV (particle imaging) measurements were made across a slice of the plume.

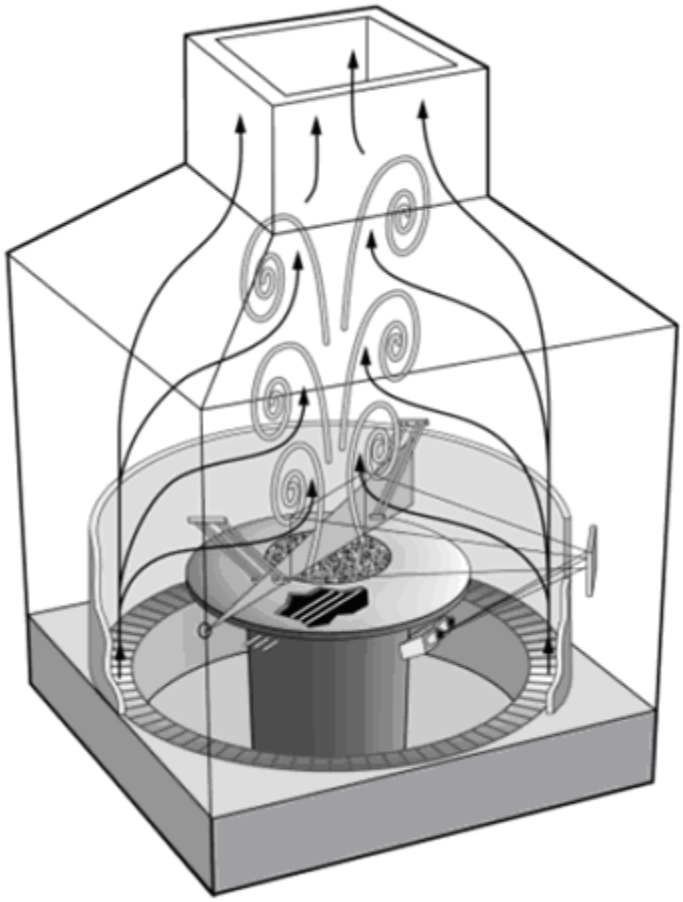

Figure 14: Drawing of Sandia FLAME Facility

A FDS geometry model was created that encompassed the entire FLAME facility with two computational grids. The first grid spanned the main building and pyramid top, and the second grid spanned the chimney. A uniform grid size of 4.8 cm was used for both grids. A cut-away view of this geometry is shown in Figure 15. The annulus at the bottom is the air inlet and the yellow circle is the plume source.

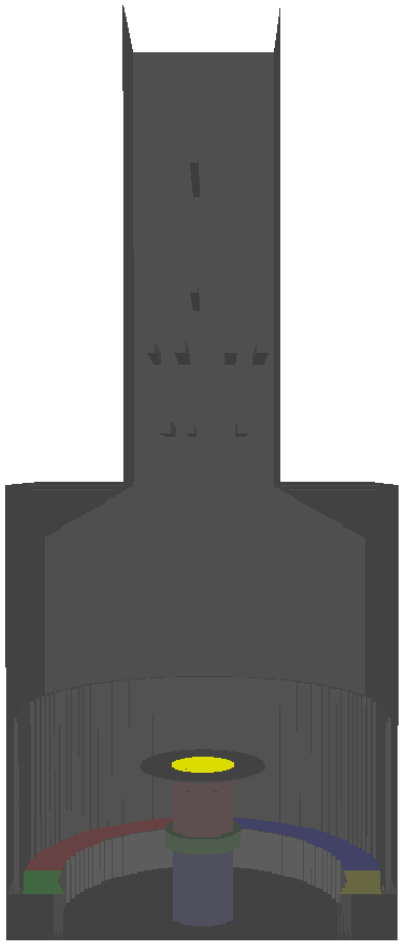

Figure 15: Cut-away View of FDS model of FLAME Facility

6.5 Helium Plume

The helium plume test injected a mixture of helium, oxygen, and acetone (used for the PLIF) through a 1 m diameter diffuser at a uniform velocity profile of 0.325 m/s with an air inlet source velocity of 0.15 m/s. Measurements of the mass fraction and the radial and vertical velocity components were made across the burner diameter plume at various heights up to 0.8 m.

The FDS simulation of the helium plume used the geometry as shown in Figure 15. Since the measured ambient temperature and helium source temperature were within a degree, the FDS computation was performed isothermally. Additionally, the FDS baroclinic torque model was activated. A 60 s simulation was performed with the final 45 s averaged for each grid location in a single plane through the burner centerline for comparison with the experiment. Results of the FDS computations are shown in Figure 16 through Figure 18 below. In each of the plots, the measured data (solid line) is shown along with its reported error (circles).

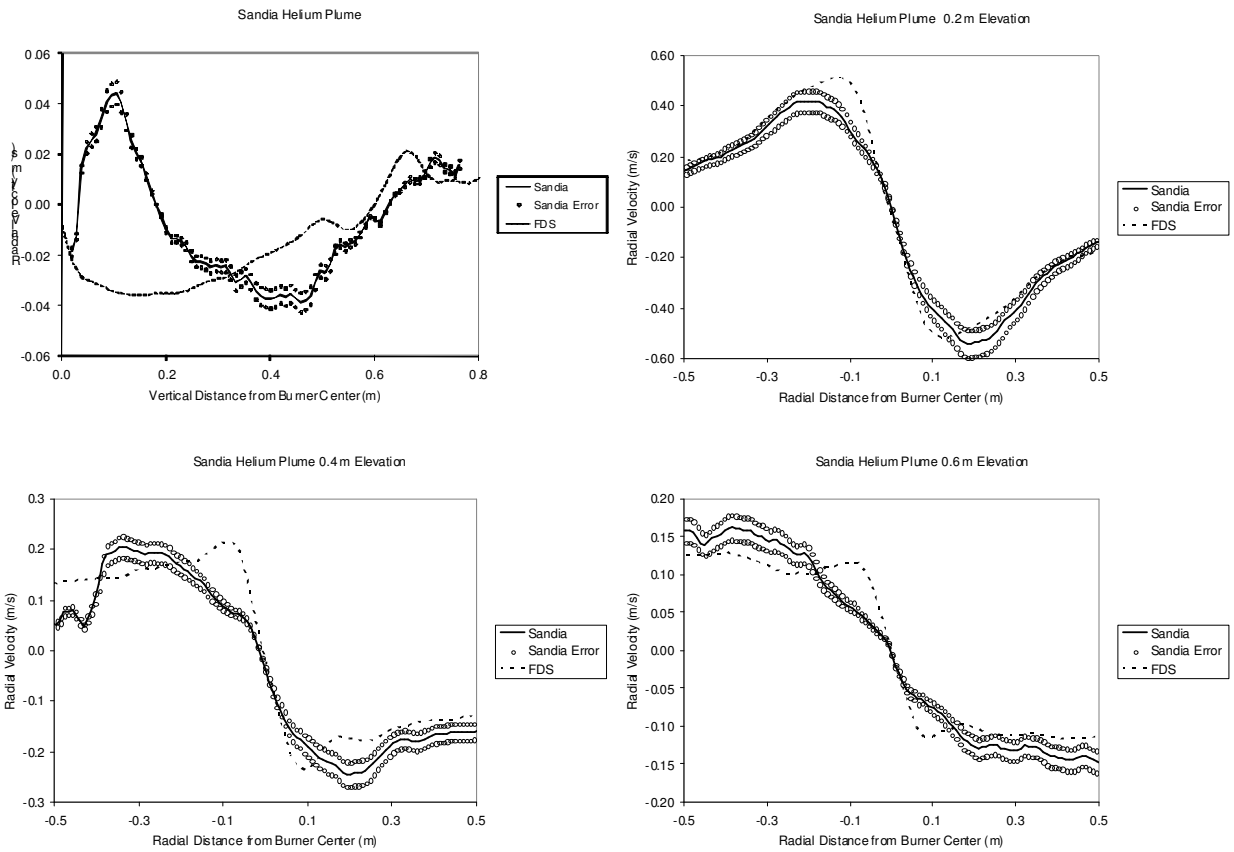

Figure 16: Sandia Helium Benchmark Case Radial Velocity Profiles, FDS vs. Data

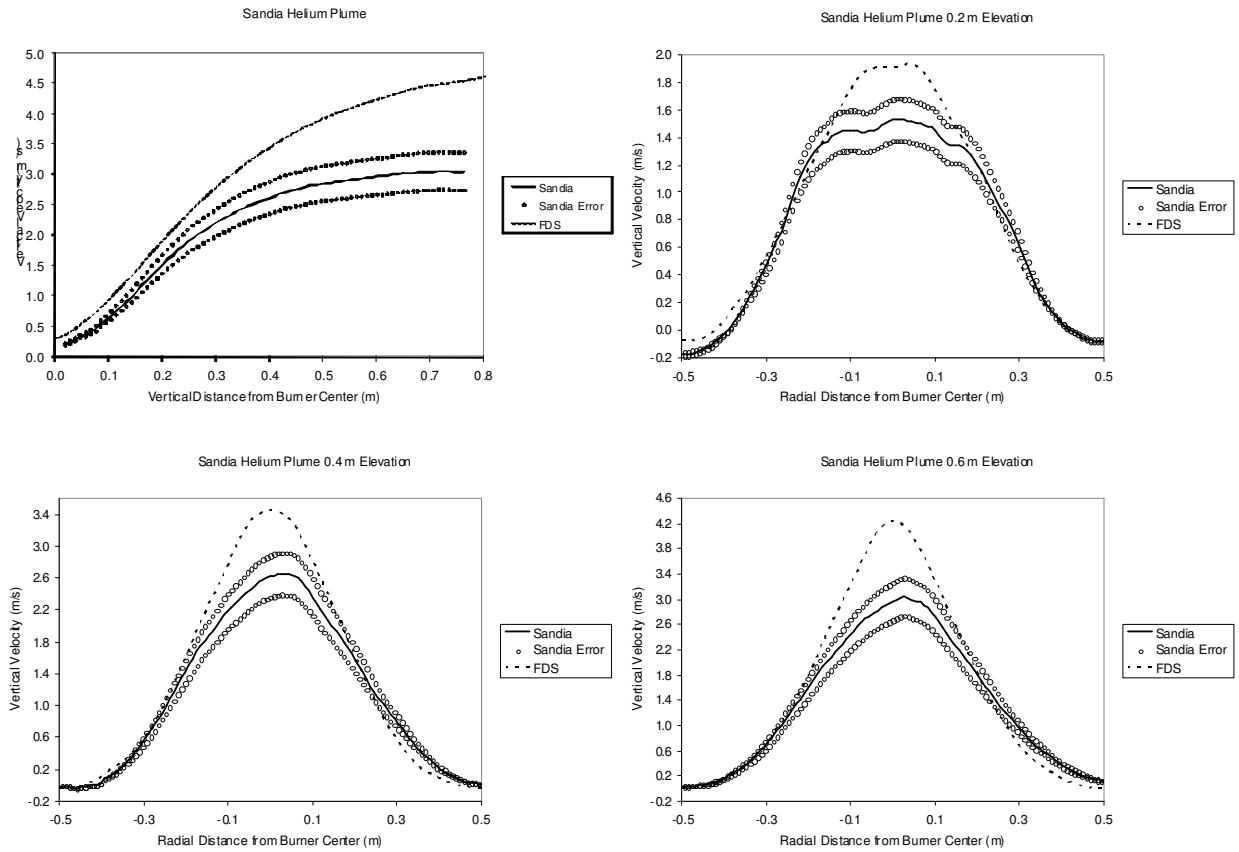

Figure 17: Sandia Helium Benchmark Case Vertical Velocity Profiles, FDS vs. Data

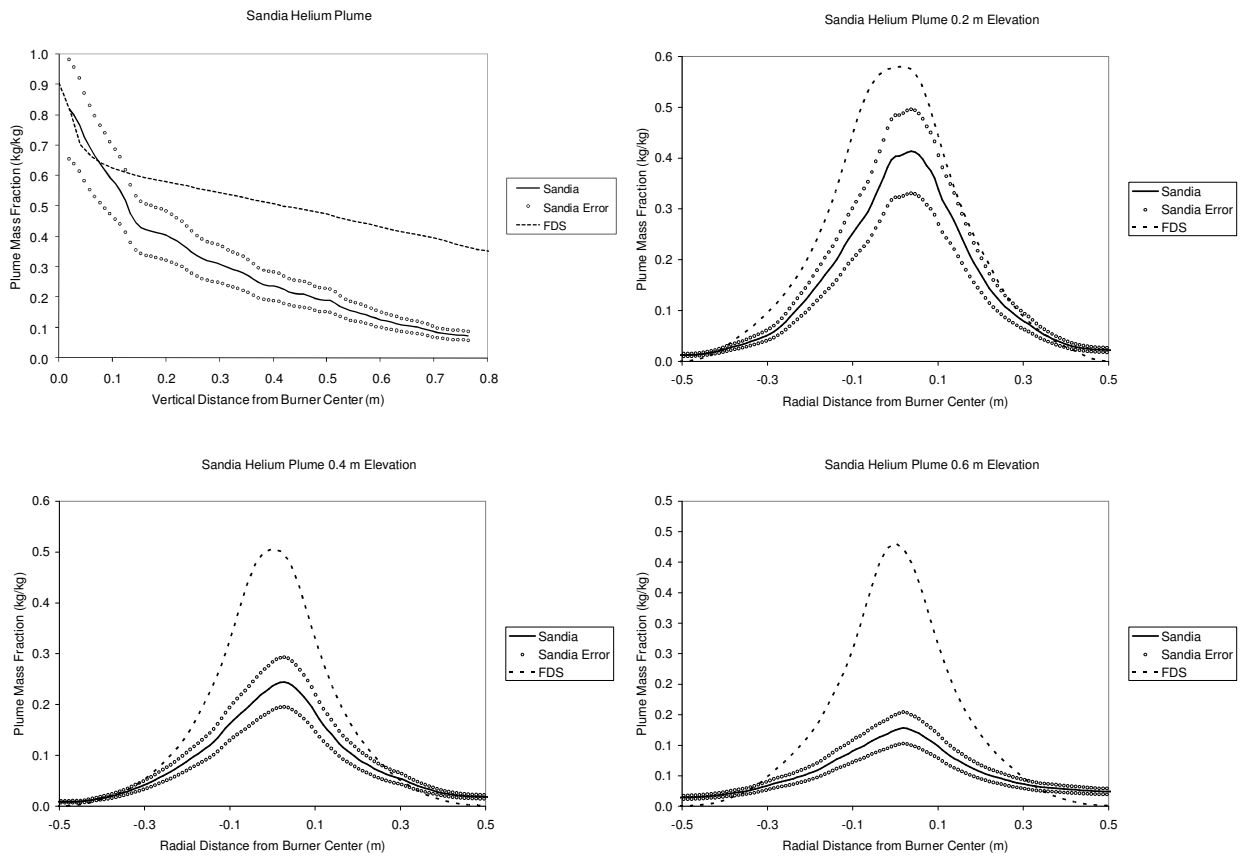

Figure 18: Sandia Helium Benchmark Case Helium Concentration Profiles, FDS vs. Data

The following observations are made from the measured data:

- The peaks of the measured concentration profiles do not lie at the centerline for any of the measured elevations. This could represent an error in assigning the radial coordinate to the measured data, a bias in the plume inlet, or a lack of sufficient timewise data to obtain an accurate average.
- The measured data is not symmetric about the peak. This is most noticeable in the radial velocity plots. The lack of symmetry suggests either a non-symmetric inlet condition or a lack of sufficient timewise data to obtain an accurate average.

The following observations are made from the FDS results.

- FDS is overpredicting the vertical velocity in the plume.
- FDS overpredicts the helium concentration at higher locations with an error that worsens with elevation. Since the buoyancy force and hence the plume acceleration is determined by this quantity, the aforementioned high velocities are not unexpected. This suggests a problem in predicting the entrainment; however, the methane simulation results do not show this same behavior where the buoyancy force is generated by the heat release rate.

- FDS is slightly overpredicting the radial velocity low in the plume and underpredicting it high in the plume. This is consistent with the helium concentration profiles. FDS is not capturing the plume entrainment higher up in the plume.

6.6 Methane Fire

The methane fire test injected methane through a 1 m diameter diffuser at a uniform velocity profile of 0.074 m/s with an air inlet source velocity of 0.32 m/s. Measurements of the radial and vertical velocity components were made across the burner diameter plume to a height of 0.8 m.

The FDS simulation of the methane fire used the geometry as shown in Figure 15. The two parameter mixture fraction, single step chemistry model was used for the simulation. A 30 s simulation was performed with the final 20 s averaged for comparison with the experiment. Results of the FDS computations are shown in Figure 19 through Figure 21 below. In each of the plots the measured data (solid line) is shown along with its reported error (circle symbols). For two of the elevations, data is also shown from computations made by Desjardin (2005). It is noted that unlike the helium data, the methane data for the left and right sides of the plume was averaged together, hence the symmetry about the plume axis.

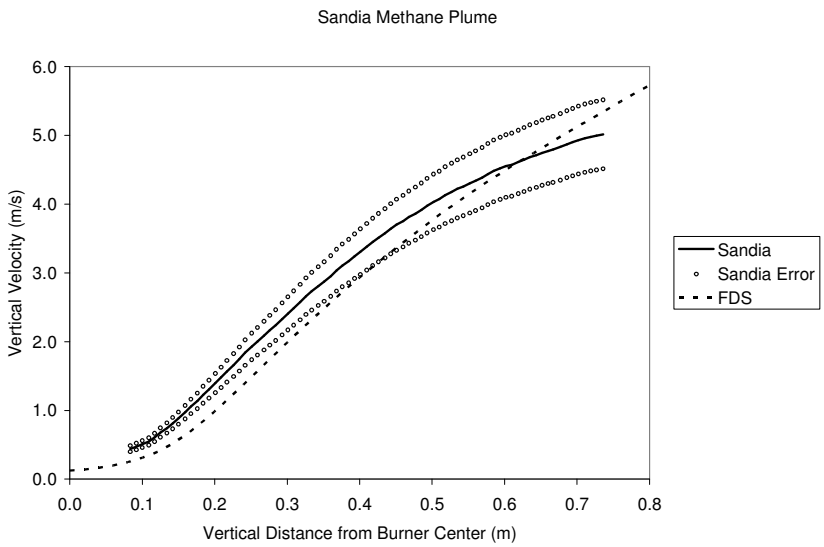

Figure 19: Methane Benchmark Case Centerline Vertical Velocity, FDS vs. Data

The other model is by Desjardin (2005), and it uses a modified strained laminar flamelet model and a high-performance computing architecture. The Desjardin computation shown has a 2.4 cm grid and simulated 3 s of the plume and consumed 19.2 hours of clock time on 128 processors (820 CPU hours/second of simulation) vs. the FDS simulation with its 2 cm grid that simulated 30 s of the plume using 92.4 hours of clock time on 1 processor (3.1 CPU hours/second of simulation).

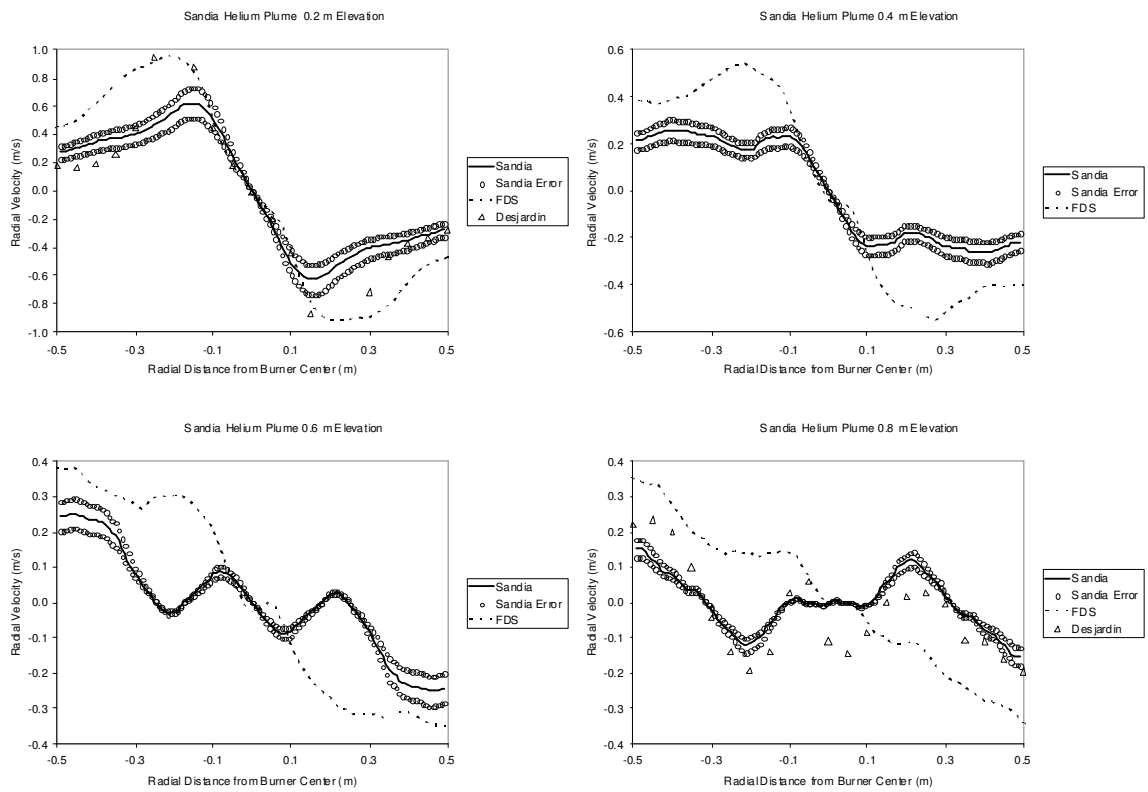

Figure 20: Methane Benchmark Case Radial Velocity Profiles, FDS vs. Data

The following observations are made from the FDS results.

- FDS predictions of the vertical velocity about the centerline lie slightly below the experimentally measured values in the lower region of the plume. At the upper region of the plume, while the predictions are within the measured values, the trend is towards an overprediction.
- FDS predictions of the radial profile of vertical velocity exaggerate the double hump about the centerline at all locations and overpredicts the velocity at the outer edge of the plume. This probably results from the infinitely fast chemistry and mixing time assumptions currently being made with the end result over predicting combustion at the plume edges vs. the plume interior.
- FDS predictions of the radial velocity are closer to the measured data at the lowest measurement location compared to the upper measurement location. At higher locations the FDS predictions show similar features and magnitudes as compared to the data, but with a wider plume width. This reflects the aforementioned observation of the wider distribution seen in the vertical velocity.
- FDS performance is similar to that seen in the Desardin results.

•

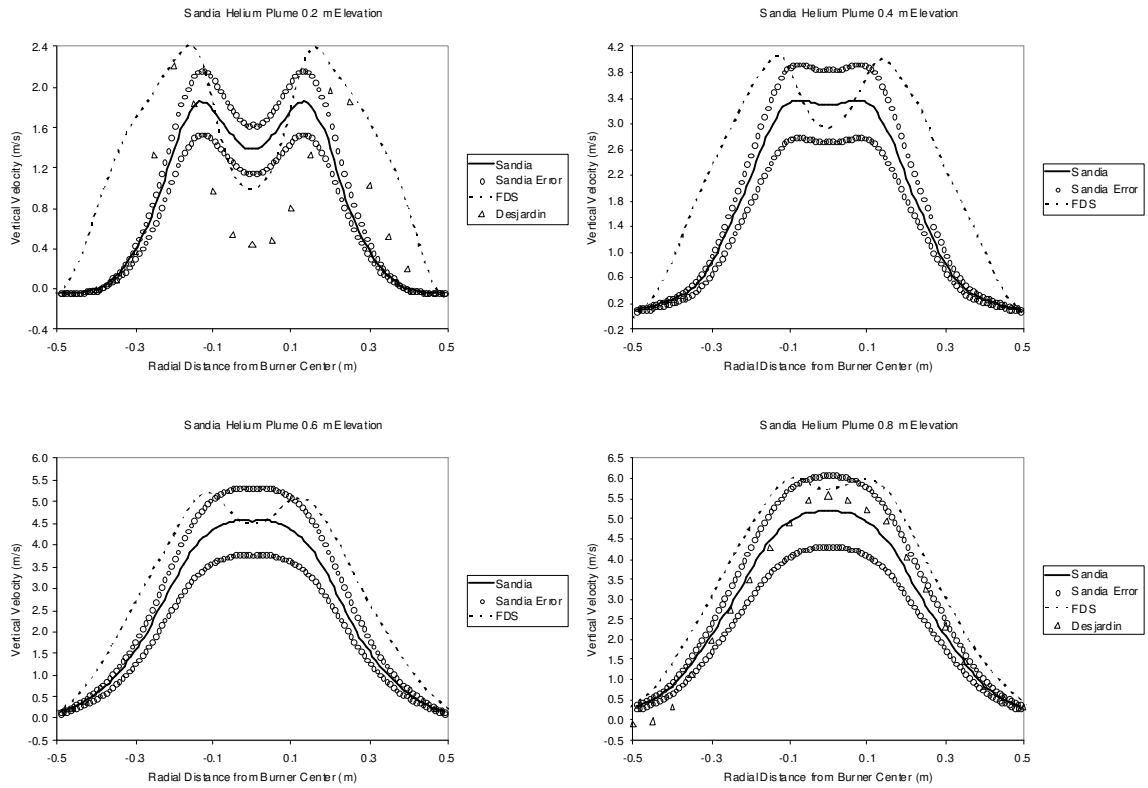

Figure 21: Methane Benchmark Case Vertical Velocity Profiles, FDS vs. Data

7.0 Support of NIST Fire Testing

7.1 Reduced Scale Enclosure Test Support

The NIST RSE has been reconstructed for a new round of fire testing. The testing objectives include the shakedown of new instrumentation and data acquisition equipment, an attempt to better account for all the carbon mass of the fuel, examine the impact of a wide range of fuels, and to provide a well documented set of validation data for fire models. Planning of new instrumentation layouts began in December of 2005 with the first round of tests beginning in March 2006. A second round of tests occurred in August, 2006.

To aid in planning the instrumentation layouts a series of FDS v4 simulations were performed. Velocity, temperature, and species concentration contour plots were generated. Additionally, FDS simulations were performed using an external wind field that represented potential asymmetries of hood induced flow around the compartment due to the overall layout of the test facility. Figure 22 below shows an example of the computations. The figure shows temperature and carbon dioxide concentrations in the doorway for a range of fire sizes. The predictions indicated that for lower fire sizes, regions of elevated temperature and combustion product concentrations appear in the upper corners of the doorway. This indicated the need for probes both along the doorway centerline and along the edges for the upper doorway. It is noted that this behavior was observed during testing.

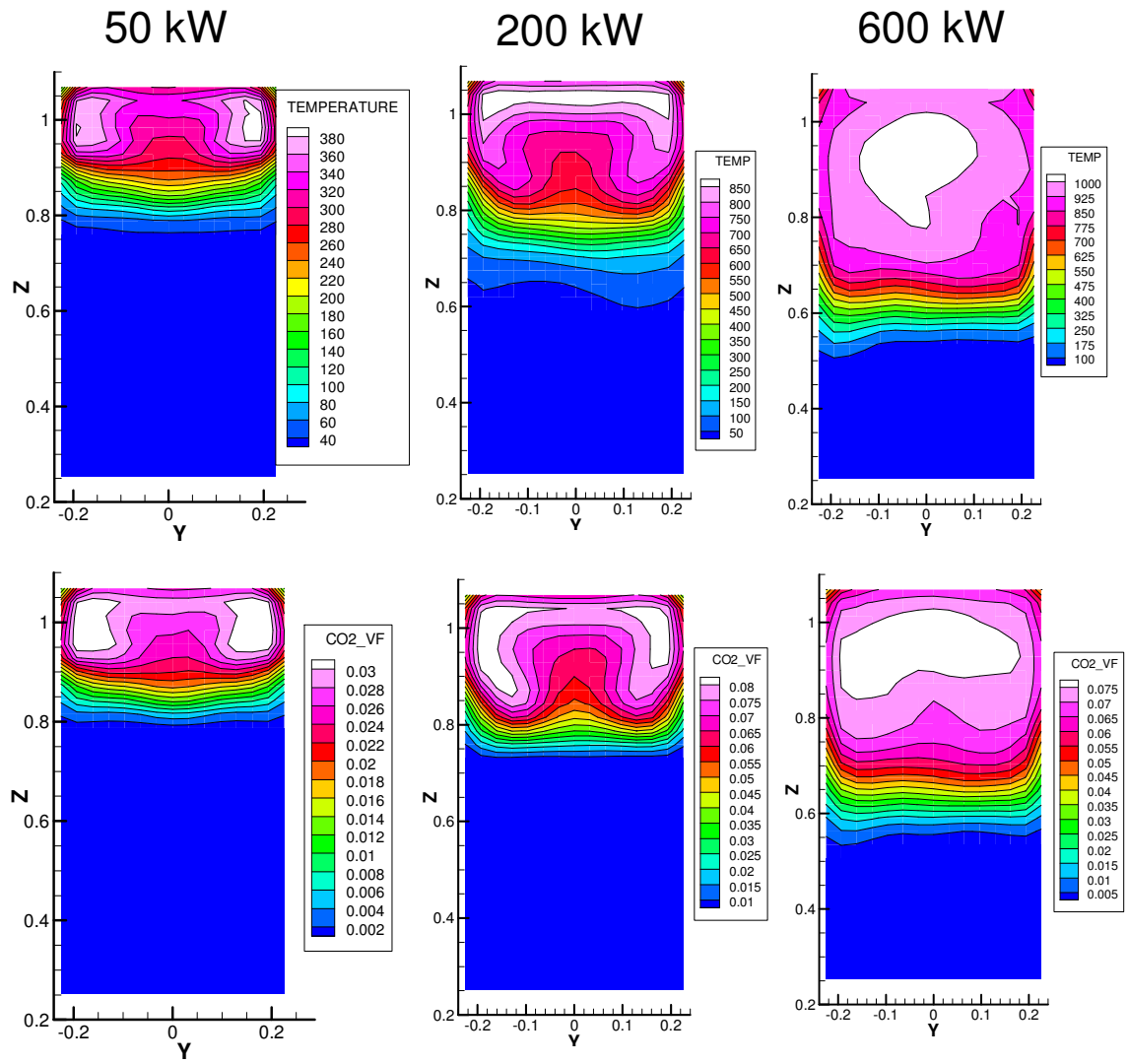

Figure 22: FDS v4 Predictions of Temperate and CO_2 in the RSE Doorway

Additionally a spreadsheet template was provided that demonstrated the advantage of viewing the test data in terms of mixture fraction space. Simply plotting together the raw species measurements can reveal gross problems with the data acquisition, but subtle problems may not be revealed. This can be seen in Figure 23 and Figure 24 below which show test data from an early shakedown test in terms of the data collected and the data collected plotted in terms of mixture fraction. The data plotted in Figure 23 looks reasonable. CO_2 and CO concentrations are within expected levels. The lowest measured O_2 corresponds to the highest measured fuel. The mixture fraction plot; however, indicates a possible sampling line leak. At high values of *Z*, the fuel lies between the two fuel curves for Reactions 2 and 3. This suggests that little extinction is occurring as significant extinction would result in data above the two curves. The sum of the CO_2 and CO mass fractions is approximately equal to the ideal CO_2 curve. This also indicates that the fuel is near fully combusted. However, there is a sizeable O_2 mass fraction that

indicates about 10 % extinction. Since this is not observed in the other data, it suggests oxygen is entering the sampling line.

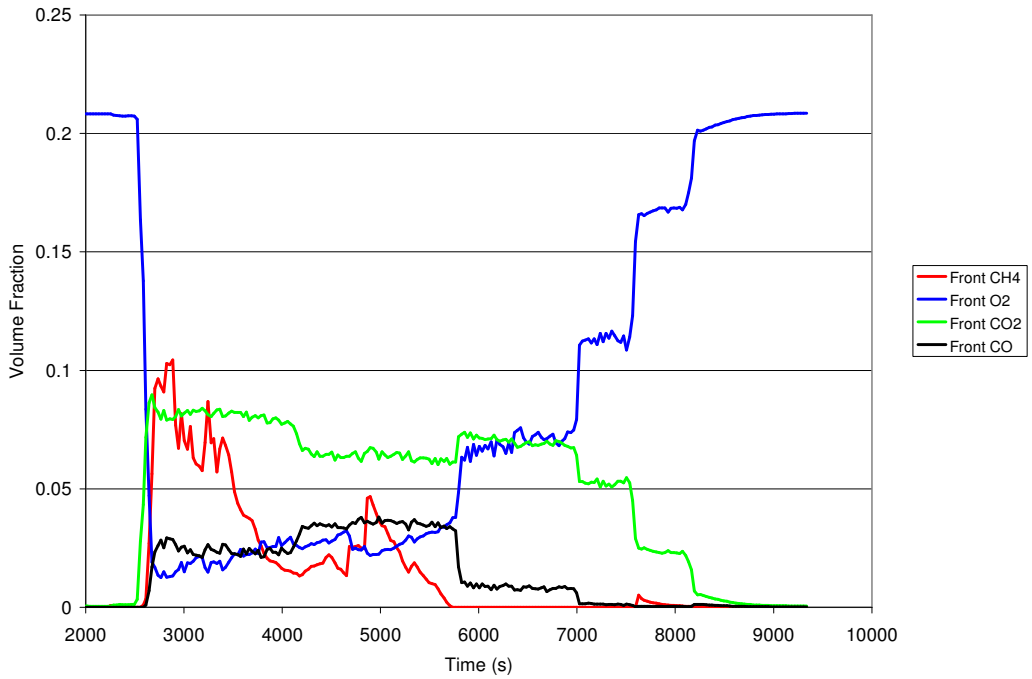

Figure 23: RSE Test Data as Volume Fraction vs. Time

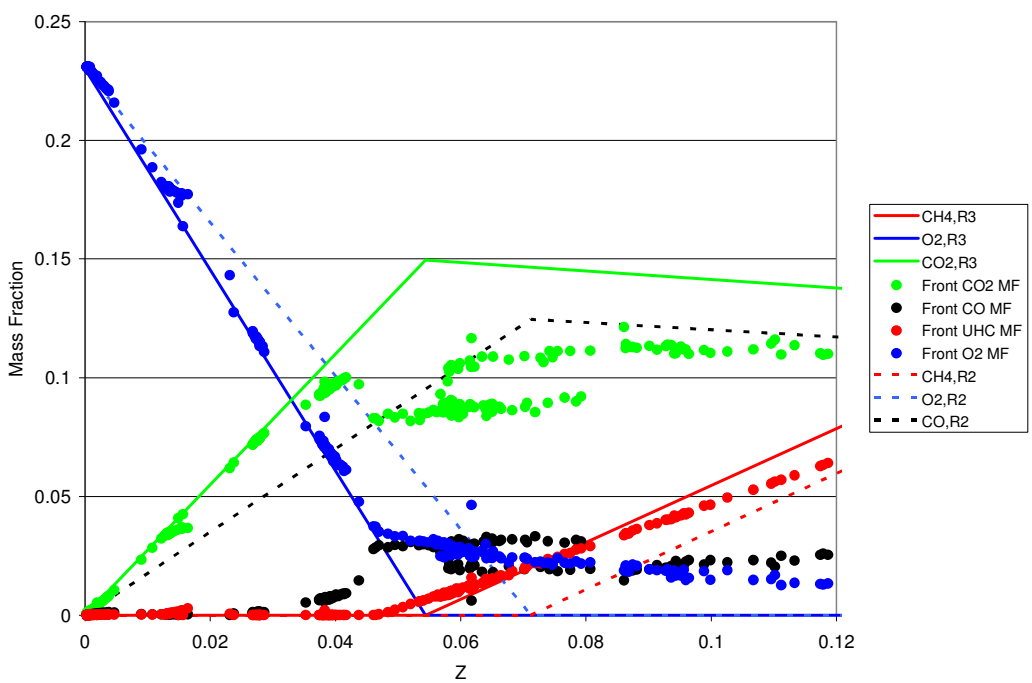

Figure 24: RSE Test Data in Mixture Fraction Space

7.2 Full Scale Testing

In 2008, NIST extended the testing begun in the RSE test series to a full sized ISO 9705 compartment. 32 tests involving 10 fuels were performed in the compartment. The width of the doorway opening was varied to enable higher equivalence ratios at smaller fuel mass loss rates. During the planning phase for this test series, a series of FDS v5 simulations of contstant power fires were performed to investigate the upper layer O_2 concentration and temperature as a function of fire size for various door openings. The results were used to aid in planning the fire sizes and door widths used in the actual test series. Figure 25 and Figure 26 below show results of these computations for the fully open doorway. Additional runs were performed for other doorway widths.

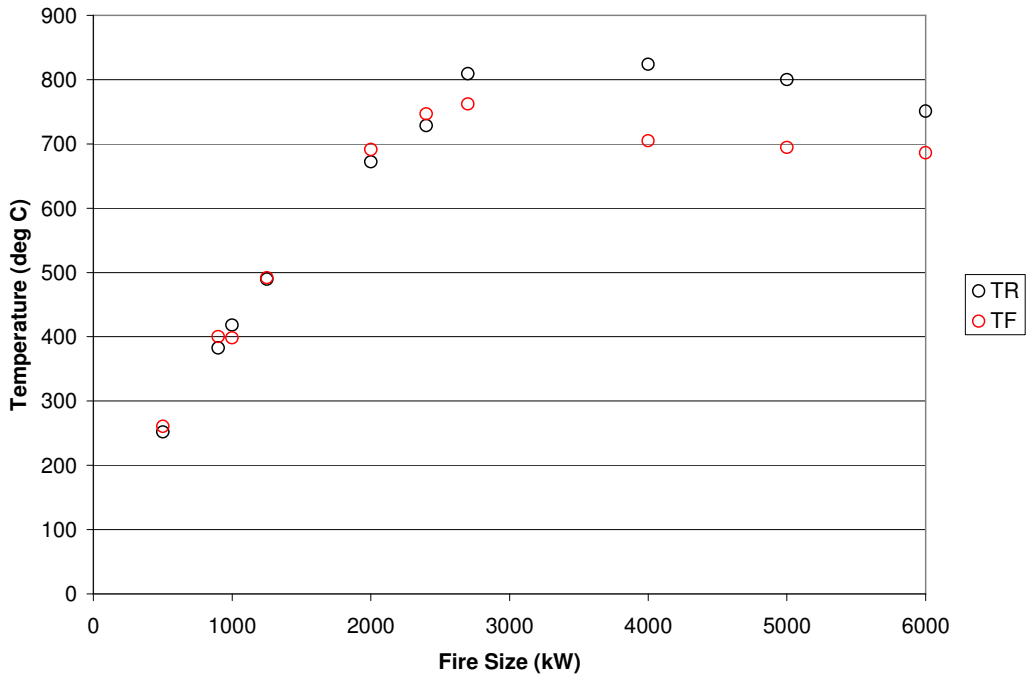

Figure 25: Pre-test Predictions of Temperature as a Function of Fire Size in an ISO 9705 Compartment with a Standard Doorway (TR = rear and TF = front)

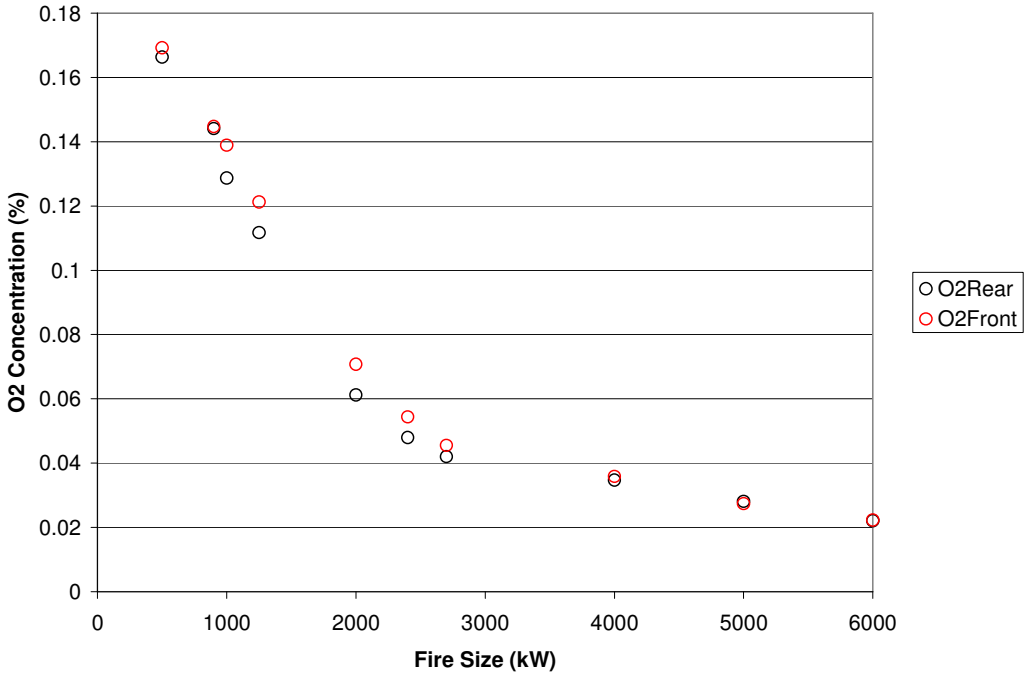

Figure 26: Pre-test Predictions of Oxygen Concentration as a Function of Fire Size in an ISO 9705 Compartment with a Standard Doorway

8.0 User Support

For most of its development history, user support consisted of direct communication by users with the lead author, Kevin McGrattan. This approach was workable when the user base was a small number of people, but with the increasing popularity of FDS it became unworkable.

- Users were unaware of problems being reported by other users resulting in multiple reports of the same problem.
- Users were unaware of feature requests being made by other users.
- Users were unable to learn from the diagnosis of input errors by other users.
- Only one individual was receiving communication from users rather than the entire development team.
- As time passed, reports of problems in emails got lost within the overall email log. Manually maintaining a separate database would have taken effort that would otherwise be focused on addressing the issues .

The solution was to make use of public domain tools available on the internet. In particular the entire development environment was placed on Google Code and a discussion group was started on Google Groups. The creation of these sites was done by Bryan Klein from the NIST BFRL.

8.1 Google Code

Google Code is Google's web based server for open source applications. It provides a number of features of great benefit to both the developers and users. Google Code provides revision control using Subversion (discussed previously in this report), issue tracking using a web based interface, download support, and Wiki pages. FDS and Smokeview were added as projects by Bryan Kelin and the project URL is http://code.google.com/p/fds-smv.

Issue tracking provides an interface via which a user can report a potential bug, report a documentation error, or request an enhancement (see Figure 27). The report includes the version of software used, a description of the problem, and allows for the attachment of supporting files (inputs, outputs, etc). Once reported any member of the development team can view the report and decide on its validity. If the report is valid, it is assigned to a developer. Each time a developer updates the status of a report, the original user automatically receives an email with the update. One particularly useful feature is that reports are classified as either open or closed. An open report is a report that has just been made, is currently being worked on, or is awaiting verification of a fix. A closed report is an issue that has been fixed and verified or an issue that was declared invalid. Open issues are easily viewed through the web browser interface. All open and closed issues can be searched. In this manner, the developers know who is working on what and what remains to be done and the users have a record of what bugs are known (and their status). A summary of the author's contributions to the issue tracker is shown in Appendix B.

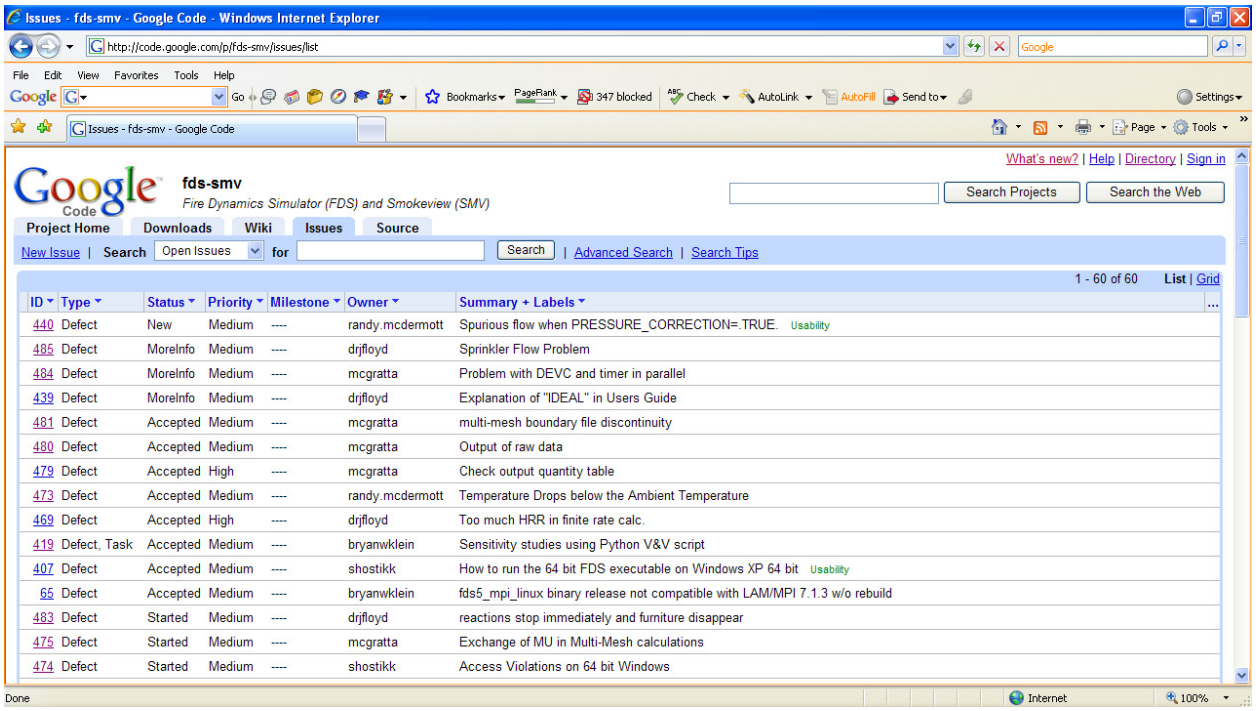

Figure 27: Screenshot of Issue Tracker

Since its inception in May, 2007, there have been 456 issues reported to the tracker. This is an average of almost one issue per day since the tracker inception. Most issues are resolved within a couple of days of being reported to the tracker. Not all issues are bug reports for FDS or Smokeview. Some issues are invalid reports (i.e. user error either in inputs or in not keeping up

to date with releases), and some issues are requests to clarify documentation. This level of reporting; however, was not seen with prior versions of FDS. It is clear that the issue tracker has lowered to barrier to bug reporting to the point where the general user community is willing to take the time to report bugs. Without this reporting, many of these bugs would long go undiscovered.

Download support consists of a web interface listing the current versions of the software (see Figure 278). Each item can be tagged with the type of release (major, minor, maintenance [bug fix]) and the operating system for which it is valid. Older versions of the software can be deprecated, which means they are still available for download (changing the "Current Downloads" in the drop down box), but are not visible by default so users can easily see the latest versions. The Google Code download interface tracks the number of times each file has been downloaded.

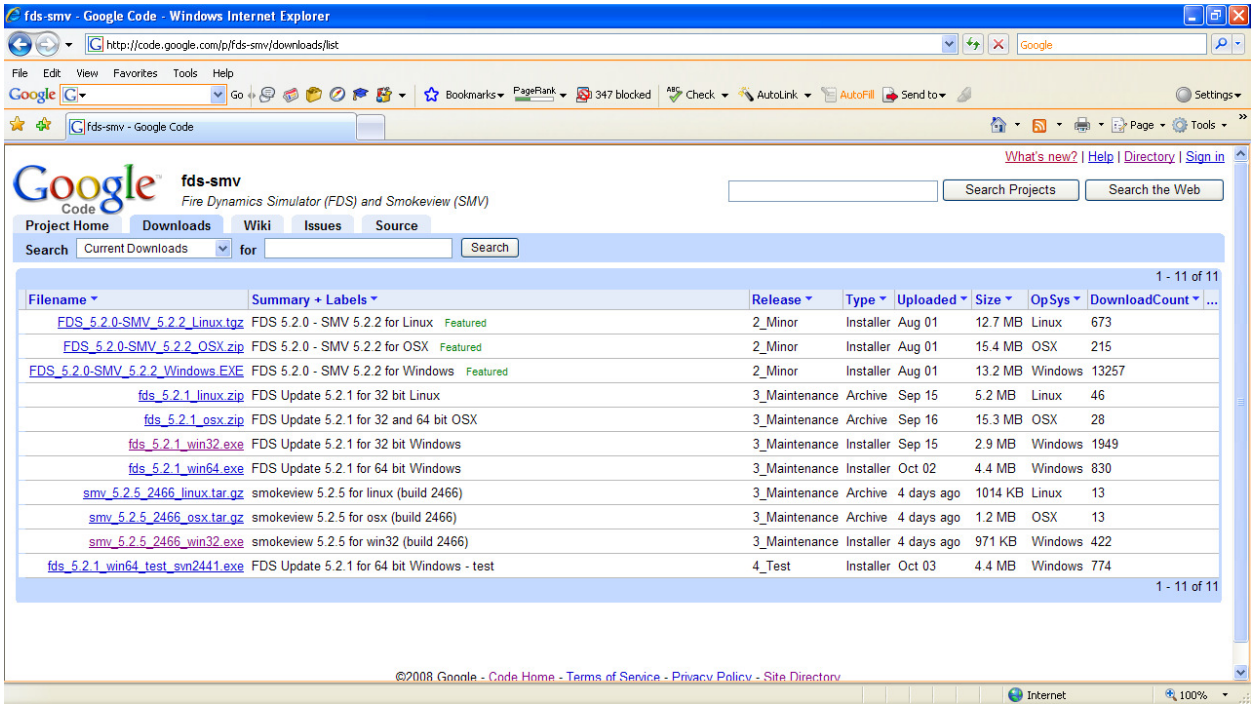

Figure 28: Screenshot of Downloads Page

The Wiki pages allow the developers to create online documentation addressing various aspects of the project such as the FDS Road Map. These pages are all editable by the developers and are under revision control. Additionally the user community can provide comments on any item which can be viewed by both the development team and the overall user community.

8.2 Discussion Forum

An online discussion forum was created by Bryan Klein using Google Groups, http://groups.google.com/group.about. The group is open to anyone to read and search the discussions. To post to the group requires requesting a membership through the web based interface for the group (this is done to prevent spambots from posting non-topical commercial

advertisements). The discussion forum is a place for users and the developers to discuss the use and future development of FDS and Smokeview. With the forum, a user having problems developing an input file can now post a question and potentially get responses from any other user and not just a member of the development team. The benefits are threefold: some user support is now provided by other users reducing the burden on the development team, users with questions will likely get a faster response, and the entire user community can learn from the experience of other users as revealed via the discussions. A summary of the author's participation in the discussion forum is given in Appendix C.

Since the creation of the forum in March, 2007, 4902 posting have been made. Ignoring the first two months of the forum (when its existence was not well publicized), there have been an average of almost 10 postings/day. The forum currently has almost 700 members of which 100 are active posters in the forum. The fact the most members are "lurkers" is quite common in online forums. Success of the forum in terms of meeting its goals are mixed. Some users do answer questions for other users, but not as much as the developmemt team would like. In general, most questions are answered within the next business day of being posted. However, the culture of first searching the forum prior to asking a question has not been fully established in this community. The developers do observe the same questions being asked repeatedly; however, it is not known how many times those questions were not asked as a result of someone searching the forum. In all, the forum is a successful way of providing support to the user community.

9.0 Ouput Compression

The Smokezip capability created by Glenn Forney allows the user to greatly reduce the size of the Smokeview output files by replacing the native 4-btye real numbers with a 1 byte integer from 0 to 255. This greatly reduces the file size, and if appropriate upper and lower limits are chosen, the Smokeview visualization is not impacted. However, this reduction impedes the ability to use those files for engineering analysis. For example if the u-velocity in a calculation ranged from -20 m/s to +20 m/s, this approach would limit one to velocity increments of 0.16 m/s.

An alternative output approach was developed to have a highly reduced file size while still maintaining a level of precision over a large order of magnitude in the output. This approach writes the outputs as a 2-byte real number rather than a 4-byte real number. This is a 50 % savings in file size. 2-byte real numbers are not part of the IEEE standard; therefore, an approach to write them was developed. The format of the two-byte real is shown in the figure below.

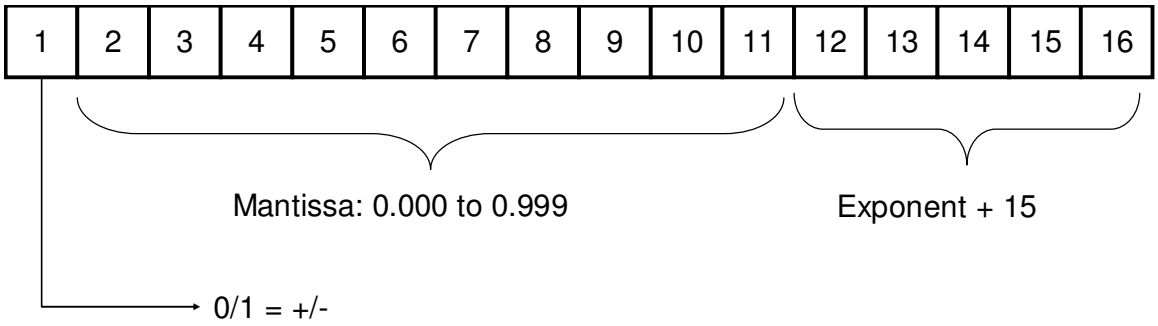

Figure 29: Two-byte Real Numbers

This format allows for real numbers ranging from +/- $1x10^{-15}$ to +/- $9.99x10^{15}$ to be represented with three digits of precision. This level of precision is more than adequate for engineering analysis as it is far less than any of the uncertainties typically associated with fire modeling. As an example the number $-1.02x10^{-5}$ would be encoded as follows:

- bit 1: 1 since the value is negative
- bits 2 to 10: 102 in binary is 0001100110
- bits 11 to 16: -5 + 15 = 10 in binary is 01010

Thus, encoding $-1.02x10^{-5}$ would result in 1000110011001010.

An additional advantage of this approach is that it should be much more compressible than the 4-byte reals using Run Length Encoding (RLE). With 4-byte reals, near ambient conditions will show temperatures with a small amount of noise (20.000001, 20.0000012, etc.). RLE cannot compress those as they are not identical; however, with 2-byte reals those numbers are identical and can be compressed by RLE. By combining RLE with 2-byte real numbers a large reduction in file size should be possible while still maintaining the ability to use the files for engineering analysis.

10.0 References

Beyler, C. (1986), "Major Species Production by Diffusion Flames in a Two-Layer Compartment Fire Environment," Fire Safety Journal, 10:1 (pp 47-56).

Beyler, C. (2002), "Flammability Limits of Premixed Diffusion Flames". In DiNenno, P., ed. Handbook of Fire Protection Engineering, 3rd ed. Quincy, MA: National Fire Protection Association.

Blanchat, T., (2001), "Characterization of the Air Source and the Plume Source at FLAME", SAND2001-2227, Albuquerque, NM: Sandia National Laboratories.

Bryner, N., Johnsson, E., and Pitts, W. (1994), "Carbon Monoxide Production in Compartment Fires – Reduced-Scale Test Facility," NISTIR 5568, National Institute of Standards and Technology, Gaithersburg, MD.

Bundy, M., et al. (2007), "Measurments of Heat and Combustion Products in Reduced-Scale Ventilation-Limited Compartment Fires," National Institute of Standards and Technology Report NIST TN 1483, Gaithersburg, MD.

Desjardin, P. (2005), "Modeling of Conditional Dissipation Rate for Flamelet Models with Application to Large Eddy Simulation of Fire Plumes", *Combustion Science and Technology*, **177** (pp 1883-1916).

Floyd, J., McGrattan, K., Hostikka, S., and Baum, H. (2003), "CFD Fire Simulation Using Mixture Fraction Combustion and Finite Volume Radiative Heat Transfer," *Journal of Fire Protection Engineering,* **13**:1 (pp 11-36).

Floyd, J.E. and McGrattan, K.B. (2007), "Multiple Paramter Mixture Fraction with Two Step Combustion Chemistry for Large Eddy Simulation," Interflam 2007, Royal Holloway College, UK.

Floyd, J.E. and McGrattan, K.B. (2008a), "Extending the mixture fraction concept to address under-ventilated fires," Fire Safety Journal, Elsevier Ltd, accepted July 8.

Floyd, J. and Mcgrattan, K.B. (2008b), "Validation of A CFD Fire Model Using Two Step Combustion Chemistry Using the NIST Reduced-Scale Ventilation-Limited Compartment Data", 9th International Symposium on Fire Safety Science, IAFSS, Karlsruhe, Germany.

Gottuk, D. and Lattimer, B. (2002), "Effect of Combustion Conditions on Species Productions," ". In DiNenno, P., ed. Handbook of Fire Protection Engineering, 3rd ed. Quincy, MA: National Fire Protection Association.

Grosshandler, W. (1993), "RADCAL: A Narrow-Band Model for Radiation Calculations in a Combustion Environment," NIST Technical Note TN-1402, National Institute of Standards and Technology, Gaithersburg, MD.

Linteris, G. and Rafferty, I. (2003), "Scale Model Flames for Determining the Heat Release Rate from Burning Polymers," Fourth International Symposium on Scale Modeling (ISSM-IV).

Mowrer, F. (2002), Private communication.

Murphy, J. and Shaddix, C. (2004)," Soot Properties and Species Measurements in a Two-Meter Diameter JP-8 Pool Fire: 2003 Test Series", SAND2004-8085, Albuquerque, NM: Sandia National Laboratories.

Norton, T., Smyth, K., Miller, J., Smooke, M. (1993), "Comparison of Experimental and Computed Species Concentration and Temperature Profiles in Laminar, Two-Dimensional Methane/Air Diffusion Flames," *Combustion Science and Technology*, **90** (pp 1-34).

O'Hern, T., Weckman, E., Gerhart, A., et al. (2004), "Experimental Study of a Buoyant Helium Plume", SAND2004-0549J, Albuquerque, NM: Sandia National LaboratoriesSmyth, K. (1999), http://fire.nist.gov/fire/flamedata.

Smyth, K. (1996), "NO Production and Destruction in a Methane/Air Diffusion Flame," Combustion Science and Technology, 155 (pp 151-176).

Tieszen, S., O'Hern, T., Schefer, R., Weckman, E., and Blanchat, T. (2002), "Experimental Study of the Flow Field In and Around A One Meter Diameter Methane Fire", *Combustion and Flame*, **129** (pp 378-391).

Westbrook, C. and Dryer, F. (1981), "Simplified Reaction Mechanisms for the Oxidation of Hydrocarbon Fuels in Flames", *Combustion Science and Technology*, **27** (pp 31-43).

Appendix A – Issue Tracker Activity

The author participated in 209 issues during the 2005-2008 grant period. Additional issues were responded to while FDS was being hosted on SourceForge, but the account is no longer active to allow retrieval of data.

Issue #	Status	Assigned To	Description	Issue #	Status	Assigned To	Description
442	Invalid	drjfloyd	why the fire can not burn	174	Verified	gforney	Transparency of 0-thickness cell
439	MoreInfo	drjfloyd	Explanation of "IDEAL" in Users Guide	168	Invalid	----	Solid fuels that burn at a specific rate
437	Fixed	drjfloyd	Flow problem between meshes	165	WontFix	gforney	Sawtooth, Colour, Surf_IDS / Surf_ID6
431	Invalid	mcgratta	new problem with fire and sprinkler	163	WontFix	drjfloyd	y(CO2) ?
427	Fixed	drjfloyd	Problem with function BLACKBODY_FRACTION	162	Verified	bryanwklein	Mesh Boudaries => Incorrect error message
426	WontFix	mcgratta	Very fast decrease of the temperatures of the smoke Performance	161	Fixed	drjfloyd	Optical density Usability
420	WontFix	mcgratta	Ambient temperature - TMPA (default value)	160	Invalid	drjfloyd	pressure not change with same fire in both open and sealed volume
409	WontFix	drjfloyd	getting high HRR and low CO	146	Duplicate	gforney	smv-bndf on Obstructions Usability
408	Fixed	drjfloyd	BOUNDARY_DEFAULT feature does not work for default boundaries defined by FDS	145	WontFix	drjfloyd	no default isosurface in parallel LINUX
403	Invalid	drjfloyd	VEL/VOLUME_FLUX creates velocity errors in domain when pulling air out through a VENT	144	WontFix	drjfloyd	Somkeview sv5p0_win32_0906_2007.exe
401	Duplicate	mcgratta	Velocity / Volume Flux boundary at computational domain not computing correctly Performance	143	WontFix	drjfloyd	SVN link from Google Code shows incorrect link
400	Fixed	bryanwklein	VnV csv file and Excel comma padding Usability	137	WontFix	mcgratta	Temperature after sprinkler operation
392	Verified	drjfloyd	Virtual memory Performance	136	Duplicate	drjfloyd	New problem with CUSTOM control activation.
390	OnHold	drjfloyd	Enhancement: Define Numbers of columns in devc output file	135	Verified	drjfloyd	Problem with a CUSTOM control activating a TIME_DELAY control Usability
380	Fixed	drjfloyd	Error in reaction product formula	134	Verified	drjfloyd	Finite Rate reactions not working
375	Fixed	drjfloyd	Entry misspelled in index	133	Verified	drjfloyd	TRANSPARENCY and ISOF
368	Invalid	drjfloyd	DYNAMIC_PRESSURE parameter	132	OnHold	drjfloyd	TRANSPARENCY Usability
361	Verified	gforney	plot3d 3d isos not working	128	Verified	mcgratta	Access violation error message Usability
360	OnHold	mcgratta	Water vapor pressure Performance	127	Verified	drjfloyd	Wall Temperature in FDS
359	Invalid	drjfloyd	Compile FDS5.1.6 for AIX5.3	126	Verified	gforney	Boundary File Wall Temperature in SMV
357	OnHold	mcgratta	Summarize the input production of additional species, and its balance. Usability	124	Verified	drjfloyd	Water Droplet Action - Delayed Sprinkler Discharge
353	WontFix	mcgratta	particles (air) are penetrating ceiling concrete Performance	123	Verified	drjfloyd	Water Droplet Action
352	Duplicate	drjfloyd	Cp in condensed phase, again	121	Invalid	drjfloyd	Dry pipe system (cont.)
351	Duplicate	drjfloyd	problems with quantity 'other'	120	Verified	drjfloyd	Dry pipe delay
349	WontFix	drjfloyd	Mixture Fraction Effects on Obscuration When Specifying Smoke with Species ID	119	Duplicate	drjfloyd	Edit/clip geometry in SMV
345	Invalid	drjfloyd	Could FDS calculate jet correctly ?	118	Verified	gforney	Edit/clip geometry in SMV
344	Verified	bryanwklein	On screen print Usability	113	Verified	drjfloyd	CTRL and DEADBAND don't deactivate VENTs
343	Verified	bryanwklein	Numerical Instability on FDS 5.1.4 SVN 1593 on OS X Usability	111	Verified	mcgratta	Restart problem and the DEVC/PROP line Performance

Issue #	Status	Assigned To	Description	Issue #	Status	Assigned To	Description
342	Verified	shostikk	Cp in condensed phase	109	WontFix	drjfloyd	Non-Standard Fortran Call
340	Invalid	drjfloyd	DEVC _ measurements temperature	108	Duplicate	drjfloyd	Problem adding sprinkler to couch example file
336	Verified	mcgratta	[SPEC_ID] vs [SPEC_ID]_VF	107	Verified	drjfloyd	FDS Users Guide
335	Fixed	drjfloyd	Output of "OTHER"	106	AltInputs	drjfloyd	Usage of RAMP of a during simulation created object
333	WontFix	drjfloyd	Possible optimization loss in dump.f90	105	Verified	drjfloyd	COLUMN_DUMP_LIMIT non-functional
327	Fixed	drjfloyd	pyrolysis model - combustion fuel gases	104	Invalid	drjfloyd	re open DEVC like WALL TEMPERATURE: non zero vs. zero thickness obstructions
322	WontFix	mcgratta	Transport equation solver	103	Verified	drjfloyd	DEVC like WALL TEMPERATURE: non zero vs. zero thickness obstructions
321	WontFix	mcgratta	Insufficient memory allocation Usability	102	Verified	drjfloyd	FDS5,RC5: MASS_FLUX_TOTAL and MASS_FLUX(0) behave differently
319	Verified	mcgratta	Multi-Mesh: Only OBST information for MESH 1 are written in .out file Usability	100	WontFix	mcgratta	Numerical instability with sprinkler Usability
316	Fixed	drjfloyd	Insufficient memory allocation and bus error Usability	99	Verified	drjfloyd	Problems with the calculation of HRR when using a spray burneer
315	Verified	mcgratta	Droplets disappear with multiple meshes	98	Verified	drjfloyd	coordinate information by WRITE_XYZ
314	WontFix	randy. mcdermott	Debug or Release version compiler directive	96	UnVerified	drjfloyd	forrtl: severe (157): Program Exception - access violation Performance
313	WontFix	mcgratta	Executable files for 64-bit Linux (fds_5.1.4_linux and fds_5.1.4_mpi_linux) Usability	95	Duplicate	----	Restart problem for FDS-5-RC6--SMV-5-RC6-Windows
312	OnHold	mcgratta	FDS5 vs FDS4 Performance Performance	94	Invalid	drjfloyd	Time step issue when dumping into hrr.csv file
311	Fixed	drjfloyd	VENT will not work for time < 0 Performance	93	Verified	gforney	load textures saved in ini causes crash
310	OnHold	mcgratta	Wrong position of subroutine PARTICLE_MASS_ENERGY_ TRANSFER in part.f90 Performance	92	WontFix	gforney	Smokeview Feature Request, Tours
305	WontFix	drjfloyd	Fire moving by itself	91	Duplicate	drjfloyd	Bug with tables and sprays
304	WontFix	mcgratta	Increase of temperature near the nozzle Performance	90	Invalid	----	Black objects in smoke view
294	Verified	mcgratta	Attempt to use pointer HP when it is not associated with a target	89	Verified	mcgratta	Suppression of a fire using the sprinkler system Usability
292	Verified	mcgratta	Doors will not open and close more than once. Performance	88	Invalid	drjfloyd	Numerical instability / NaN
289	WontFix	drjfloyd	Stack Overflow Error After Significant Run Time Performance	87	Verified	mcgratta	Gentle Stop on Multiple Machines Usability
286	WontFix	gforney	Play smv file without loading data	83	Verified	shostikk	fds-smv post 'out file error'?? Usability
282	Verified	drjfloyd	Error: forrtl: severe (174)	82	WontFix	drjfloyd	DEVC
281	Invalid	drjfloyd	Help with Multiple Meshes Alignment	81	Duplicate	drjfloyd	problem with burning rate and temperature after extinction (same issues)
280	Invalid	drjfloyd	Multiple meshes alignment	80	Verified	bryanwklein	Memory Allocation error running RC6
279	WontFix	drjfloyd	Removal of Obstruction using DEVC	79	Verified	mcgratta	Heat Release Rate Usability
276	Fixed	drjfloyd	DEVC XB input read limit set too small	78	Verified	shostikk	problem with burning rate and temperature after extinction
275	WontFix	mcgratta	DEVC-timer (TIME) problem in FDS5_MPI Performance	76	Verified	drjfloyd	RESTART feature
274	WontFix	drjfloyd	pyrolysis cell size glitch?	75	Verified	drjfloyd	Multi-orifice nozzles
273	Invalid	drjfloyd	Compartment still loosing energy	74	Invalid	drjfloyd	Devices to create and remove obstacles and holes

Issue #	Status	Assigned To	Description	Issue #	Status	Assigned To	Description
272	Invalid	drjfloyd	stange results: the air inside an inert compartment cools down	73	WontFix	drjfloyd	Double namelist entry on one line
265	Invalid	drjfloyd	Problem with restart feature.	72	Verified	----	fds5 rc5 core dump on Segfault. FDS compiled with f95 on solaris.
264	Fixed	drjfloyd	Numerical Instability and Sprinkler	71	Verified	drjfloyd	Error in FDS5 RC5 when using controlled nozzles
263	Verified	gforney	Smokeview stops loading/unloading slice files Performance	70	Verified	drjfloyd	Problem with dry pipe sprinkler delay
258	Verified	mcgratta	Pressure Boundary Conditions Usability	69	Verified	drjfloyd	Bucket_Test_2, typo in DEVC line
252	WontFix	drjfloyd	calculated hrr larger than input-value	68	Verified	drjfloyd	Documentation, Extra gas species parameter ABSORBING not discussed.
250	Fixed	drjfloyd	Access Violation Usability	67	Verified	drjfloyd	Documentation (V&V guide)
249	Verified	mcgratta	equivalent fans blowing air in opposite direction	66	Verified	drjfloyd	concern in fire.f90
248	WontFix	drjfloyd	Application of Wind and Pressure Coefficient	64	Verified	bryanwklein	User guide manual malfunctioning
244	WontFix	mcgratta	Protect existing RESTART files during write process. Security	63	WontFix	drjfloyd	Be careful when placing DEVC...
243	Verified	mcgratta	Change AWMPUA to count all OBST and not just the floor	60	Verified	gforney	Modification to Motion/View Dialog Box
242	Invalid	drjfloyd	Problem on simulation of water spray and fuel spray	59	Verified	drjfloyd	No "Fire Resolution Index"?
241	Invalid	drjfloyd	insufficient virtual memory?	58	Verified	mcgratta	Radiant Fluxe Usability
239	Fixed	drjfloyd	'Spread-rate' function dows not wok with VENT control logic	57	Verified	mcgratta	Temperature problem (temperature below ambient)
237	Fixed	drjfloyd	Problem on aspiration detection modelling Performance	55	WontFix	mcgratta	Stop after 1st timestep
236	OnHold	bryanwklein	Segmentation Fault on Intel MacPro Usability	53	OnHold	drjfloyd	Non-physical temperature increases (Divergence equation) Usability
235	Verified	mcgratta	Problems with measuring the mass of soot Performance	51	Verified	gforney	SMV particles QUANTITIES: bug or feature
233	Invalid	drjfloyd	VENT ERROR	50	Invalid	bryanwklein	CO and slice file – still some problems
231	Invalid	drjfloyd	Cannot colour meshes	49	Verified	gforney	moving grid with stopped time will start time
228	Verified	bryanwklein	Source Code of the new version of FDS 5.0.2	48	Verified	mcgratta	Numerical Instability when using droplets
226	Invalid	gforney	Re: We cannot open your program	46	Duplicate	mcgratta	Restart feature Usability
225	Invalid	drjfloyd	We cannot open your program	45	Verified	drjfloyd	User guide corrections
224	Verified	drjfloyd	restarting problem Usability	44	Invalid	drjfloyd	Ability to specify Smagoronsky constant
223	Verified	drjfloyd	Add RELATIVE HUMIDITY output quantity	43	Verified	----	HRR output
222	Invalid	drjfloyd	Comparing HRR using FDS4.07 and FDS5.0.0	42	Verified	bryanwklein	Increase string size for working directory path. Usability
220	Verified	drjfloyd	enhancement, quote device ID strings in CSV output	41	WontFix	drjfloyd	Furnace Simulation
216	Verified	shostikk	(box_burn_away case) Material quickly vanishes without a REFERENCE_TEMPERATURE	36	WontFix	----	Absorption coefficient
214	Verified	drjfloyd	Vent message on startup is misleading	35	Verified	drjfloyd	bug in finite rate combustion model
213	UnVerified	gforney	SMV scrambling text above colorbar again..	33	Verified	drjfloyd	Vent (VEL) close problem
210	Invalid	drjfloyd	RAMP_Q	32	Verified	mcgratta	Humidity problem
208	Verified	randy.mcdermott	Multiple meshes	30	Verified	gforney	Possible to show total HRR somewhere in SmokeView? Usability
207	WontFix	drjfloyd	'MIN' statistic in DEVC incorrectly reporting quantity TEMPERATURE	29	Invalid	drjfloyd	varying FLOW_RATE of a sprinkler

Issue #	Status	Assigned To	Description	Issue #	Status	Assigned To	Description
206	WontFix	drjfloyd	DEVC PROBLEM	28	Verified	drjfloyd	RC4: SLCF quantity carbon monoxide not appropriate for SLCF

Appendix B – Source Commits

The author had 227 commits during the 2005-2008 grant period.

Revision	Date	Summary	Revision	Date	Summary
r21	5/2/2007	Created wiki page through web user interface.	r583	9/12/2007	apply TIME_SHIRNK_FACTOR to DEVC of QUANTITY='TIME'
r22	5/2/2007	Edited wiki page through web user interface.	r584	9/12/2007	add output to .out for TIME_SHRINK_FACTOR and correct output for T_END, also correct TIME_DELAY control function and the various DT_???? on &DUMP for the TIME_SHRINK_FACTOR
r23	5/2/2007	Edited wiki page through web user interface.	r587	9/12/2007	fix nu_o2 (forgot the O_z in the fuel)
r24	5/2/2007	Edited wiki page through web user interface.	r588	9/12/2007	correct eq 3.42 for Z2. Missing soot h fraction multiplier on nu_s
r25	5/2/2007	Edited wiki page through web user interface.	r615	9/18/2007	Add checks to MESH processing to ensure that MIN < MAX for XB inputs
r26	5/2/2007	Edited wiki page through web user interface.	r645	9/19/2007	Fix error in computing HRR for CO reaction when CO_PRODUCTION=.TRUE> Modify EVALUATE_RAMP calls to use actual time for RAMPs that are active from the code start and relative time otherwise. This should allow one to have a HRR curve from a test, but set a T_BEGIN to being part way into the test. Manual updated to caution user when setting T_BEGIN to test time based control functions.
r27	5/2/2007	Edited wiki page through web user interface.	r646	9/19/2007	Fix typo T_BEGIN to T_BEGIN
r28	5/2/2007	Edited wiki page through web user interface.	r651	9/20/2007	Edited wiki page through web user interface.
r29	5/2/2007	Edited wiki page through web user interface.	r655	9/20/2007	Edited wiki page through web user interface.
r31	5/4/2007	Fixed RGB in input tables, removed T_CREATE and REMOVE, fixed _NAME to _ID for CTRL and DEVC, added new parameters to OBST table	r656	9/20/2007	Edited wiki page through web user interface.
r32	5/4/2007	fixed CB = to MB =	r658	9/20/2007	Add update to controls and open/close status prior to run start.
r33	5/4/2007	fixed beam detector select case from 'obscuration' to 'path obscuration'	r662	9/21/2007	attempt to change special chars
r34	5/4/2007	fix initial_state in OBST to FALSE	r663	9/21/2007	Edited wiki page through web user interface.
r35	5/4/2007	Added error trapping when &SURF requires a material but no &MATL lines are specified.	r665	9/21/2007	Errors in how the recursion was being done for controls resulted in order dependent behavior during the recursion.
r36	5/4/2007	Fix error when intializing a DEVC or CTRL used for multiple HOLE's or across multiple MESHes	r667	9/21/2007	Better explanation for CUSTOM CTRL functions (Issue 177)
r38	5/7/2007	limit TANH for RAMP to [0,1]	r695	9/26/2007	Fix undefined var error in ctrl.f90 (Issue 187) Modify evaluate ramp for drop insert (to account for non-zero T_BEGIN) Fix undefined var errors (YY_SUM_W) in fire.f90
r39	5/7/2007	force DV%MESH to be 1 for TIME (so user doesn't have to worry about what gets put for XYZ).	r696	9/26/2007	INTENT in for ITMP in func.f90 Limit max temp to 5000 K in read CLIP
r43	5/8/2007	fix timestep at 0.01 s	r702	9/27/2007	Adjust wall-drop interactions to improve wall heat flux when drop completely evaporates or hits boiling temp
r50	5/9/2007	fix ctrl bug change time in output files to actual time rather than next output interval when meshes are synched	r706	9/28/2007	Change Z to ZZ when refering to mixture fraction to avoid conflicts with Z(K).

Revision	Date	Summary	Revision	Date	Summary
r63	5/14/2007	fix for humidity	r708	9/28/2007	FDS Source: fix uninit vars giving error in debug when running charring_solid.fds
r64	5/14/2007	add humidity to misc table	r710	9/28/2007	FDS Source: Source cleanup. Have routines use PI from CONS rather than expense of recalcing. Also defined SQRTPI which was being computed in a few spots
r78	5/17/2007	.part to .prt5	r711	9/28/2007	FDS Source: Seemed to have missed a Z to ZZ
r79	5/17/2007	fix read_core error due to reading TMP_S for open cells	r712	9/28/2007	FDS Source: Delete unused variables. Attempt to remove gap alignment issues in type.f90
r80	5/18/2007	Fix SURF INVISIBLE Fix instability with particles	r720	10/1/2007	FDS Documentation: alphabatize beta testers
r81	5/18/2007	better error messages for bad SLCF quantities	r721	10/1/2007	FDS Source: SPECIES_BC was being processed for N_SPECIES==0 except if MASS_FLUX(0)=0. Need to not do for N_SPECIES == 0 expect if SPECIFIED_MASS_FLUX and MASS_FLUX(0) /= 0 and then only need to portions of the routine.
r82	5/18/2007	remove debug statement	r736	10/2/2007	FDS Docs: No changes, but resetting my keyword subsitution makes SVN think I modified them.
r88	5/21/2007	FR bug fix	r750	10/3/2007	FDS Source: Add SMOKE_ALBEDO (on &MISC) and SVN_REVISION_NUMBER outputs to .smv file (keywords ALBEDO and REVISION)
r154	5/28/2007	fix finite rate error Trouve found add TABL input add TABL sprinkler spray distribution remove debug statements	r757	10/3/2007	FDS User Guide: Issue 195. Units to SURF table and DT_ISOF in ISOF sectioni
r155	5/29/2007	mods to spray pattern logic and syntax checking. added details to manual	r759	10/4/2007	FDS Source: Issue 27 . Added default RGB values rather than -1 for COLOR='INVISIBLE'. This appears to fix the problem
r156	5/29/2007	test case for spray patterns	r776	10/5/2007	FDS Source: Extend STATISTICS on DEVC to include VOLUME MEAN (volume weighted average) and MASS MEAN (mass weighted average)
r157	5/29/2007	add spray pattern test case	r871	10/24/2007	FDS Source: Issue 27. COLOR='INVISIBLE' now works but still have problems with TRANSPARENCY
r159	5/29/2007	tweaks to spray pattern stuff.	r909	10/29/2007	FDS Source: FDS Documentation: Issue 214, clarify meaning of vent warning message in both code and in User's Guide
r160	5/29/2007	compiler error due to use of variable name for IF block name	r919	10/31/2007	FDS Source: Issue 220. Added quote marks around DEVC and CTRL ids in the csv files to allow the use of commas in a DEVC_ID or CTRL_ID.
r161	5/30/2007	error trapping for duplicate MATL and for non-existing MATL (SURF reference)	r927	11/2/2007	FDS Source: Remove MW_SOOT assignment from READ_MISC and move location in READ_REAC
r170	5/31/2007	Fix DUMP default descriptions and added the new inputs on TIME and fixed SYNCRHONIZE default	r945	11/7/2007	FDS Source: Fix Y_N2 in func for Y_F_INLET < 1
r185	6/6/2007	write CHID to .smv file	r977	11/12/2007	FDS Source: Issue#224 added UII, UIID, OME_E, TAU_E, and the rad counters to the restart file.
r190	6/7/2007	fix (of sorts) to wall evap problem. comment unused SUM?? in main attempt to align types	r980	11/13/2007	FDS Documentation: Add units to MASS_FLUX in U Guide, Fix nu_o2prime for CO_PRODUCTION in guide
r191	6/7/2007	update keywords	r982	11/14/2007	FDS Source: Correct bug in RADCAL CO2 routine for ATOT(3)

Revision	Date	Summary	Revision	Date	Summary
r192	6/7/2007	update keywords	r1003	11/20/2007	FDS Source: Added new routines GET_QUANTITY_INDEX and GET_PROPERTY_INDEX to read.f90 to collect the OUTPUT_QUANTITY and PROPERTY lookups in one place. Also added QUANTITY='RELATIVE HUMIDITY' for Issue 223.
r203	6/12/2007	remove fire resolution index	r1004	11/20/2007	FDS Source FDS Documentation: Issue 161 added QUANTITY='optical depth' where OD = K / 2.3
r205	6/12/2007	notes on array syntax	r1037	11/29/2007	FDS Source: Added logical flag AL2O3. Using this flag changes RHO_SOOT and the soot optical properties to by that of Al2O3 (rocket motor).
r211	6/13/2007	source cleanup	r1074	12/5/2007	FDS Source: Tweaks to AL2O3
r212	6/13/2007	fix deletion of hard return	r1079	12/7/2007	FDS Source: Modify output formatting for VENT overlap error
r215	6/14/2007	remove dead code	r1094	12/12/2007	Edited wiki page through web user interface.
r217	6/15/2007	Fix YYS error in COMBUSTION_MF	r1098	12/13/2007	Edited wiki page through web user interface.
r226	6/20/2007	add some info on obscuration to vis section.	r1099	12/13/2007	Edited wiki page through web user interface.
r227	6/20/2007	fix burner size, issue 67	r1114	12/17/2007	FDS Source: Issue 237. Made fix to time weighted average of aspiration history used in computing the total system response
r232	6/21/2007	remove x-tra comma	r1115	12/17/2007	FDS Source: Forgot to remove a debug statement.
r233	6/21/2007	expand discussion of control functions and devices. Fix and tweak debug and DEVC and CTRL processing.	r1126	12/19/2007	Edited wiki page through web user interface.
r238	6/25/2007	fix to spray pattern error. degree -> radian conversion being done for each device using the pattern rather than once for the property.	r1127	12/20/2007	FDS Source: Issue 239. Fix logic for vents with SPREAD_RATE so they work properly with CTRL or DEVC.
r245	6/25/2007	recommitt changes to spray pattern fix error in dump_core	r1133	12/28/2007	FDS Source: Add checks for isothermal before entering radiation or combustion routine
r249	6/27/2007	fix bug. need to set SOOT_H_FRACTION to zero if H=0	r1151	1/3/2008	FDS Source: Fix state relationship file generation in dump.f90. Fix Y_CO2, Y_O2 in GET_MASS_FRACTION (error was only present if CO_PRODUCTION with CO_YIELD > 0. Only significant it CO_YIELD was large)
r269	7/10/2007	Modiifed wall convective limits for droplets	r1197	1/16/2008	FDS Source: Issue#250. Array misalignment in OMESH%IJKW assignment
r270	7/11/2007	Added tolerance check	r1215	1/21/2008	FDS Source: Issue#161 fixed case select statement in dump.f90
r271	7/11/2007	remove debug	r1233	1/24/2008	FDS Source: Tuning in func.f90. FORALL replacement of nested DO LOOPS
r276	7/12/2007	various array limit/undefined variable fixes	r1254	1/30/2008	FDS Source: MVAP limit based on cell gas mass
r277	7/12/2007	fix misc array, undefined, subrountine call errors	r1268	2/4/2008	FDS Source: Modified removal of droplets when approaching MAXIMUM_DROPLETS to allow insertion of a constant number of droplets each DT_INSERT. When MAXIMUM_DROPLETS is appeared, droplets older than the insertion cycle (MAXIMUM_DROPLEST / TOTAL_INSERTION_RATE) are killed until the number of droplets = MAXIMUM_DROPLETS - number inserted each DT_INSERT
r278	7/12/2007	additional undefined variable fixes	r1280	2/7/2008	FDS Source: Apply TIME_SHRINK_FACTOR to *.q file name generation

Revision	Date	Summary	Revision	Date	Summary
r301	7/17/2007	move TMP_F,_W,_B=TMP_INNER into THERMALLY THICK IF block	r1282	2/7/2008	FDS Source: Remove debug in part.f90
r303	7/18/2007	fix CP_MF in divg.f90 to include other species (i.e. water vapor from drops)	r1283	2/7/2008	FDS Source: Debug removal
r304	7/18/2007	Fixes to setting TMP_INNER, FRONT, BACK in read.f90	r1284	2/7/2008	FDS Documentation: Modify caution on controlling HOLEs to include CTRL
r305	7/18/2007	additional changes for TMP_FRONT and INNER logic	r1291	2/8/2008	FDS Documentation: Note the INERT means wall temp is TMPA.
r306	7/18/2007	TMP_INNER init to TMPA-TMPM	r1301	2/11/2008	FDS Source: Fix bug for MW_SOOT calc when H=0
r312	7/19/2007	Smyth's WP slot burner	r1310	2/13/2008	FDS Source: reorganize end of timestep ouput processing so KILL control function dumps a restart.
r313	7/19/2007	refs for slot burner	r1311	2/13/2008	FDS Source: Fix Issue#276 Change XB error trapping for DEVC from <-1E3 to <=-1E6
r315	7/20/2007	Modify slot burner, add Beyler and First RSE (Bryner/Pitts)	r1312	2/13/2008	FDS Documentation: Clarify windows start instructions
r318	7/23/2007	add PART_COUNTER to DUMP_CORE and READ_CORE	r1317	2/14/2008	FDS Documentation: Add WALL_THICKNESS to output table
r326	7/23/2007	move figures into sub directories	r1323	2/15/2008	FDS Source: Change limit of X0 check for firespread vent. Fix bug in CREATE_OR_REMOVE. Add logic to set TW when creating an OBST.
r337	7/25/2007	fix mass addition of droplets when DT > DT_INSERT	r1325	2/15/2008	FDS Source: FORALL breakup in mass.f90 for cache optimization. Tweaks to EBU for fire.f90. Drop cycle in part.f90 if already at M_VAP_MAX.
r356	7/30/2007	IF statement in WALL_BC prevented entry into species_bc with 0 species and a MASS_FLUX(0) in the input.	r1338	2/19/2008	FDS Source: Issue#282. Added input error check to prevent the input MASSLESS=.TRUE. when particles evaporate
r357	7/30/2007	correct UWS for MASS_FLUX_TOTAL inlet	r1412	3/6/2008	FDS Source: Issue#292, force latch to .FALSE. for CUSTOM CTRL FUNCTION_TYPE
r364	8/1/2007	put back code for COLUMN_DUMP_LIMIT	r1506	3/26/2008	FDS Source: Change velo so that VEL_T gets atmospheric profile (for U and V only). Add new DEVC RADIATIVE_FLUX_GAS (partially completes Issue#58)
r372	8/1/2007	add explicit typing for real number (_EB)	r1508	3/26/2008	FDS Source: Issue#311 Previous fix for RAMPs when T_BEGIN < 0 broke the TAU logic. This has been fixed (hopefully) for anything that uses a TAU.
r373	8/1/2007	fix Y_CORR and MW_MF_CORR calc to avoid Div 0.	r1509	3/26/2008	FDS Documentation: Update U Guide for RADIATIVE_FLUX_GAS
r380	8/2/2007	Fix missing quote Issue 107	r1516	3/27/2008	FDS Documentation: Fix error in nu_CO_2 definition for two-step chemistry
r390	8/3/2007	tweaks to column_dump_limit	r1531	4/3/2008	FDS Source: Add rev number gather for vege.
r400	8/6/2007	Change mesh assignment for timer devices so that xyz need not be in a grid.	r1532	4/3/2008	FDS Source: Add vege revision number check
r422	8/7/2007	add some missing entries for namelists	r1548	4/9/2008	FDS Source: Issue #312. Changes made to GET_MASS_FRACTION and GET_MOLECULAR_WEIGHT routines.
r425	8/8/2007	fix non-standard call text (no longer use flush and don't need getcl for Lahey)	r1549	4/9/2008	FDS Documentation: Issue #327. Added more explantion re:HEAT_OF_COMBUSTION on MATL vs REAC line.
r444	8/10/2007	correct Eq 3.48	r1554	4/10/2008	FDS Source: Fix local Unix LF setting in SmartSVN
r450	8/13/2007	Fix to DEADBAND logic and U Guide example	r1557	4/10/2008	FDS Source: Further speedups by changing GET_parameter routines in func.f90
r451	8/13/2007	remove debug lines	r1570	4/15/2008	FDS Source: Issue#335 reported by Stephen.Olenick. Added missing initialization of RCON_MF(OTHER_INDEX).

Revision	Date	Summary	Revision	Date	Summary
r464	8/21/2007	add ctrl to flush buffers	r1572	4/15/2008	FDS Source: Add CHKMemErr for AINV
r465	8/21/2007	Add new NIST logo to FDS guides	r1576	4/15/2008	FDS Source: Update to generation of Kappa for mixture fraction. Deletion of GET_F,GET_F_C, and the SPECIES state relationship arrays. Clean up of func.f90 from recent overhaul of GET_ functions.
r467	8/21/2007	remove 1line from archive	r1595	4/21/2008	FDS Source: Fixes initialization error reported by fds4hhpberlin. Add initialize statements for Z2Y_C and Z2MW_C.
r468	8/21/2007	remove Tech Admin Under Sec	r1597	4/21/2008	FDS Source: Add KILL_DIAMETER to particle_class_type and set in read.f90 to 1/4 of MINIMUM diameter. Use in remove_droplets instead of fixed rdmin
r471	8/23/2007	fix time delay example	r1598	4/21/2008	FDS Source: missing comma after KILL_DIAMETER in type def
r472	8/23/2007	changes to TIME_DELAY example	r1604	4/23/2008	FDS Source: Unitialized variables
r476	8/24/2007	New method of getting mass fractions, mu, cp, k, and d for mixture fraction. Eliminates table lookup.	r1613	4/28/2008	FDS Documentation: Add other and other mass fraction to QUANTITY table
r478	8/24/2007	New writeup on getting species from mixture fraction	r1643	5/7/2008	FDS Source: Remove IZ2ZZ and replace ZZ2KAPPA with YY2KAPPA. Adjust weighting of IYY in SPECIES%KAPPA to be power law.
r486	8/27/2007	Fix 'MIXTURE_FRACTION2' => 'MIXTURE_FRACTION_2'	r1645	5/7/2008	FDS Source: Minor formatting in radi.f90
r487	8/27/2007	missing TMP_THR in material type	r1740	6/2/2008	FDS Source: Modify fuel and o2 lookup at boundaries to use mass_flux or mass_fraction, if specified, rather than YY_W
r492	8/28/2007	tech guide updates (in progress) func.f90 mods for get mass fraction.	r1753	6/4/2008	FDS Source: modify O2 depletion accounting in first reaction step of fire.f90 combustion_mf
r493	8/28/2007	fix Y_N2	r1765	6/9/2008	FDS Documentation: Correct sprinkler spelling error in index (Issue #370 reported by emanuele.gissi)
r494	8/28/2007	continued updates to combustion section	r1777	6/11/2008	FDS Documentation: H_2 product term missing from equation on p69 (&REAC)
r495	8/28/2007	corrections to CO production relations	r1790	6/12/2008	FDS Source: Fix array pointer.
r496	8/28/2007	fixes to combustion to account for CO_YIELD and to GET_MASS_FRACTION for Y_CO	r1858	6/20/2008	FDS Source: Changes in Q_UPPER in fire.f90 and move Q_AVG calc. Add limit to leakage calc in divg.f90
r497	8/28/2007	Fix so transparency works without having to specify a color or RGB	r1913	6/27/2008	FDS Source: Partially addresses Issue #390, Added DEVC_COLUMN_LIMIT and CTRL_COLUMN_LIMIT to allow user to set the number of columns in the respective output files
r500	8/29/2007	add nu_M & b to combustion section	r1914	6/27/2008	FDS Documentation: Add DEVC_COLUMN_LIMIT and CTRL_COLUMN_LIMIT to U Guide
r501	8/29/2007	explain M better	r1924	6/30/2008	FDS V&V: Add Smyth_Slot_Burner files to Validation directory
r502	8/29/2007	fix broken FINITE_RATE	r1991	7/9/2008	FDS Documentation: Update validation config w/Smyth burner
r511	8/30/2007	CTRL fix for CUSTOM continued changes with new GET_MF functions	r1992	7/9/2008	FDS Documentation: Smyth slot burner plots and Validation script
r513	8/30/2007	unbreak smv fix	r2027	7/15/2008	FDS Documentation: Updates to validation guide sections on Beyler hood and Pitts RSE
r514	8/30/2007	fix CF%T_CHANGE logic	r2061	7/23/2008	FDS Source: Fix Z2_MIN_CALC in fire.f90.
r521	8/31/2007	change Z_4 to Y_EXTRA	r2073	7/29/2008	FDS Documentation: Pagination changes
r547	9/7/2007	Increase .smv real number precision. RGB values to #.## can't resolve 1/255 which is 0.004	r2075	7/29/2008	FDS Documentation: Formatting to User's Guide.

Revision	Date	Summary	Revision	Date	Summary
r548	9/7/2007	Add check for <=0 mass flux in spray pattern table	r2079	7/30/2008	FDS Source: Create SET_OFTEN_USED in PREC to handle PI constants. Not all compilers accept the use of ATAN in a PARAMETER statement.
r554	9/10/2007	fix ABSORBING when a mixture fraction species is on the SPEC line and a REAC has been specified	r2081	7/30/2008	FDS Source: Add FOTH back to prec.f90
r564	9/11/2007	Test of SVN keyword expansion for Date and Revision.	r2083	7/30/2008	FDS Source: Fix to prec.f90 add ONSI
r565	9/11/2007	2nd Test of Keyword expansion	r2098	7/31/2008	FDS Source: Fix for Issue#427 reported by ianrosswilliams
r566	9/11/2007	Add Revision and Date keywords to source files Add subroutine to first module in all source to return revision and date Add subroutine to main to find newest rev and use that rev and date to set version info.	r2154	8/11/2008	Smokeview: Modify smoke_test.fds for initial density of 1 kg/m^3
r567	9/11/2007	Add and tested code to extract newest subversion revision number from the source.	r2162	8/12/2008	FDS Source: Minor changes to evaluation of BBFRAC
r582	9/12/2007	RAMP for a CUSTOM &CTRL had been given the type of TIME which means that TIME_SHRINK_FACTOR is applied. Changed type to CONTROL			
r21	5/2/2007	Created wiki page through web user interface.	r583	9/12/2007	apply TIME_SHIRNK_FACTOR to DEVC of QUANTITY='TIME'
r22	5/2/2007	Edited wiki page through web user interface.	r584	9/12/2007	add output to .out for TIME_SHRINK_FACTOR and correct output for T_END, also correct TIME_DELAY control function and the various DT_???? on &DUMP for the TIME_SHRINK_FACTOR
r23	5/2/2007	Edited wiki page through web user interface.	r587	9/12/2007	fix nu_o2 (forgot the O_z in the fuel)
r24	5/2/2007	Edited wiki page through web user interface.	r588	9/12/2007	correct eq 3.42 for Z2. Missing soot h fraction multiplier on nu_s
r25	5/2/2007	Edited wiki page through web user interface.	r615	9/18/2007	Add checks to MESH processing to ensure that MIN < MAX for XB inputs
r26	5/2/2007	Edited wiki page through web user interface.	r645	9/19/2007	Fix error in computing HRR for CO reaction when CO_PRODUCTION=.TRUE> Modify EVALUATE_RAMP calls to use actual time for RAMPs that are active from the code start and relative time otherwise. This should allow one to have a HRR curve from a test, but set a T_BEGIN to being part way into the test. Manual updated to caution user when setting T_BEGIN to test time based control functions.
r27	5/2/2007	Edited wiki page through web user interface.	r646	9/19/2007	Fix typo T_BEGIN to T_BEGIN
r28	5/2/2007	Edited wiki page through web user interface.	r651	9/20/2007	Edited wiki page through web user interface.
r29	5/2/2007	Edited wiki page through web user interface.	r655	9/20/2007	Edited wiki page through web user interface.

Appendix C – Source Commits

The author had 485 posts to the FDS Discussion Forum during the 2005-2008 grant period.

Month	2007	2008
January	a	39
February	a	43
March	a	18
April	a	48
May	46	30
June	27	21
July	23	24
August	28	21
September	17	b
October	43	b
November	23	b
December	34	b
Total	241	244

[a]Google group started in May 2007
[b]Month not covered by reporting period

Appendix D – Interflam 2007 Paper

MULTIPLE PARAMETER MIXTURE FRACTION WITH TWO-STEP COMBUSTION CHEMISTRY FOR LARGE EDDY SIMULATION

Jason E. Floyd[1] & Kevin B. McGrattan[2]
[1]Hughes Associates, Inc. USA
[2]Building and Fire Research Laboratory, National Institute of Standards and Technology, USA

INTRODUCTION

A common approach for treating combustion in practical fire models is to use the mixture fraction, a conserved scalar to which all gas species can be related. Typically, infinitely fast chemistry is assumed, in which case the technique works well for fires scenarios in which there is an adequate supply of oxygen. A somewhat more complex approach is to create flamelet libraries that map temperature and mixture fraction to species mass fractions. This has been shown to work well in small scale simulations and is widely used in the combustion community. However, for simulations of fires in large structures, the inability to resolve flame temperatures and scalar dissipation rates, regardless of the turbulence model used, make detailed flamelet models impractical. Therefore, we seek a methodology that allows us to describe incomplete combustion and flame extinction at large scale while staying within the basic framework of the mixture fraction.

In the proposed new framework, the mixture fraction retains its classic definition as the mass fraction of gas that originates as fuel. However, with a single value of the mixture fraction it is not possible to account for products of incomplete combustion, or even the mixing of unburned fuel and oxygen. Instead, we need to decompose the mixture fraction into constitutive parts that represent the products of the different reactions. The number of components depends on the complexity of the phenomena. For example, to account for local flame extinction and also the production/destruction of CO, we need to decompose the mixture fraction into three components. This paper will document the new mixture fraction approach and test it against three sets of experimental data of varying scale: a slot burner, a hood experiment, and a compartment fire experiment. All three sets of experiments involve relatively clean burning fuels because the emphasis is on CO, not soot, production.

MATHATICAL FORMULATION

The combustion model in the Fire Dynamics Simulator (FDS), version 4,[1,2] uses only a single mixture fraction variable[3], defined in terms of the mass fractions, Y, molecular weights, W, and stoichiometric coefficients, ν, of the fuel and oxygen:

$$Z = \frac{sY_{\mathrm{F}} - \left(Y_{\mathrm{O}_2} - Y_{\mathrm{O}_2}^{\infty}\right)}{sY_{\mathrm{F}}^{I} - Y_{\mathrm{O}_2}^{\infty}} \quad ; \quad s = \frac{\nu_{\mathrm{O}_2} W_{\mathrm{O}_2}}{\nu_{\mathrm{F}} W_{\mathrm{F}}} \qquad [1]$$

The superscripts, I and ∞, denote the fuel inlet and background values, respectively. Assuming infinitely fast chemistry, all gas species can be related to Z via a set of *state relations*. However, suppose we do not want to assume an infinitely fast, temperature-independent reaction of fuel and oxygen. How can the products of the complete and incomplete reactions be tied to the single variable, Z? They cannot – there are now additional degrees of freedom in the state relations.

Decomposing the Mixture Fraction

To overcome the limitations of the current single variable mixture fraction model, additional information is required to account for CO formation and extinction. To minimize the complexity of a new combustion model and to ensure its applicability to simulations with relatively coarse numerical grids, the simplest possible two-step CO formation mechanism is assumed[4]:

$$\text{Step 1: } \mathrm{F} + \mathrm{O}_2 \rightarrow \mathrm{CO} + \text{Other Products (i.e. } \mathrm{H}_2\mathrm{O} \text{ and Soot)} \qquad [2]$$

$$\text{Step 2: } \mathrm{CO} + \frac{1}{2}\mathrm{O}_2 \rightarrow \mathrm{CO}_2 \qquad [3]$$

Implicit in this formulation is the possibility that Step 1 does not occur at all; that is, fuel and oxygen can mix but not burn. This so-called "null" reaction, which could be considered Step 0, along with the two steps listed above, demands the inclusion in the model of three variables – one to account for the total amount of unburned fuel present (Step 0), one to account for the CO produced (Step 1), and one to account for the CO that has oxidized to form CO_2 (Step 2). Derivation of these variables starts with the transport equations, shown below, for fuel, CO, and CO_2. The subscripts 1 and 2 refer to the two steps shown above.

$$\frac{\mathrm{D}Y_{\mathrm{F}}}{\mathrm{D}t} = \nabla \cdot D\rho\nabla Y_{\mathrm{F}} + \dot{m}'''_{\mathrm{F},1}, \qquad [4]$$

$$\frac{\mathrm{D}Y_{\mathrm{CO}}}{\mathrm{D}t} = \nabla \cdot D\rho\nabla Y_{\mathrm{CO}} + \dot{m}'''_{\mathrm{CO},1} + \dot{m}'''_{\mathrm{CO},2} \qquad [5]$$

$$\frac{\mathrm{D}Y_{\mathrm{CO}_2}}{\mathrm{D}t} = \nabla \cdot D\rho\nabla Y_{\mathrm{CO}_2} + \dot{m}'''_{\mathrm{CO}_2,2}. \qquad [6]$$

The production and destruction rates of the species for Steps 1 and 2 are related via:

$$\frac{\dot{m}'''_{\mathrm{F},1}}{W_{\mathrm{F}}} = -\frac{\dot{m}'''_{\mathrm{CO},1}}{xW_{\mathrm{CO}}} \quad ; \quad \frac{\dot{m}'''_{\mathrm{CO},2}}{W_{\mathrm{CO}}} = -\frac{\dot{m}'''_{\mathrm{CO}_2,2}}{W_{\mathrm{CO}_2}} \qquad [7]$$

where x is the moles of CO formed per mole of fuel burned. Now define Z_1, Z_2, and Z_3:

$$Z_1 = Y_{\mathrm{F}}; \quad Z_2 = \frac{W_{\mathrm{F}}}{W_{\mathrm{CO}}x}Y_{\mathrm{CO}}; \quad Z_3 = \frac{W_{\mathrm{F}}}{xW_{\mathrm{CO}_2}}Y_{\mathrm{CO}_2}. \qquad [8]$$

Substituting Equations 7 and 8 into Equations 4 through 6, we obtain:

$$\frac{\mathrm{D}Z_1}{\mathrm{D}t} = \nabla \cdot D\rho\nabla Z_1 - \frac{W_{\mathrm{F}}\dot{m}'''_{\mathrm{CO},1}}{xW_{\mathrm{CO}}} \qquad [9]$$

$$\frac{\mathrm{D}Z_2}{\mathrm{D}t} = \nabla \cdot D\rho\nabla Z_2 + \frac{W_{\mathrm{F}}}{xW_{\mathrm{CO}}}\dot{m}'''_{\mathrm{CO},1} + \frac{W_{\mathrm{F}}}{xW_{\mathrm{CO}}}\dot{m}'''_{\mathrm{CO},2}. \qquad [10]$$

$$\frac{\mathrm{D}Z_3}{\mathrm{D}t} = \nabla \cdot D\rho\nabla Z_3 - \frac{W_{\mathrm{F}}}{xW_{\mathrm{CO}}}\dot{m}'''_{\mathrm{CO},2}. \qquad [11]$$

Note that the source terms for the three equations cancel by design. Thus, the sum of the three components is the mixture fraction:

$$Z_1 + Z_2 + Z_3 = Y_{\mathrm{F}} + \frac{W_{\mathrm{F}}}{xW_{\mathrm{CO}}} Y_{\mathrm{CO}} + \frac{W_{\mathrm{F}}}{xW_{\mathrm{CO}_2}} Y_{\mathrm{CO}_2} = Z \qquad [12]$$

If we assume that water vapor and soot have yields that are fixed functions of CO and CO_2, then the three quantities Z_1, Z_2, and Z_3 can be used to determine the individual mass fractions of N_2, O_2, CO, CO_2, H_2O, soot, and unburned fuel. This is the precisely why the mixture fraction framework is used to track species; it reduces the number of transport equations that must be solved (in this case from 7 to 3). The process via which species are extracted from the mixture fraction parameters is discussed in the next section.

State Relations

The correspondence between the mixture fraction variables and the primitive species is known as the state relations. If a single mixture fraction variable is used in a calculation, it is easy, via a "look-up" table, to link individual gas mass fractions to the mixture fraction. However, for the above decomposition of the mixture fraction into three components, the state relations now become a function of three rather than one variable, and the computational "cost" of obtaining mass fractions during a calculation becomes significant. To reduce the computational expense, we construct a linear combination of state relations from the following three reaction pathways:

Pathway 1: $\mathrm{F} + \mathrm{O}_2 \rightarrow \mathrm{F} + \mathrm{O}_2$ (extinction / null reaction) [13]

Pathway 2: $\mathrm{F} + \mathrm{O}_2 \rightarrow \mathrm{CO} + \text{Other Products}$ (CO formation / incomplete reaction) [14]

Pathway 3: $\mathrm{F} + \mathrm{O}_2 \rightarrow \mathrm{CO}_2 + \text{Other Products}$ (CO destruction / complete reaction) [15]

Pathway 1 is the so-called "null" or "Step 0" reaction. Pathway 2 is the same as Step 1 of the two-step reaction (Eq. 2). Pathway 3 is just Step 1 + Step 2 (Eq. 2 + Eq. 3). In some sense, every molecule that makes up the combustion products originated by way of one of the three pathways. For each pathway we can define a set of state relations. This is shown for methane in Figure 1. Note that for clarity water vapor and nitrogen are omitted and Z is limited to 0.5.

Figure 1 Methane state relations for the three reaction pathways (N_2 and H_2O omitted)

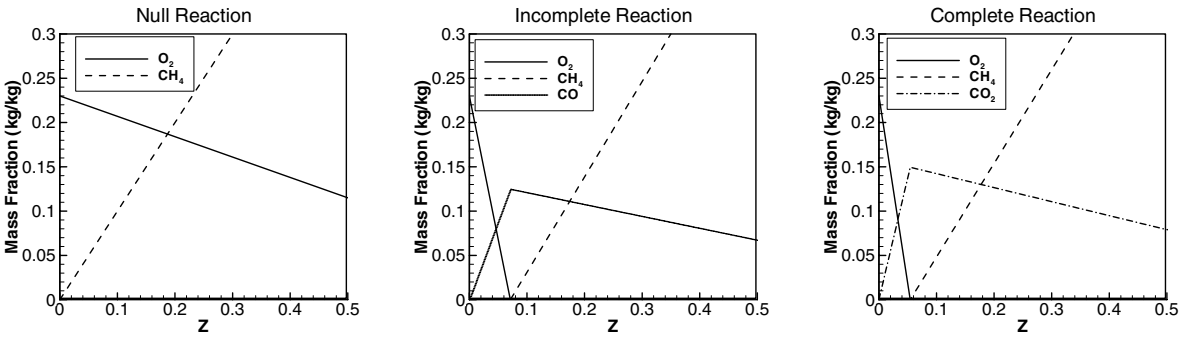

Since the state relations are piecewise-linear functions and since the above chemical reactions are linear expressions, it is postulated that the mass fractions of species can be given by linear combinations of the state relations. That is, the mass fraction of species i, Y_i, is given by:

$$Y_i(Z_1,Z_2,Z_3) = (1-c_{\mathrm{F}})\ Y_{i,1}(Z) + \ c_{\mathrm{F}}\left[(1-c_{\mathrm{CO}})\,Y_{i,2}(Z) + c_{\mathrm{CO}}\ Y_{i,3}(Z)\right], \qquad [16]$$

where c_{F} is a progress variable indicating the fraction of fuel that has not burned due to local flame extinction, c_{CO} is a progress variable indicating the fraction of CO that has been converted to CO_2, and the integer subscripts indicate the reaction pathway defined above. c_{CO} is given by:

$$c_{\mathrm{CO}} = \frac{1}{c_{\mathrm{F}}}\frac{Z_3}{Z_{3,\max}(Z)} \qquad [17]$$

where $Z_{3,max}$ is the maximum possible value of Z_3 (achieved when all the CO is oxidized). The progress variable related to fuel consumption is somewhat more complicated:

$$c_{\mathrm{F}} = \frac{Z - Z_1}{Z - Y_{\mathrm{F}}(Z)} \qquad [18]$$

$$Y_{\mathrm{F}}(Z) = \begin{cases} 0, & Z \le Z_f \\ \dfrac{Z - Z_f}{1 - Z_f}, & Z > Z_f \end{cases} \qquad [19]$$

$$Z_f = \left(1 + \frac{W_{\mathrm{O}_2}}{W_{\mathrm{F}}}\left(\frac{1}{Y_{\mathrm{O}_2}^{\infty}}\right)\left((1-c)\nu_{\mathrm{O}_2,2} + c\,\nu_{\mathrm{O}_2,3}\right)\right)^{-1} \qquad [20]$$

where c is a slightly different form of c_{co} needed to obtain the proper value of Z_f:

$$c = \frac{Z_3}{Z_2 + Z_3}. \qquad [21]$$

Figure 2 Methane State Relations for Pathway 2, Pathway 3, and $c = 0.5$ & $c_{\mathrm{F}} = 0$

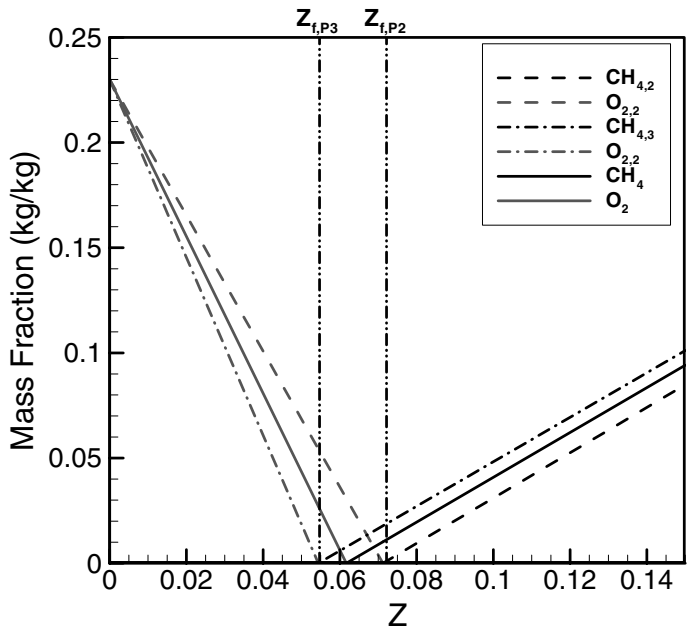

One additional step is required to obtain the mass fractions. Figure 2 shows the state relations for fuel and oxygen for Pathways 2 and 3 (dashed lines) along with a combination corresponding to $c = 0.5$ and $c_F = 0$ (solid lines). Note that above and below the stoichiometric values for Pathways 2 and 3 (vertical dashed lines), fuel and oxygen mass fractions are indeed simply linear combinations of their values from Pathways 2 and 3. However, in between the two stoichiometric values, simply taking a linear combination of the individual mass fractions would result in some oxygen surviving from Pathway 3 and some fuel surviving from Pathway 2. Since c_F is zero in this example (no extinction), fuel and oxygen cannot coexist. Therefore, in between the two stoichiometric values a correction is needed to account for the consumption of residual fuel and oxygen. This correction, $Y_{corr,i}$, is given by:

$$Y_{corr,i} = \begin{cases} c_{CO}\ s \dfrac{\nu_i W_i}{\nu_F W_F} Y_{F,3} & Z \le Z_f \\ \left(1 - c_{CO}\right) s \dfrac{\nu_i W_i}{\nu_{O_2} W_{O_2}} Y_{O_2,2} & Z > Z_f \end{cases}, \qquad [22]$$

where s is -1 for reactants and +1 for products.

While the state relations appear complicated, it is important to remember that they simply serve to translate the mixture fraction variables back into species mass fractions. This is not the "combustion model," but rather an accounting procedure that allows us to solve half as many transport equations as we would otherwise have to do. While there is computational cost in translating the mixture fraction variables to species mass fractions, the cost is far less than that of solving the full set of transport equations. The combustion model is described next.

Combustion Model

The new combustion model implemented in FDS version 5 includes the two reaction steps described in Eqs. 2 and 3, along with the possibility of local extinction (Pathway 1). Transport equations are solved for the three components of the mixture fraction. At each time step of the calculation, the procedure described above is used to extract the individual species mass fractions from the mixture fraction variables. Then, an empirical criterion is used to decide whether or not Step 1, oxidation of fuel to CO and other products, can occur. If the temperature and oxygen mass fraction of a given cell and that of its neighbors are too low to support combustion (the black region of Figure 3), then Step 1 cannot occur. The neighboring cells represent either the fuel or oxidizer stream of classical diffusion flame theory. The local flammability criterion is based on the critical adiabatic flame temperature, as described by Beyler[5], and a simplified thermodynamic analysis by Mowrer[6]. The criterion determines if the energy released by consuming the maximum possible amount of oxygen can raise the local temperature above the critical flame temperature. If so, then Step 1 is allowed. Because large scale fire simulations usually have grid cell sizes far greater than the flame width, it is not appropriate to use a detailed kinetics model as the flame temperature and local strain rate are not available.

If the local environment is assumed to support combustion, Step 1 just depletes either fuel or oxygen, releasing the corresponding amount of energy into the grid cell, up to an empirically-based maximum value. This maximum value is based on two assumptions. First, that a flame sheet can generate no more than 200 kW/m^2 of energy[7]; second, that the numerical grid is resolved enough such that any grid cell is cut by only one flame sheet.

Figure 3 Flammability Criteria

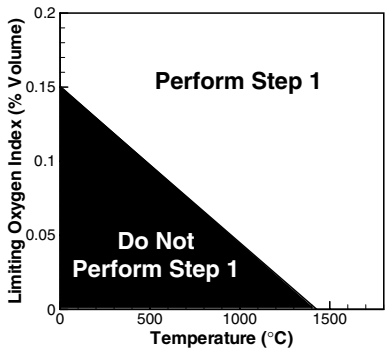

The limitation of this simple extinction model is that it is based on the conditions of the oxidizer stream, not the fuel stream. In other words, for any particular grid cell, an adequate oxygen supply in any of its neighboring cells automatically triggers Step 1 of the reaction to occur. In reality, low temperatures and/or low concentrations of fuel may still lead to flame extinction, but the model does not account for this. As will be discussed in the results section below, this means that the model may over-predict the burning rate and thus over-predict exhaust product concentrations in scenarios where fuel rich gases meet ambient air along an interface.

Step 2 of the reaction, the oxidation of CO, is determined by one of two methods depending on the outcome of Step 1. The first method presumes that if Step 1 results in any heat production in a given grid cell, then a flame (and flame temperatures) are present and the conversion of CO is "fast." For this case the maximum possible CO conversion is assumed, again limited by the upper bound on the local volumetric heat release rate. If no heat is produced in Step 1, it is presumed that a flame is not present and, therefore, the existing temperature is an accurate representation of the conditions in the cell. A finite rate computation[4] is then performed to determine the rate of CO oxidation. Oxidation of CO means that Z_2 becomes Z_3 using the source terms in Eq. 10 and Eq. 11.

A side benefit of the new combustion model is that it no longer requires the computation of the gradient of the mixture fraction normal to the flame sheet to determine the heat release rate. Past versions of FDS were susceptible to inaccuracies in the heat release rate because of this computation. Even though the transport algorithm is mass conserving globally, local numerical defects (known as "overshoots" and "undershoots") exist. These defects coincide with steep gradients and they led to unrealistically high and low local heat release rates. Attempting to correct both the numerical defects and the heat release rate often resulted in errors in the global heat release. The new mixture fraction formulation does not require the calculation of gradients, resulting in more accurate values of the local heat release rate and more flexibility in using "flux-correction" schemes to reduce the numerical defects in the transport algorithm.

VALIDATION

The new combustion model discussed above was implemented in FDS and tested against three sets of experimental measurements: a methane-air Wolfhard-Parker slot burner[8,9,10], selected Beyler hood experiments[11], and selected tests from the NIST reduced scale enclosure (RSE)[12].

Laminar Diffusion Flame from a Slot Burner

The Wolfhard-Parker slot burner consists of an 8 mm wide central slot flowing fuel surrounded by two 16 mm wide slots flowing dry air with 1 mm separations between the slots. The slots are 41 mm in length. The experimental errors have been reported as 5 % for temperature and 10 % to 20 % for the major species[9]. A 3D direct numerical simulation of one quarter of the burner with two symmetry planes was performed for the slot burner with a 0.5 mm grid resolution, 390,000 total grid cells. While the Wolfhard-

Parker burner is often discussed as a 2D flame, there are 3D effects that come into play when modeling the flame. In 2D, all computed quantities including radiation transport are mirrored at the symmetry boundary. Modeling the burner in 2D resulted in poorer predictions of temperature as radiant energy could not escape normal to the burner's axis. The post-flame CO was set to zero and the soot yield was also set to zero. The simulation was run for 4 s which took 104 hours on a single 2.4 GHz processor. While this seems a long time, it is noted that 0.5 mm grid resolution requires timesteps of 0.06 ms.

Figure 4 shows predicted and measured temperatures at three elevations above the burner. The model predicts a flame that is slightly narrower (5.5 mm vs. 6.5 mm or a 15 % error) and cooler (1700 °C vs. 1800 °C or a 5 % error) than measured. The model also predicts higher centerline temperatures. These results are not surprising. The new combustion model considers the first step, fuel to CO, to be infinitely fast, assuming that the local oxygen concentration satisfies the criteria of Figure 3. This is true in the vicinity of the lip of the burner. In reality, the cold fuel and air streams do not react infinitely fast there and some oxygen penetrates the flame at the base, resulting in cooler gases being entrained into the core of the flame with a resulting drop in the centerline temperature.

Figure 4. Predicted and measured temperature at three elevations (7 mm, 9mm and 11 mm) above a methane-air slot burner

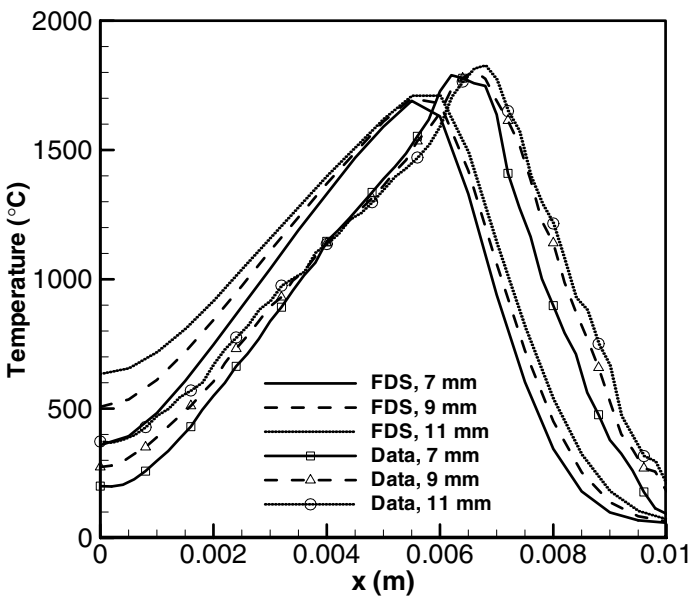

Figure 5 shows predicted and measured values of $CH_4 + O_2$, CO, CO_2 at three elevations above the burner along with a contour plot of CO near the burner lip (black rectangle is burner). Note that a small quantity of oxygen exists along the burner center per the observation made above. Along the centerline, the model predicts lower values of fuel and higher values of products than measured. The species profiles are also slightly narrower than measured, echoing the temperature plot in Figure 4. Again, this is likely due to the higher amounts of combustion at the burner lip resulting from the infinitely fast first step. The peak CH_4 values along the burner centerline have errors ranging from 6 % to 13 %, the peak CO_2 values in the flame have errors ranging from 3 % to 10 %, and the peak CO values in the flame have errors ranging from 9 % to 25 %. Given the reported 10 % to 20 % species measurement uncertainty, the new combustion model predicts well both the magnitude and shape of the mixture fraction profiles

The contour of CO illustrates the combustion model quite well. At the burner lip, fuel and oxygen first meet. Since ambient levels of oxygen exist on the air side of the slot and the temperatures are relatively low at the burner lip, combustion occurs and converts Z_1 to Z_2. This consumes the oxygen present and the CO does not have an opportunity to fully convert to CO_2. As the CO rises in the flame, oxygen is

entrained and the temperatures are high enough that the CO reacts with the entrained oxygen to form CO_2. Eventually, at a point high enough in the flame, all of the fuel is consumed and all of the CO is oxidized.

Figure 5. Predicted and measured mole fractions at three elevations (7 mm, 9mm and 11 mm) above a methane-air slot burner, along with contours of CO near the burner lip

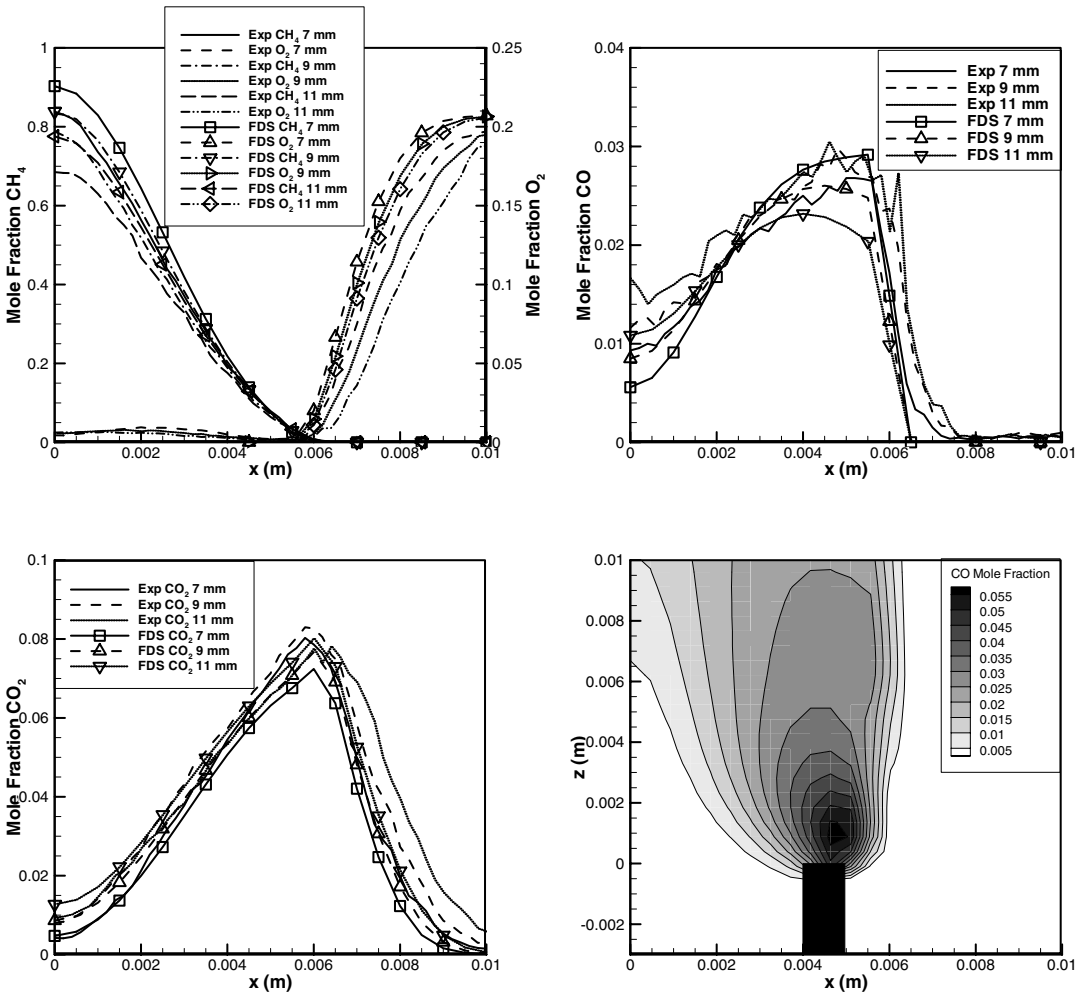

Beyler Hood Experiments

Beyler performed a large number of experiments involving a variety of fuels, fire sizes, burner diameters, and burner distances beneath a hood[11]. The hood consisted of concentric cylinders separated by a gap. The inner cylinder was shorter than the outer and this allowed combustion products to be removed uniformly from the hood perimeter. The exhaust gases were then analyzed to determine species concentrations. The burner could be raised and lowered with respect to the bottom edge of the hood. Based on the published measurement uncertainties, species errors are estimated at 6 %.

Simulations using the two step finite rate combustion model were performed for a number of the propane tests using a 19 cm burner. The cylindrical hood was transformed in the model into an equivalent area square box while preserving the height. A 1.4 cm grid was used with a total of 729,000 grid cells. As with the slot burner simulations, the first step was considered always infinitely fast and the second step was temperature dependent. It took 50 hrs to complete a 300 s simulation on a single 2.4 Gz processor.

Figure 6 shows species predictions made by the two step model compared with measured data for a range of fire sizes and burner positions. The dotted lines indicate the estimated measurement uncertainty. The model predicts the time-averaged species concentration at the hood exhaust vent. CO_2 predictions are

within the measurement uncertainty for all but one of the simulations performed. For the well-ventilated fires (-10 cm), CO, CO_2, and unburned fuel predictions match the data. As the fires become under-ventilated, CO is over-predicted while fuel and O_2 are under-predicted. The most likely explanation for the discrepancy is that the model assumes fuel and oxygen react infinitely fast in the vicinity of near ambient conditions. This occurs at the lower edge of the hood were the vitiated layer is adjacent to the ambient air below the hood, and as a result layer burning is occurring in the model which depletes the fuel and O_2 and creates CO. This is not unexpected, and indicates that more work is required to establish the conditions under which combustion in the first step, conversion of fuel to CO, will be allowed.

Figure 6. Comparison of measured and predicted species concentrations in the Beyler hood experiments, dotted lines show experimental uncertainty

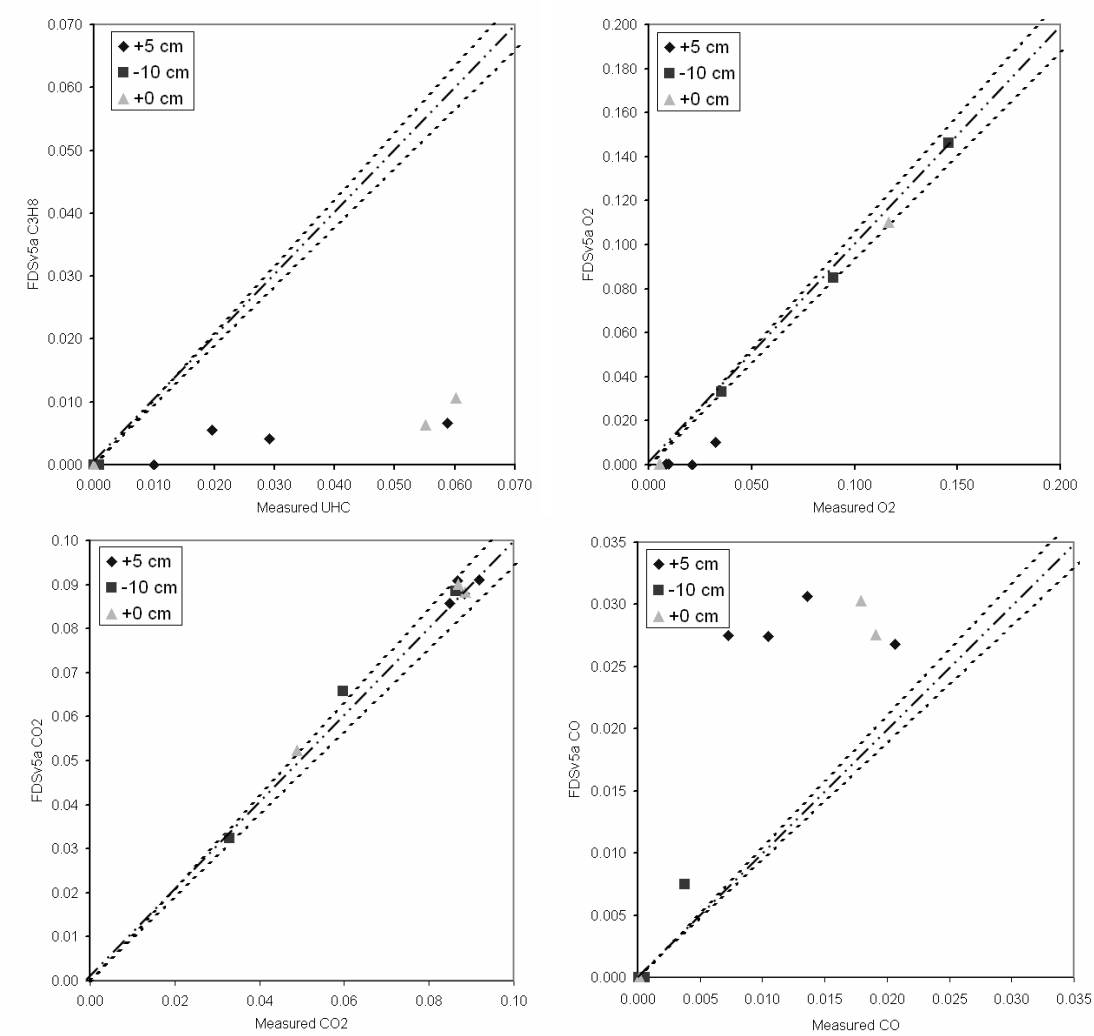

NIST Reduced Scale Enclosure

The NIST Reduced Scale Enclosure (RSE)[12] is a 40 % scaled version of the ISO 9705 compartment. It measures 0.98 m wide by 1.46 m deep by 0.98 m tall. The compartment contains a door centered on the small face that measures 0.48 m wide by 0.81 m tall. A 15 cm diameter natural gas burner was positioned in the center of the compartment. The burner was on a stand so that its top was 15 cm above the floor. Species measurements were made inside the upper layer of the compartment at the front near the door and near the rear of the compartment. The natural gas experiments were selected as currently the interest is in modeling CO production rather than CO and soot production.

Nine fire sizes were simulated: 50 kW, 75 kW, 100 kW, 150 kW, 200 kW, 300 kW, 400 kW, 500 kW, and 600 kW. The tests were modeled using properties of the natural gas supplied to the test facility[13,14]. The model geometry included the compartment interior along with a 0.6 m deep region outside the door that was modeled using a 2.4 cm grid resolution for a total of 240,000 grid cells. The wall boundary condition used a reduced material density for the compartment lining. This was done so that the computation would reach steady state in less time. Each fire size was simulated for 300 s which took approximately 45 hours on a 2.4 GHz processor.

Figure 7 shows the measured and predicted CO_2 and CO concentrations. The measured values are from the test series performed Bryner, Johnsson, and Pitts[12]. The model matches the data up to a fire size of 300 kW, including the location of the peak CO_2 concentration at 200 kW. For larger fires the model predicts more CO surviving in the upper layer than measured, along with correspondingly lower CO_2 levels. At 300 kW the model predicts front and rear concentrations of 7.7 % and 7.4 % CO_2 vs. 7.5 % and 7.7 % in the data. At 600 kW the respective CO_2 values are 6.5 % and 5.3 % vs. 6.1 % and 6.8 % in the data. For CO at 300 kW the model predicts 2.2 % and 2.4 % vs. 1.8 % and 2.0 % in the data. For CO at 600 kW the model predicts 3.2 % and 3.8 % vs. 2.9 % and 2.1 % in the data. As the compartment becomes under-ventilated, the model under-predicts CO_2 and over-predicts CO. The relative error increases as the compartment becomes more under-ventilated. However, note that the absolute model under-prediction of CO_2 in the rear (1.5 %) is equivalent to the absolute over-prediction of CO (1.7 %). This implies that part of the model error results from the assumption of infinitely fast chemistry for the first step. Furthermore, since the model as implemented performs the two steps sequentially, higher CO is predicted where the first step consumes all of the available oxygen.

Figure 7 Predicted and measured CO_2 and CO concentrations for the NIST RSE experiments of Bryner, Johnsson, and Pitts[12]

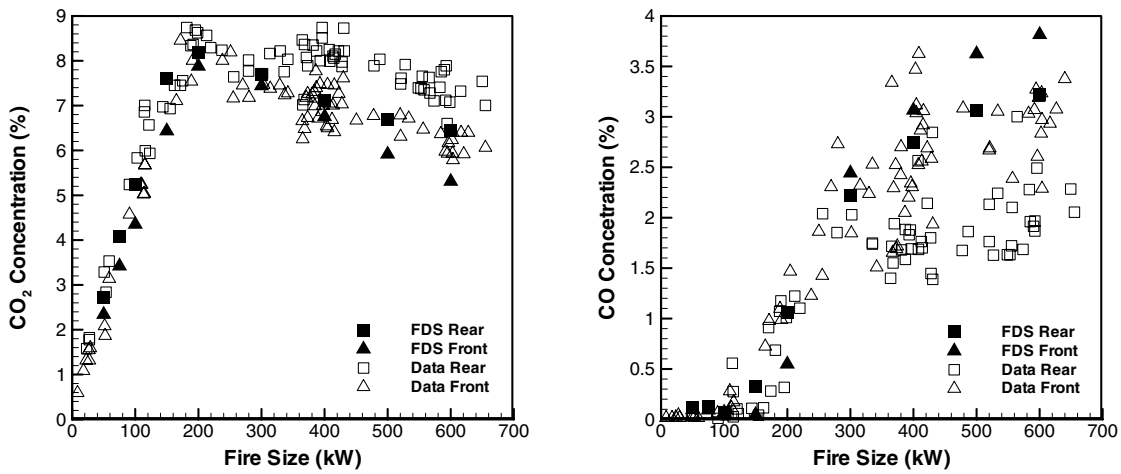

CONCLUSIONS

A combustion model based on a multiple parameter mixture fraction has been developed to account for local extinction and incomplete combustion, in particular, the formation and destruction of carbon monoxide. The new model was used to simulate three sets of experiments. The first experiment was a methane-air slot burner. The model successfully predicted the peak CO concentration as a function of elevation within the flame with errors ranging from 6 % to 25 % of the measurements and the overall flame temperature 5 % of the measurements. This is compared to experimental uncertainties of 10 % to 20 % for species and 5 % for temperatures. Since the current implementation of the two-step model assumes the first step is infinitely fast, it predicted a slightly narrower flame as combustion occurred at the burner lip rather than at a slight stand-off distance. The second set of experiments, conducted by Beyler, was designed to create a vitiated fire environment under a small hood. Predictions of species concentrations for the well-ventilated experiments correlate very well with the data (within the

experimental uncertainty of 6 %). For the higher equivalence ratio experiments, the model under-predicts fuel and oxygen and over-predicts CO. This appears to be a result of the model not being able to predict extinction at the base of the hood. The final set of experiments was a set of reduced-scale enclosure fires at NIST. The new model generally matched the trends seen in the data, though with an approximately 1 % to 2 % by volume error in the CO (relative error of 10 % to 80 %) and CO_2 (relative error of 10 % to 20 %) predictions for the under-ventilated fires. Overall, the validation results indicate that the new method tends to over-predict CO formation because of its assumption that the first step of the reaction is infinitely fast.

There is room for improvement to the current approach while remaining within the developed mixture fraction framework. A better method of determining when to allow the first step of the reaction to occur should result in improved predictions of CO formation. It is also noted that the current mixture fraction framework could be extended to a fourth parameter that could be used for tracking soot formation. However, a point of diminishing returns is reached as the number of mixture fraction variables approaches the number of primitive species, defeating the purpose of the mixture fraction approach.

ACKNOWLEDGEMENTS

The first author is supported by the Building and Fire Research Laboratory of the National Institute of Standards and Technology via its Fire Grants Program.

REFERENCES

[1] McGrattan, K., Hostikka, S., Floyd, J., Baum, H. and Rehm, R. 2007 *Fire Dynamics Simulator (Version 5): Technical Reference Guide*. NIST SP 1018-5. Gaithersburg, MD: National Institute of Standards and Technology.

[2] McGrattan, K., Klein, B., Hostikka, S., and Floyd, J. 2007. *Fire Dynamics Simulator (Version 5): User's Guide*. NIST SP 1019-5. Gaithersburg, MD: National Institute of Standards and Technology.

[3] Floyd, J., McGrattan, K., Hostikka, S., and Baum, H., 2003. CFD Fire Simulation Using Mixture Fraction Combustion and Finite Volume Radiative Heat Transfer, *Journal of Fire Protection Engineering,* **13** (1), pp.11-36.

[4] Westbrook, C. and Dryer, F., 1981. Simplified Reaction Mechanisms for the Oxidation of Hydrocarbon Fuels in Flames, *Combustion Science and Technology*, **27**, pp.31-43.

[5] Beyler, C., 2002. Flammability Limits of Premixed Diffusion Flames. In DiNenno, P., ed. *Handbook of Fire Protection Engineering*, 3rd ed. Quincy, MA: National Fire Protection Association.

[6] Mowrer, F., 2002. Private communication.

[7] Linteris, G. and Rafferty, I. 2003. Scale Model Flames for Determining the Heat Release Rate from Burning Polymers, *Fourth International Symposium on Scale Modeling (ISSM-IV)*.

[8] Smyth, K., 1999. *Fire Experimental Results*. [online]. Available from: http://fire.nist.gov/fire/flamedata [cited on 6 June 2007].

[9] Norton, S., Smyth, K., Miller, J., and Smooke, M., 1993. Comparison of Experimental and Computed Species Concentration and Temperature Profiles in a Laminar Two-Dimensional, Methane/Air Diffusion Flame, *Combustion Science and Technology*, **90**, pp.1-34.

[10] Smyth, K., 1996. NO Production and Destruction in a Methane/Air Diffusion Flame, *Combustion Science and Technology*, **155**, pp.151-176.

[11] Beyler, C., 1986. Major Species Production by Diffusion Flames in a Two-Layer Compartment Fire Environment, *Fire Safety Journal*, **10**(1), pp.47-56.

[12] Bryner, N., Johnsson, E., and Pitts, W., 1994. *Carbon Monoxide Production in Compartment Fires – Reduced-Scale Test Facility*. NISTIR 5568. Gaithersburg, MD: National Institute of Standards and Technology.

[13] Bundy,M., Hamins, A., Johnsson, E., Kim, S., Ko, G., and Lenhert, D. 2007. *Measurements of Heat and Combustion Products in Reduced-Scale Ventilation-Limited Compartment Fires.* NIST Technical Note TN-1483 (in internal review). Gaithersburg, MD: National Institute of Standards and Technology.

[14] Jonsson, E., Bundy, M. and Hamins, A. 2007 Reduced-Scale Enclosure Fires – Heat and Combustion Product Measurements. *Interflam 2007*. London, England. Interscience Communications.

Appendix E – Fire Safety Journal Paper

Extending the Mixture Fraction Concept to Address Under-Ventilated Fires

J.E. Floyd[1] K.B. McGrattan[2]

[1] Hughes Associates, Inc.

3610 Commerce Dr., #817

Baltimore, Maryland, USA, 21227

P:410.737.8677, F:410.737.8688, jfloyd@haifire.com

[2]Building and Fire Research Laboratory, National Institute of Standards and Technology,

Gaithersburg, Maryland, USA

Abstract

A common technique in computational fluid dynamics (CFD) modeling of fire is to assume single step, infinitely fast combustion, in which case the transport equations of all gas species can be combined into one for a single conserved scalar called the mixture fraction. While this approach is adequate for many engineering applications, for fire scenarios that require predictions of CO formation or flame extinction, this approach is inadequate. This paper describes a method of extending the mixture fraction concept to address two-step chemistry. The two-step chemistry allows for flame extinction and the prediction of CO formation and destruction. The mixture fraction is decomposed into components representing the states of the two-step chemistry. The new model is demonstrated with two test cases: a slot burner using direct numerical simulation (DNS) and a reduced scale enclosure using large eddy simulation (LES). Results of the new model are compared with experimental data and simulations using single-step chemistry.

Nomenclature

a,b,x,y,z	Mole proportions
$\frac{\mathrm{D}}{\mathrm{D}t}$	Substantial derivative
D	Diffusion coefficient
K	Reaction rate constant
$\dot{m}_i'''$	Species i production rate (kg i/m^3-s)
R	Universal gas constant
T	Time (s)
T	Temperature (K)
W_i	Molecular weight of species i (kg i/kmol i)
X_H	Hydrogen atom fraction
Y_i	Mass fraction of species i (kg i/kg)
Y_i^I	Fuel inlet mass fraction of species i (kg i/kg)
Y_i^∞	Ambient mass fraction of species i (kg i/kg)
y_i	Yield of species i (kg i/kg fuel)
s	Stoichiometric oxygen to fuel mass ratio
Z_i	Mixture fraction component
ϕ	Equivalence ratio
ρ	Density (kg/m^3)
ν_i	Stoichiometric coefficient of species i
ν_{CO}	Fixed yield stoichiometric coefficient of CO
ν'_{CO}	Stoichiometric coefficient of CO

1. The mixture fraction concept

In the classic Burke-Schumann description of a diffusion flame [1], the combustion process can be described by way of a single conserved scalar, the mixture fraction, which represents the mass fraction of the gas originating in the fuel stream. It can be expressed in various ways, usually as linear combinations of fuel and product species. Here we adopt:

$$Z = \frac{sY_\mathrm{F} - \left(Y_{\mathrm{O}_2} - Y_{\mathrm{O}_2}^\infty\right)}{sY_\mathrm{F}^I - Y_{\mathrm{O}_2}^\infty} = Y_\mathrm{F} + \frac{Y_{\mathrm{H_2O}} W_{\mathrm{H}_2}}{W_{\mathrm{H_2O}}} + \frac{Y_{\mathrm{CO}_2} W_\mathrm{C}}{W_{\mathrm{CO}_2}} + \ldots \tag{1}$$

where s is the stoichiometric oxygen to fuel mass ratio. For fire modeling with simple combustion chemistry, the mixture fraction is a useful concept, as it reduces the computational expense of having multiple gas species transport equations. However, the mixture fraction alone only provides one degree of freedom. In the absence of additional scalar parameters (i.e. some form of reaction progress variable), one is limited to the

assumption that combustion is infinitely fast or, in other words, fuel and oxygen burn instantly and completely on contact, regardless of temperature and other local conditions. This means that there is no way to model extinction, CO and soot production/destruction, pre-mixed combustion, ignition, and various other phenomena of interest in fire science.

Does this mean that we ought to abandon the mixture fraction approach? No. The principal reason for adopting a mixture fraction-based combustion model is to reduce the number of species transport equations that must be solved and thereby reduce the overall computer time required. To overcome its limitations, but keep its benefits, we have extended the mixture fraction approach to account for incomplete combustion. This method has been incorporated into the computational fluid dynamics (CFD) model Fire Dynamics Simulator (FDS) [2][3] and a number of validation test cases have been run. Two examples are given in this paper: a methane-air slot burner and a small-scale compartment fire experiment.

2. Generalizing the mixture fraction concept

There exist in the combustion literature, numerous reaction mechanisms for various hydrocarbon fuels. Many of these are intended for small-scale simulations and involve dozens of reactions and species. For example, one mechanism for methane combustion in air includes 58 reactions with 16 species [4]. This is a level of complexity that is undesirable for a practical fire model as tracking 16 species would greatly increase the computational resources required (both memory and time) and many of the reactions would occur at length scales never encountered in a typical large-scale simulation. Simpler reaction mechanisms have been derived that collapse the very complex schemes down to four reactions [5] that include separate steps for the oxidation of H_2 to H_2O and CO to CO_2. Even this, however, is more complex than desired as it involves five parameters (one each for fuel, CO_2, CO, H_2, and H_2O). It is additionally observed that for fire protection applications, H_2 in under-ventilated fires is not as critical as CO, since H_2 is essentially non-toxic.

Since it is desired to minimize the complexity of a new combustion model and to ensure its applicability to simulations with large grid sizes, the simplest possible CO formation and extinction mechanism is used. The following two-step combustion is assumed [6]:

$$\text{Step 1: } \mathrm{F} + \mathrm{O}_2 \rightarrow \mathrm{CO} + \text{Other Products} \tag{2}$$

$$\text{Step 2: } \mathrm{CO} + \frac{1}{2}\mathrm{O}_2 \rightarrow \mathrm{CO}_2 \tag{3}$$

In the first step, fuel and oxygen react to form carbon monoxide and other combustion products. Other products (soot, water vapor) are considered to have fixed yields. In the second step, carbon monoxide reacts with oxygen to form carbon dioxide. No assumptions need to be made at this point about reaction rates. This scheme is designed primarily for hydrocarbon fuels. Fuels containing oxygen, such as wood, can generate CO directly from pyrolysis reactions [7] and this method presumes that CO and other products are formed proportionately to oxygen consumption.

The description of the two-step reaction above, with extinction, requires three independent variables. One to keep track of the amount of fuel present, a second to track how much of that fuel has reacted to form CO, and a third to track how much of the CO has reacted to form CO_2. For practical reasons, the variables should be conserved, should provide a numerically stable method of computing the heat release rate, and should uniquely determine the gas species. To derive these variables, consider linear combinations of the transport equations for fuel, carbon monoxide, and carbon dioxide:

$$\frac{\mathrm{D}Y_{\mathrm{F}}}{\mathrm{D}t} = \nabla \cdot D\rho\nabla Y_{\mathrm{F}} + \dot{m}'''_{\mathrm{F},1}, \tag{4}$$

$$\frac{\mathrm{D}Y_{\mathrm{CO}}}{\mathrm{D}t} = \nabla \cdot D\rho\nabla Y_{\mathrm{CO}} + \dot{m}'''_{\mathrm{CO},1} + \dot{m}'''_{\mathrm{CO},2}, \tag{5}$$

and

$$\frac{\mathrm{D}Y_{\mathrm{CO}_2}}{\mathrm{D}t} = \nabla \cdot D\rho\nabla Y_{\mathrm{CO}_2} + \dot{m}'''_{\mathrm{CO}_2,2} \tag{6}$$

where the numerical subscripts on the mass production terms refer to the two reaction steps. Note that

$$\frac{\dot{m}'''_{\mathrm{F},1}}{W_{\mathrm{F}}} = -\frac{\dot{m}'''_{\mathrm{CO},1}}{\nu_{CO} W_{\mathrm{CO}}} \tag{7}$$

and

$$\frac{\dot{m}'''_{\mathrm{CO},2}}{\nu_{CO} W_{\mathrm{CO}}} = -\frac{\dot{m}'''_{\mathrm{CO}_2,2}}{\nu_{CO_2} W_{\mathrm{CO}_2}}. \tag{8}$$

By substituting Eqs. (7) and (8) into Eqs. (5) and (6) respectively, and multiplying the equations by an appropriate scalar constant (scalar multiplication does not affect the conservation of mass), we derive the following transport equations for the three mixture fraction variables:

$$\frac{\mathrm{D}Z_1}{\mathrm{D}t} = \nabla \cdot D\rho\nabla Z_1 + \dot{m}'''_{\mathrm{F},1}, \tag{9}$$

$$\frac{\mathrm{D}Z_2}{\mathrm{D}t} = \nabla \cdot D\rho\nabla Z_2 - \dot{m}'''_{\mathrm{F},1} + \frac{W_F \dot{m}'''_{\mathrm{CO},2}}{\nu_{CO} W_{\mathrm{CO}}}, \tag{10}$$

and

$$\frac{\mathrm{D}Z_3}{\mathrm{D}t} = \nabla \cdot D\rho\nabla Z_3 - \frac{W_F \dot{m}'''_{\mathrm{CO},2}}{\nu_{CO} W_{\mathrm{CO}}} \tag{11}$$

where $Z_1 = Y_{\mathrm{F}}$, $Z_2 = \frac{W_{\mathrm{F}}}{\nu_{CO} W_{\mathrm{CO}}} Y_{\mathrm{CO}}$, and $Z_3 = \frac{W_{\mathrm{F}}}{\nu_{CO_2} W_{\mathrm{CO}_2}} Y_{\mathrm{CO}_2}$. Note that the source terms in the mixture fraction transport equations sum to zero. Physically, this is simply mass conservation. The decrease in Z_1 (fuel combining with oxygen to form CO and other products) is equal to the increase in Z_2, and the decrease in Z_2 (CO combining with oxygen to form CO_2) is equal to the increase in Z_3. When the three mixture fraction variables are summed, the resulting quantity represents all the mass that was originally fuel, and is equal to the mixture fraction itself:

$$Z_1 + Z_2 + Z_3 = Y_F + \frac{W_F}{\nu_{CO} W_{CO}} Y_{CO} + \frac{W_F}{\nu_{CO_2} W_{CO_2}} Y_{CO_2} = Z \tag{12}$$

In short, we can replace the transport equations for all the gas species with the three mixture fraction variables. The source terms in these equations depend on the specific form of the combustion model that is described below as follows.

Recovering the species mass fractions from the mixture fraction variables is relatively easy and computationally efficient. To derive the necessary formulae, first consider Eqs. 2 and 3 written completely in terms of all the species:

$$\mathrm{C_xH_yO_zN_aM_b} + \nu_{O_2}\mathrm{O_2} \rightarrow \nu_{H_2O}\mathrm{H_2O} + (\nu'_{CO} + \nu_{CO})\mathrm{CO} + \nu_S \mathrm{soot} + \nu_{N_2}\mathrm{N_2} + \nu_M \mathrm{M} \tag{13}$$

$$\nu'_{CO}\left(\mathrm{CO} + \frac{1}{2}\mathrm{O_2} \rightarrow \mathrm{CO_2}\right) \tag{14}$$

The parentheses in Eq. (14) are there to indicate that the two reactions sum to the complete combustion reaction for the fuel. Note that CO has two stoichiometric coefficients where ν'_{CO} applies to the CO that can be converted to CO_2 and ν_{CO} applies to the CO that exists post-flame. The combustion model to be discussed later in this paper is not capable of predicting the small levels of CO that still exist in well-ventilated fires; hence, the need to preserve this empirical value. M is a species that represents that portion of the fuel that is not C, H, O, or N.

Next, some additional quantities are defined. The fuel stream may be specified as diluted given by Y_F^I, the mass fraction of fuel in the fuel stream. The diluent is presumed to be nitrogen with a mass fraction of $Y_{N_2}^I = 1 - Y_F^I$. The ambient mass fractions of oxygen, $Y_{O_2}^\infty$, and nitrogen, $Y_{N_2}^\infty = 1 - Y_{O_2}^\infty$, are also specified. Accounting for fuel dilution and the atom fraction of hydrogen in the soot, X_H, the mixture fraction parameters are given as follows:

$$Z_1 = \frac{Y_F}{Y_F^I}, \tag{15}$$

$$Z_2 = \frac{W_F}{W_{CO}\left(x - (1 - X_H)\nu_S\right)} \frac{Y_{CO}}{Y_F^I} \tag{16}$$

and

$$Z_3 = \frac{W_F}{W_{CO2}\left(x - (1 - X_H)\nu_S\right)} \frac{Y_{CO2}}{Y_F^I}. \tag{17}$$

The mass fractions of the species are then given by

$$
\begin{bmatrix}
0 & Y_{\mathrm{F}}^{I} & 0 & 0 \\
Y_{\mathrm{N_2}}^{\infty} & Y_{\mathrm{N_2}}^{I} & \dfrac{\nu_{\mathrm{N_2}} W_{\mathrm{N_2}}}{W_{\mathrm{F}}} Y_{\mathrm{F}}^{I} & \dfrac{\nu_{\mathrm{N_2}} W_{\mathrm{N_2}}}{W_{\mathrm{F}}} Y_{\mathrm{F}}^{I} \\
Y_{\mathrm{O_2}}^{\infty} & 0 & -\dfrac{\nu'_{\mathrm{O_2}} W_{\mathrm{O_2}}}{W_{\mathrm{F}}} Y_{\mathrm{F}}^{I} & -\dfrac{\nu_{\mathrm{O_2}} W_{\mathrm{O_2}}}{W_{\mathrm{F}}} Y_{\mathrm{F}}^{I} \\
0 & 0 & \dfrac{(\nu'_{\mathrm{CO}} + \nu_{\mathrm{CO}}) W_{\mathrm{CO}}}{W_{\mathrm{F}}} Y_{\mathrm{F}}^{I} & 0 \\
0 & 0 & 0 & \dfrac{\nu_{\mathrm{CO_2}} W_{\mathrm{CO_2}}}{W_{\mathrm{F}}} Y_{\mathrm{F}}^{I} \\
0 & 0 & \dfrac{\nu_{\mathrm{H_2O}} W_{\mathrm{H_2O}}}{W_{\mathrm{F}}} Y_{\mathrm{F}}^{I} & \dfrac{\nu_{\mathrm{H_2O}} W_{\mathrm{H_2O}}}{W_{\mathrm{F}}} Y_{\mathrm{F}}^{I} \\
0 & 0 & \dfrac{\nu_{\mathrm{S}} W_{\mathrm{S}}}{W_{\mathrm{F}}} Y_{\mathrm{F}}^{I} & \dfrac{\nu_{\mathrm{S}} W_{\mathrm{S}}}{W_{\mathrm{F}}} Y_{\mathrm{F}}^{I} \\
0 & 0 & \dfrac{\nu_{\mathrm{M}} W_{\mathrm{M}}}{W_{\mathrm{F}}} Y_{\mathrm{F}}^{I} & \dfrac{\nu_{\mathrm{M}} W_{\mathrm{M}}}{W_{\mathrm{F}}} Y_{\mathrm{F}}^{I}
\end{bmatrix}
\times
\begin{bmatrix}
1 - \mathrm{Z}_1 - -\mathrm{Z}_2 - -\mathrm{Z}_3 \\
\mathrm{Z}_1 \\
\mathrm{Z}_2 \\
\mathrm{Z}_3
\end{bmatrix}
=
\begin{bmatrix}
Y_{\mathrm{F}} \\
Y_{\mathrm{N_2}} \\
Y_{\mathrm{O_2}} \\
Y_{\mathrm{CO}} \\
Y_{\mathrm{CO_2}} \\
Y_{\mathrm{H_2O}} \\
Y_{\mathrm{S}} \\
Y_{\mathrm{M}}
\end{bmatrix}. \tag{18}
$$

The stoichiometric coefficients are given by:

$$
\begin{aligned}
\nu_{\mathrm{N_2}} &= \frac{\mathrm{a}}{2} & \nu_{\mathrm{H_2O}} &= \frac{\mathrm{y}}{2} - X_{\mathrm{H}} \nu_{\mathrm{S}} \\
\nu'_{\mathrm{O_2}} &= \frac{\nu'_{\mathrm{CO}} + \nu_{\mathrm{H_2O}} - \mathrm{z}}{2} & \nu'_{\mathrm{CO}} &= \mathrm{x} - \nu_{\mathrm{CO}} - (1 - X_{\mathrm{H}}) \nu_{\mathrm{S}} \\
\nu_{\mathrm{O_2}} &= \nu_{\mathrm{CO_2}} + \frac{\nu_{\mathrm{H_2O}} - \mathrm{z}}{2} & \nu_{\mathrm{CO}} &= \frac{W_{\mathrm{F}}}{W_{\mathrm{CO}}} y_{\mathrm{CO}} \\
\nu_{\mathrm{CO_2}} &= \mathrm{x} - (1 - X_{\mathrm{H}}) \nu_{\mathrm{S}} & \nu_{\mathrm{S}} &= \frac{W_{\mathrm{F}}}{W_{\mathrm{S}}} y_{\mathrm{S}} \\
\nu_{\mathrm{M}} &= \mathrm{b} & W_{\mathrm{S}} &= X_{\mathrm{H}} W_{\mathrm{H}} + (1 - X_{\mathrm{H}}) W_{\mathrm{C}}
\end{aligned} \tag{19}
$$

where y_{CO} and y_{S} are the user-specified post-flame yields of CO and soot and a, b, x, and y are from the specification of the fuel molecule in Eq. (13). In short, the individual gas species mass fractions are just linear combinations of the three mixture fraction variables, and the solution of transport equations for the three mixture fraction variables rather than the eight species reduces the computational expense of the entire simulation roughly by 30 %.

3. Numerical advantages of the mixture fraction decomposition method

The decomposition of the mixture fraction discussed in the previous section is not the only way to generalize the concept. There are combustion models that still retain the "total" mixture fraction, *Z*, for species tracking, but also solve a transport equation for a "progress variable" (often denoted by the letter *c*) that indicates, via a value between zero and one, the

completeness of the combustion reaction [8]. Z and c alone can describe a single reaction with the possibility of local extinction. The formulation can be extended, via another progress variable, to account for CO production/destruction. Indeed, the decomposition of the mixture fraction described in the previous section can also be reformulated in terms of only two mixture fraction variables, Z_1 and Z_3, if we want to neglect the incomplete combustion step and only allow complete combustion with the possibility of local extinction.

Mathematically, these various formulations of the basic transport equations are equivalent. They are simply book-keeping strategies designed to reduce the computational expense of the simulation. However, there are numerical advantages to the mixture fraction decomposition ($Z = \sum_i Z_i$) when implemented in a large-scale fire model. The first advantage has to do with the calculation of the heat release rate; the second has to do with boundary and initial conditions.

A very important consideration in a fire model is the computation of the local volumetric heat release rate. In the classic formulation, the heat release rate is proportional to the gradient of Z across the "flame sheet;" that is, the interface between fuel and oxygen. On a relatively coarse numerical grid, this computation can be awkward, as the value of Z can change dramatically at the interface when there are not a sufficient number of grid cells to resolve it. Consider a horizontal profile of Z across a coarsely defined fire, shown in Fig. 1 (shaded region is burner location). A common problem with finite differencing schemes whose spatial accuracy is higher than first order is that regions with steep gradients typically exhibit "under-shoots," where the variable drops below some obvious lower bound. For example, in the Fig., the mixture fraction, Z, drops below zero. Although a negative value of the mixture fraction is physically meaningless, the numerical scheme is mass conserving overall. In other words, a local dip below zero is offset somewhere else (the slight increase in Z above zero seen near the dips). There are numerous ways of correcting these local defects [9], but all of these methods will compromise the accuracy of any heat release rate calculation that is based on the gradient of the mixture fraction across the flame sheet, where these under-shoots typically occur. The reason for the inaccuracy is that the correction of the under-shoot is typically achieved by redistributing fuel mass across the flame sheet, which effectively alters the heat release rate.

The advantage of the mixture fraction decomposition approach is that Z_1 represents the fuel mass fraction, and the heat release rate can be computed directly from the conversion rate of fuel to products. There is no need to compute gradients of a single mixture fraction variable, and thus the problem associated with under-shoots is eliminated. This was a crucial consideration in the adoption of the decomposition approach in FDS, starting with version 5, released in October 2007 [2].

A second major advantage of the mixture fraction decomposition approach has to do with boundary conditions. Because the mixture fraction components, Z_i, represent linear

combinations of species mass fractions, their initial and boundary conditions are easily formulated. However, the same cannot be said for the progress variable, c. The progress variable is well defined within the fuel and product streams because it indicates the relative completeness of the combustion process. However, its value initially and in the far field is not well defined, as there are no reactants or products initially or in the far field. Over the course of a fire simulation, the value of the progress variable in the exhaust plume might go from 1 (complete combustion) to 0 (no combustion). What value should be assigned to c in the far field that is consistent with these two extremes? Whether it be 0 or 1, there will inevitably be problems associated with the "artificial" diffusion of c that are inherent in any finite difference formulation of the transport equations. Artificial diffusion is essentially the "smearing" of the variable's value over the numerical mesh, another unavoidable consequence of the numerics. Because c represents the state of the combustion process, changes in its value imply a reaction has or has not occurred. As with the problem associated with the calculation of the heat release rate, we do not want to adopt any numerical scheme for which unavoidable numerical defects compromise the integrity of the underlying physical model.

This discussion of the advantages and disadvantages of these various mixture fraction formulations may seem completely divorced from the actual physics of fire. It is important to keep in mind, however, that these abstract concepts do have physical meaning, and the choice of one scheme over another often has more to do with numerical, rather than physical, considerations. Indeed, up to this point, the actual physics of the combustion process have not even been discussed, but rather the numerical framework that is to support the combustion model. The physical assumptions underlying the combustion model are discussed next.

4. Combustion model

In this section, we discuss the details of the combustion model that was implemented in FDS. The model is fairly simple and empirically based because of the fact that FDS is used for large-scale fire simulations, and the numerical grid is typically on the order of 10 cm or higher. It is important to keep in mind that the mixture fraction decomposition idea put forward in the previous section will support any number of variants on the combustion model discussed as follows.

Consider the two-step reaction outlined in Eqs. (2) and (3). The first reaction step, the incomplete reaction of fuel and oxygen that forms CO and other products, could potentially occur in any grid cell that contains both fuel and oxygen, assuming conditions are appropriate. One possible means of determining flammability is via the critical adiabatic flame temperature [10]. On coarse numerical grids typical of large-scale fire simulations, there is only limited information with which to determine the viability of a flame in a particular region of the flow field. Using only the local temperature and oxygen concentration, an argument can be made that a flame is viable for values that lie in the upper right half of the diagram shown in Fig. 2. For local temperatures and oxygen

concentrations falling below the line, the critical flame temperature cannot be reached and Step 1 is not allowed. Details are given in Ref. [2].

There are several limitations associated with this simple flammability argument. First, the rule is applicable to low strain rate flames typically found in fires and cannot predict phenomena such as blow off. Second, if flammability is permitted, there is often an abundance of fuel or oxygen in the particular grid cell due to the numerical error that inevitably results from using a coarse grid. Allowing either the fuel or oxygen to be consumed instantaneously leads to an unrealistic local heat release rate, but limiting the reaction rate is problematic as well because the local temperature is only an average over a fairly large grid cell and cannot be used to estimate the reaction rate. Empirical arguments must be used to control the rate of reaction. In FDS, an upper limit is placed on the volumetric heat release rate. Recent research has suggested that low strain rate diffusion flames cannot achieve heat release rates greater than about 200 kW/m^2 of flame area [11]. Dividing this value by the width of the grid cell provides a limit on the local volumetric heat release rate. In the specific FDS version used for this paper, no additional limitations were applied based on mixing constraints; however, such limitations are currently being investigated.

The second step of the reaction, the conversion of CO to CO_2, can occur in any grid cell where oxygen and CO exist. However, unlike Step 1, it can be argued that the computed local temperature away from the flame region *can* be relied upon for use in calculating the reaction rate, even on a relatively coarse grid, because the gradient of temperature is not nearly as steep. Of course, "away from the flame" is somewhat vague, especially in regard to a compartment undergoing flashover. In FDS, the strategy is as follows. If fuel, oxygen and CO exist in a grid cell for which flammability is viable, Step 1 of the reaction takes preference in consuming the fuel and oxygen, followed by the instantaneous conversion of CO to CO_2 if there is enough oxygen left over and if the upper bound in the volumetric heat release rate has not been reached. It is presumed that a flame, and therefore a flame temperature, is present and CO will oxidize rapidly consuming the maximum possible amount of CO and O_2 in the grid cell. Away from the flame, that is, where fuel is not present or oxygen levels do not meet the criteria in Fig. 2, it is presumed that a flame is also not present and therefore the computed cell temperature is appropriate in the following expression for the oxidation rate of CO [12].

$$k(T) = 2.53 \times 10^{12}\, e^{\frac{-199547}{RT}} \text{ cm}^3\text{/mol-s} \tag{20}$$

In summary, the two-step reaction mechanism described above consists of a fast (instantaneous) reaction of fuel and oxygen to form CO and other products, followed by a slow conversion of CO to CO_2 if the temperature is high enough and there is enough oxygen available. This process is illustrated in the flowchart shown in Fig. 3.

5. Validation

The extended mixture fraction, two-step combustion model was implemented in FDS, version 5, and compared against two very different experiments. The first was a small methane-air, Wolfhard-Parker slot burner diffusion flame [13]-[15]. The second was a set of selected experiments performed at NIST in a reduced scale enclosure (RSE) [16]. The objective of the exercise was to (1) ensure that the new methodology is valid, (2) determine if the two-step approach is significantly better than the one-step, and (3) make sure that the methodology is sound not just for small laminar diffusion flames simulated using direct numerical simulation (DNS), but also for practical, large-scale fire scenarios performed with large eddy simulation (LES).

For both geometries, the current FDS submodels for radiation heat transfer and surface heat transfer were used. Surface heat transfer is computed using a one-dimensional (1D), multi-layer, heat conduction solver. Radiation heat is computed using a finite volume method [17] using 104 control angles. Spectrally, the slot burner used a wide band approach that uses nine spectral bands whereas the RSE used a gray gas approach. Absorption coefficients are precomputed using RADCAL [18] and tabulated as a function of the mixture fraction components, temperature, and spectral band.

5.1 Slot burner

The Wolfhard-Parker slot burner consisted of an 8 mm wide central slot flowing fuel surrounded by two 16 mm wide slots flowing dry air with 1 mm separations between the slots. The slots were 41 mm in length and 3 mm high. Velocity, temperature, and species profiles for a methane flame for various heights above the burner are archived on the NIST web page [13]. The experimental errors were reported as 5 % for temperature [14] and 10 % - 20 % [14] for the major species.

A three-dimensional (3D) simulation was performed for one quarter of the slot burner with a uniform 0.5 mm numerical grid. The grid study used grids of 0.25, 0.5, and 1.0 mm. The 0.5 and 0.25 mm grid had no change in flame position and differences in the peak temperature, peak velocity, and CO and CO_2 gas concentrations were less then 10. Symmetry boundary conditions were assumed because the flow field was laminar. The computational domain was 32 mm by 32 mm by 48 mm with 393,000 grid cells. A two dimensional simulation was also performed, but the results were less accurate because radiative losses along the axis of symmetry are not possible in a two-dimensional (2D) computation. The 3D simulation was run for 4 s of physical time, requiring 104 h of CPU time on a 2.4 GHz Intel processor. While this might sound like a very costly calculation, it is typical of DNS. While DNS is typically not practical for fire protection engineering applications, it is a useful approach for evaluating the new combustion methodology.

Fig. 4 shows predicted temperature profiles using both a single and two-step reaction scheme, plotted as a function of the distance from the burner centerline at heights of 7 mm and 11 m above the burner. Both the single and two-step model predicted a flame that is slightly narrower and slightly cooler than the data. The single- and two-step models,

respectively, predicted a 5.5 and 6 mm wide flame vs. the measured 6.5 mm (15 % and 8 % error). It is possible that the width error resulted from assumptions made in creating the FDS input. The fuel and air inlets were presumed to be uniform in both temperature and mass flux. Some or all of the width errors could be accounted for by non-uniformities in the inlet flow. Additionally, above the region displayed was a screen to stabilize the flame. That region was not included and its omission may also contribute to the error in width. Lastly, there is a noticeable shift in the width when going from one-step to two-step chemistry, and some portion of the width error could result from the lack of species such as H_2. The peak flame temperature, however, should not be greatly affected by these assumptions. It is observed that the one-step reaction scheme under-predicted the peak measured temperatures by 11 % and 7 % at 7 and 11 mm, respectively, while the two-step scheme only under-predicted these measurements by 3 % and 4 %, respectively. The two-step version predicted higher centerline temperatures and the single-step version predicted slightly lower centerline temperatures. If the two-step profiles are expanded by the 0.5 mm width error (presuming the width error was due to input uncertainties), then the two-step predictions would match the measured data except along the centerline.

The overall results are not surprising as the first reaction step is infinitely fast. Thus, combustion occurs at the grid cell immediately above the lip of the burner. In reality, the cold fuel and air streams do not react infinitely fast and some oxygen penetrates the flame at the base. This lower amount of combustion in the experiment at the burner lip results in cooler gases being entrained into the core of the flame with a resulting drop in the centerline temperature. The single-step version predicted lower temperatures throughout the flame and this was likely a result of the single parameter model not capturing the appropriate heat release distribution vertically over the burner.

Fig. 5 shows predicted and measured fuel and oxygen profiles for the single- and two-step reaction schemes, plotted as a function of the distance from the burner centerline at a height of 7 and 11 mm above the burner. The two-step predictions of the fuel concentration lie within the uncertainty at all locations. The one-step predictions lie below the uncertainty bounds near the edge of the flame but are otherwise within the uncertainty bounds. Both schemes predicted oxygen concentrations above the uncertainty bounds, but the two-step predictions are significantly improved. The over-prediction of the oxygen concentration resulted primarily from the prediction of a narrower flame, as seen in the temperature predictions shown in Fig. 4. If the predicted width were stretched to match the experimental width, the two-step predictions would match the measured data. Notice that both reaction schemes failed to predict the small amount of oxygen that was measured at the burner centerline because both schemes employ a fast primary reaction that does not allow any oxygen to penetrate the flame sheet.

Fig. 6 shows predicted and measured carbon dioxide and carbon monoxide concentration profiles at two elevations above the burner. The two-step predictions for CO_2 generally lie within the uncertainty bounds of the measurements, except for regions outside the flame resulting from the narrower flame prediction. The one-step scheme over-predicted CO_2 inside the flame - not surprising as the scheme only produced CO_2 in a one-step complete

reaction. The two-step predictions of CO at the 7 mm height generally lie within the uncertainty bounds except near the edge of the flame (due to the narrower flame prediction) and at the flame centerline. At the 11 mm height, the two-step predictions are lower than the measured data. The CO predictions show a decrease in the peak value as a function of height above the burner whereas the measurements show a slight increase (errors in the peak concentrations of CO are 5 % at 7 mm and 30 % at 11 mm). This result was likely due to a combination of the infinitely fast first reaction combined with allowing the second reaction to be infinitely fast in those cells where the first reaction has occurred.

The predictions of CO provide an excellent illustration of the two-step combustion model. In the grid cells in the vicinity of the burner lip, fuel and oxygen react and form CO, but there was not enough oxygen available to complete the reaction. Further up in the flame, additional air was entrained and CO oxidizes to form CO_2. The two-step combustion model is relatively simple, but it does at least have the necessary mechanism to describe this very basic process. Next, the model will be shown to work well for a more practical fire scenario.

5.2 NIST RSE

The NIST Reduced Scale Enclosure (RSE) was a 40 % scaled version of the ISO 9705 compartment. It measured 0.98 m wide by 1.46 m deep by 0.98 m tall, with a door centered on the small face that measured 0.48 m wide by 0.81 m tall. A 15 cm diameter natural gas burner was positioned in the center of the compartment. The burner was on a stand so that its top was 15 cm above the floor. Species measurements were made inside the upper layer of the compartment at the front near the door and near the rear [16]. Heat release rate uncertainties were reported as 8.6 %, and CO and CO_2 concentration measurements had reported uncertainties of 0.24 %.

Fire Dynamics Simulator was used to simulate eight fires in the compartment: 50, 75, 150, 200, 300, 400, 500, and 600 kW. The tests were modeled using properties of a typical natural gas supplied to the test facility [19],[20]. The simulation included the compartment interior along with a 0.6 m deep region outside the door that was modeled using a 2.4 cm grid resolution for a total of 240,000 grid cells. The grid study used the 500 kW fire with grid sizes of 1.9, 2.4, and 3.5 cm as well as a study using the 2.4 cm with a 50 % lower CFL limit (i.e. reduced the time steps by a factor of two). Between the 1.9 cm and the 2.4 cm grids, as well as the reduced time step, there was no significant change in the location and magnitude of the heat release rate contours and discernable differences in upper layer temperatures and CO and CO_2 concentrations were less then 10 %. The wall boundary condition used a reduced material density for the compartment lining. This was done so that the computation would reach steady state in less time. Each fire size was simulated for 300 s that for the new approach took approximately 45 h on a 2.4 GHz processor.

Simulations were performed with both the single- and two-step reaction schemes. While the one-step reaction scheme does not predict CO formation, it does allow the specification of a fixed post-flame CO yield. Setting an increased CO yield to account for a higher

equivalence ratio would be a typical practice for an engineer using the one-step model; therefore, the correlation in Eq. 21 [21] was used to set the CO yield for each simulation with the equivalence ratio, ϕ, determined using Eq. 22.

$$Y_{\mathrm{CO}} = \frac{0.19}{180}\tan^{-1}\left(10\left(\phi - 0.8\right)\right) + 0.095 . \tag{21}$$

$$\phi = \frac{\dot{m}_{burner}\dfrac{\nu_{\mathrm{O}_2} W_{\mathrm{O}_2}}{W_{\mathrm{F}}}}{\dfrac{Y_{\mathrm{O}_2}^{\infty}}{2} A_{door}\sqrt{H_{door}}} . \tag{22}$$

The predicted and measured CO and CO_2 concentrations at the front and rear locations are shown in Fig. 7. The equivalence ratios in the Fig. are based upon the computed mass flow rates derived from temperature measurements made during the tests; they differ from the presumed equivalence ratios used to set the CO yield for the one-step model. Both reaction schemes capture the general trends seen in the CO_2 data. The one-step scheme over-predicted the concentrations while the two-step scheme under-predicted them. Moreover, the two-step scheme over-predicted the CO concentrations, but the amount of over-prediction was consistent with the amount of under-prediction in CO_2. The one-step scheme, using an equivalence ratio correlation for CO yield, could not replicate the measured values at the two specific locations inside the compartment. Not surprisingly, the under-prediction of CO by the one-step scheme was consistent with its over-prediction of CO_2.

At 600 kW, the two-step predictions of CO_2 at the front and rear locations were 4.9 % and 6.3 % respectively vs. the 6.1 % and 7.1 % in the data. For CO, the corresponding results were 3.6 % and 2.9 % vs. 2.9 % and 2.1 %. Note, however, that the absolute front and rear under-prediction in CO_2 of 1.2 % and 0.8 % was similar to the 0.7 % and 0.8 % over-prediction of CO. This implies that a significant contributor to the model error was likely the infinitely fast chemistry assumption of the first reaction combined with the sequential vs. simultaneous reaction steps.

The predicted and measured lower and upper temperatures are shown in Fig. 8. The two-step predictions show a similar trend to the data (reaching plateau at higher equivalence ratios) that is not seen in the single-step predictions. Both approaches over-predict the upper layer temperatures; however, the degree of over-prediction is much less for the two-step scheme.

5. Conclusion

A generalization of the mixture fraction concept has been proposed as a means of maintaining the practicality and efficiency of a CFD fire model while extending its ability to handle fire phenomena such as CO production and extinction. By decomposing the

mixture fraction into three parts -- fuel, products of incomplete combustion, and products of complete combustion -- we can introduce a two-step combustion model that allows for extinction and CO production. The ability of the new approach to predict CO concentrations was tested using two sets of experiments: a methane-air slot burner diffusion flame and small compartment experiments performed.

For the small-scale slot burner simulations performed at high spatial resolution, the new model predicted species concentrations generally within the 10 % to 20 % experimental uncertainty range with prediction errors of 6 % to 25 %. Temperature predictions were within the 5 % experimental uncertainty range. Improvements in all predicted quantities were achieved with the new approach and were demonstrably better than results using only a one-step reaction scheme.

For the larger scale geometry, the new model matched experiments for both well-ventilated and under-ventilated fires, whereas the one-step approach only performed well for well-ventilated fires. The two-step scheme under-predicted the oxidation of CO; however, the predictions were still within 20 % to 30 % of the measured data, a level of performance which was not possible with the one-step scheme. Upper temperature predictions were also greatly improved with the two-step scheme.

There is clearly room for improvement in the current approach. Developing improved criteria for allowing the oxidation of fuel and oxygen in the first step and perhaps the inclusion of a rate equation or mixing limitation should reduce over-predictions of CO formation. However, given the conditions discussed in the introduction, developing criteria that are broadly applicable over many length scales would not be trivial. Such criteria would have the added benefit of potentially extending the applicability of the model to re-ignition problems such as backdrafts. The mixture fraction decomposition idea could also be extended to included additional parameters. For example, the mixture fraction could be decomposed further to add a term for tracking soot formation and destruction. However, it is noted that at some point, the expense of working with a large number of mixture fraction variables becomes comparable to the cost of working with the primitive variable approach of tracking individual species, in which case its advantages disappear.

Acknowledgement

This work was funded by the United States Department of Commerce, National Institute of Standards and Technology, Building and Fire Research Laboratory through the Fire Grants Program.

References

[1] K. Kuo, Principles of Combustion, John Wiley & Sons, New York, NY, 1986.

[2] K. McGrattan, S. Hostikka, J. Floyd, H. Baum, R. Rehm, Fire Dynamics Simulator (Version 5): Technical Reference Guide, NIST SP 1018-5, National Institute of Standards and Technology, Gaithersburg, MD, 2007.

[3] K. McGrattan, S. Hostikka, J. Floyd, H. Baum, CFD fire simulation using mixture fraction combustion and finite volume radiative heat transfer, J. Fire Prot. Eng. 13 (1) (2003) 11-36.

[4] R.W. Bilger, S.H. Stårner, On reduced mechanisms for methane-air combustion in non-premixed flames, Combust. Flame. 80 (1990) 135-149.

[5] W.P. Jones, R.P. Lindstedt, Global reaction schemes for hydrocarbon combustion, Combust. Flame. 73 (1988) 233-249.

[6] C. Westbrook, F. Dryer, Simplified reaction mechanisms for the oxidation of hydrocarbon fuels in flames. Combust. Sci. Technol., 27 (1981) 31-43.

[7] X. Zhou, S. Mahalingam, A suitable mixture fraction for diffusion flames of wood pyrolysis gas, Combust. Flame. 133 (2003) 197-199.

[8] S. Ferraris, J. Wen, S. Dembele, Large eddy simulation of backdraft phenonenom, Fire Saf. J.

[9] J. Boris, A. Landsberg, E. Oran, J. Gardner, LCPFCT – a flux corrected transport algorithm for solving generalized continuity equations, NRL/MR/6410-93-7192, Naval Research Laboratory, Washington, DC, 1993.

[10] C. Beyler, Flammability limits of premixed diffusion flames. In: P. DiNenno Ed.) Handbook of Fire Protection Engineering, third ed., National Fire Protection Association, Quincy, MA, 2002.

[11] G. Linteris, I. Rafferty, Scale model flames for determining the heat release rate from burning polymers, in: Proceedings of the Fourth International Symposium on Scale Modeling (ISSM-IV), 2003.

[12] W. Tsang, R.F. Hampson, Chemical kinetic database for combustion chemistry. Part I. Methane and related compounds. J. Phys Chem. Ref. Data. (1986) 15.

[13] K. Smyth, <http://fire.nist.gov/fire/flamedata>, 1999.

[14] S. Norton, K. Smyth, J. Miller, M. Smooke, Comparison of experimental and computed species concentration and temperature profiles in a laminar two-dimensional, methane/air diffusion flame. Combust. Sci. Technol. 90 (1993) 1-34.

[15] K. Smyth, NO production and destruction in a methane/air diffusion flame. Combust. Sci. Technol. 155 (1996) 151-176.

[16] N. Bryner, E. Johnsson, W. Pitts, Carbon monoxide production in compartment fires – reduced-scale test facility. NISTIR 5568, National Institute of Standards and Technology, Gaithersburg, MD, 1994.

[17] S. Hostikka, K. McGrattan, A. Hamins, Numerical modeling of pool fires using LES and finite volume method for radiation, in: Proceedings of the 7th International Symposium on Fire Safety Science, International Association for Fire Safety Science, Worcester, MA, 2003.

[18] W. Grosshandler, RADCAL: A narrow-band model for radiation calculations in a combustion environment, NIST Technical Note TN-1402, National Institute of Standards and Technology, Gaithersburg, MD, 1993.
[19] M. Bundy, A. Hamins, E. Johnsson, S. Kim, G. Ko, D. Lenhert, Measurements of heat and combustion products in reduced-scale ventilation-limited compartment fires. NIST Technical Note TN-1483, National Institute of Standards and Technology, Gaithersburg, MD, 2007.
[20] E. Johnsson, M. Bundy, A. Hamins, Reduced-scale enclosure fires – heat and combustion product measurements, in: Interflam 2007, Interscience Communications, . London, UK, 2007.
[21] D. Gottuk, B. Lattimer, Effect of combustion conditions on species production, SFPE Handbook of Fire Protection Engineering, Chapter 2 Section 5, Society of Fire Protection Engineers, Bethesda, MD, 2002.

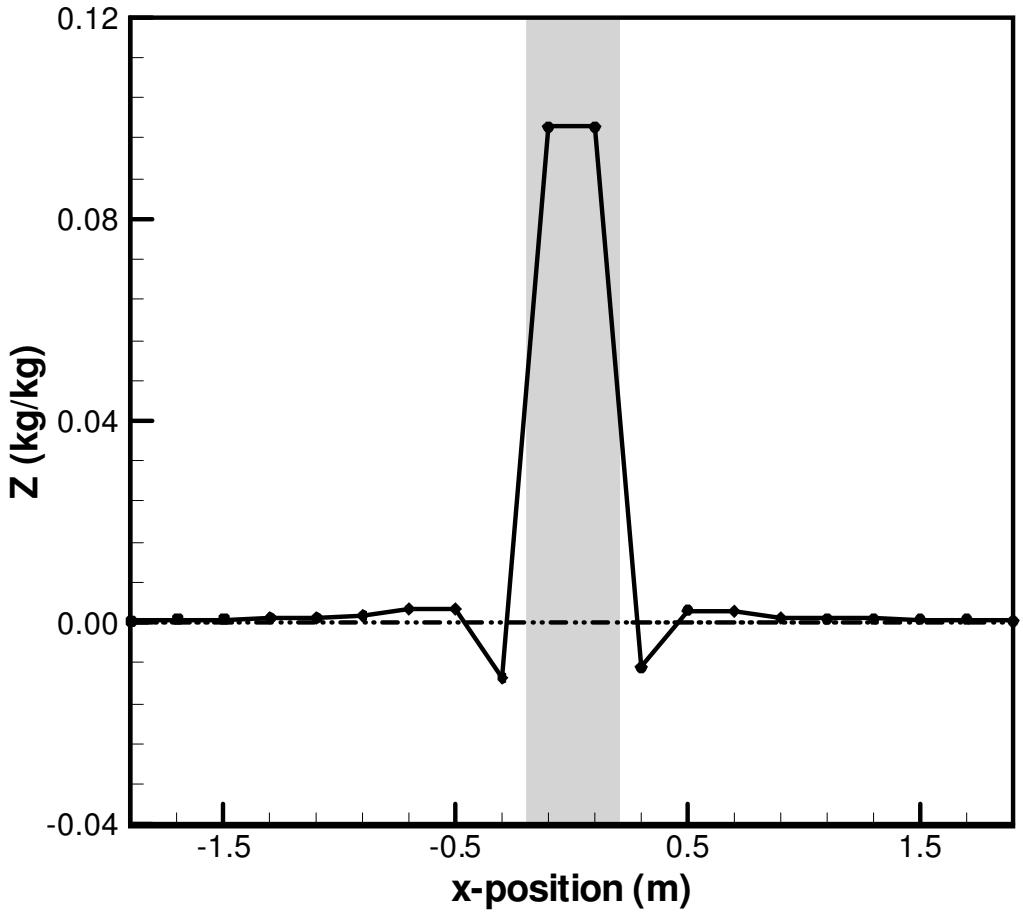

Fig. 1: An example of a numerical “under-shoot.”

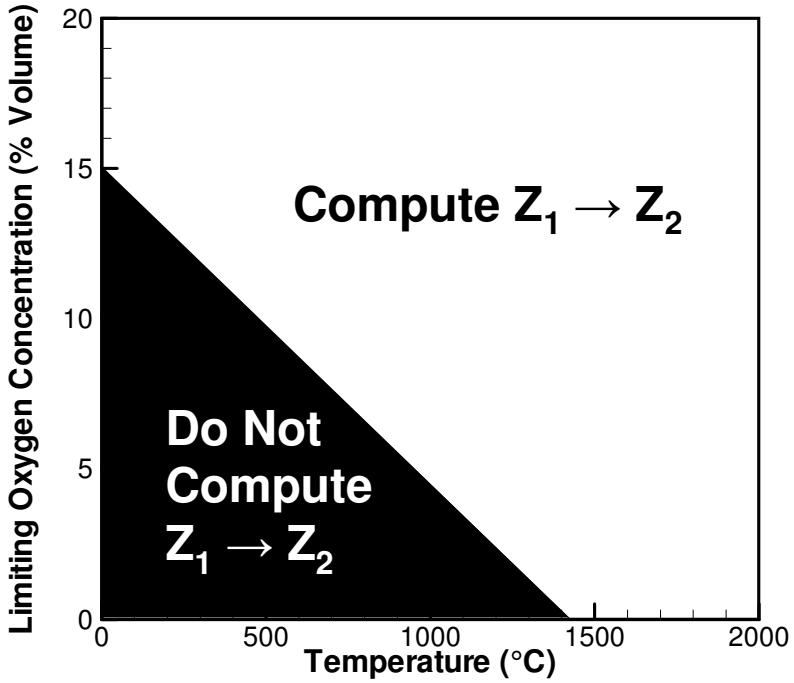

Fig. 2: Flammability criteria for reaction step 1

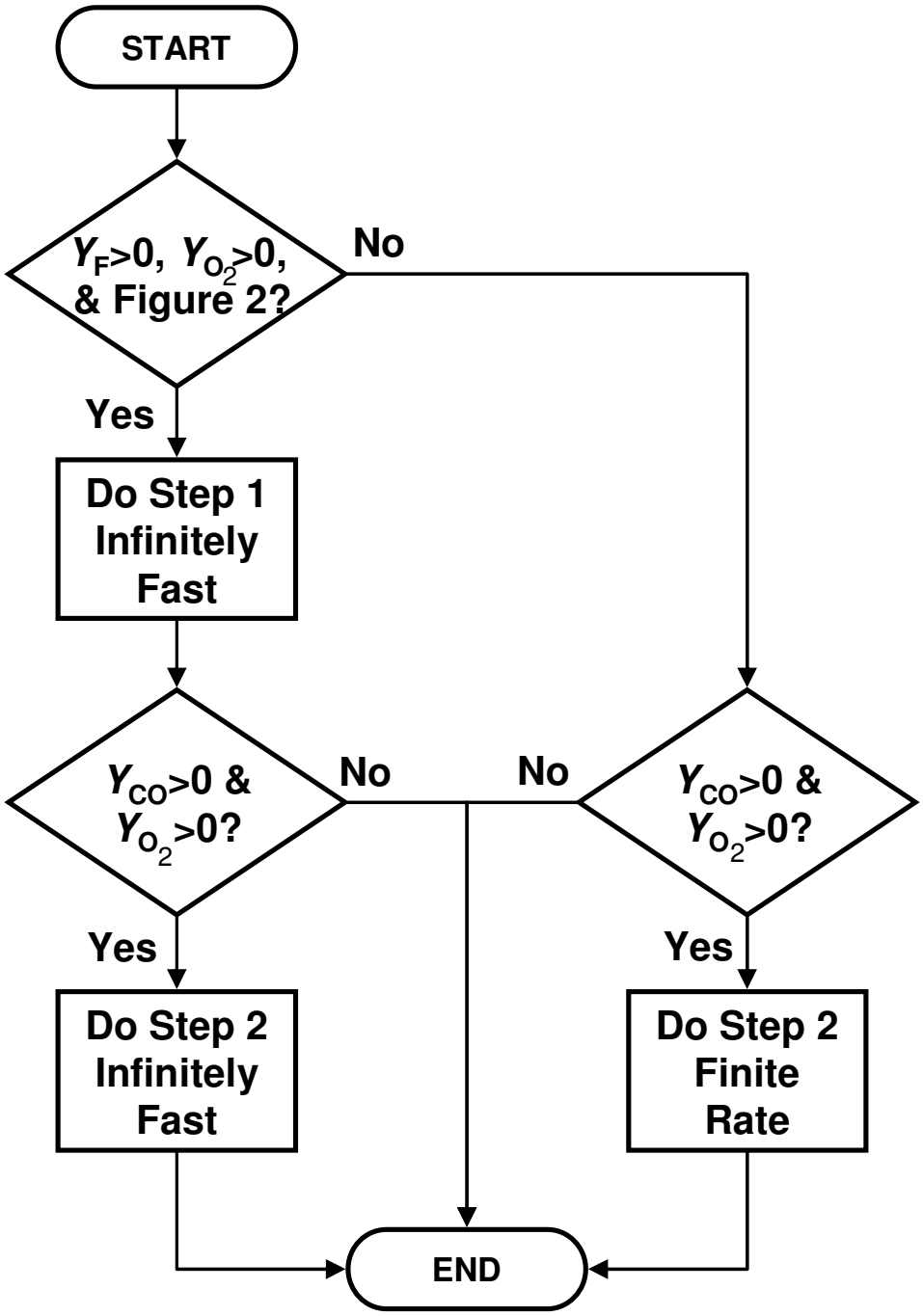

Fig. 3: Flowchart of two-step combustion model

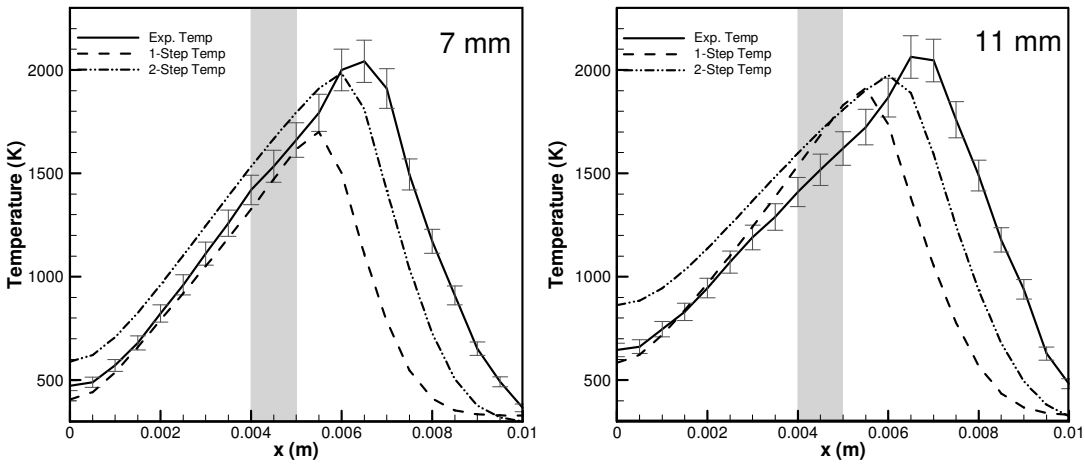

Fig. 4: Predicted and measured temperature profiles over the half-width of a methane-air slot burner (x=0 is burner centerline, shaded region is burner lip) at two elevations above the burner.

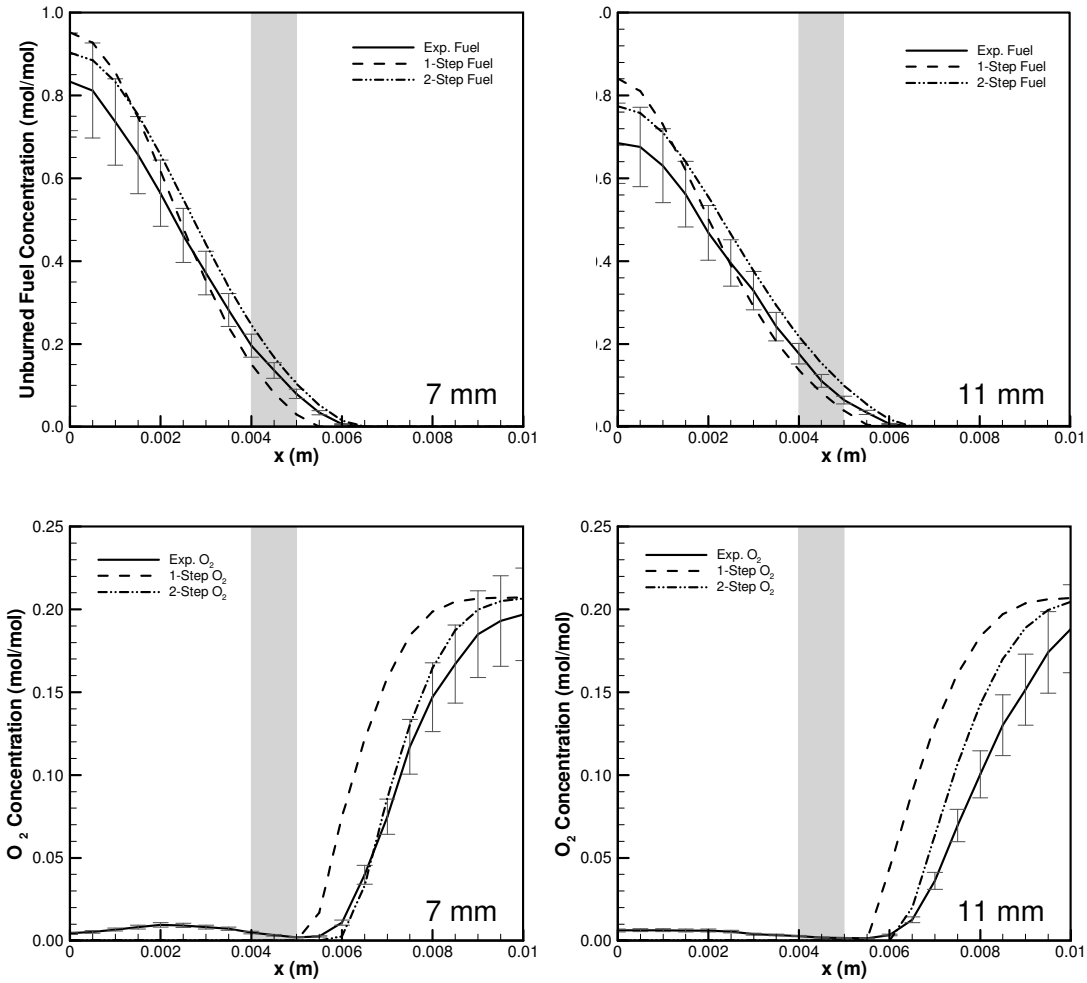

Fig. 5: Predicted and measured fuel (top) and oxygen (bottom) concentrations for a methane-air slot burner (x=0 is burner centerline, shaded region is burner lip) at two elevations above the burner.

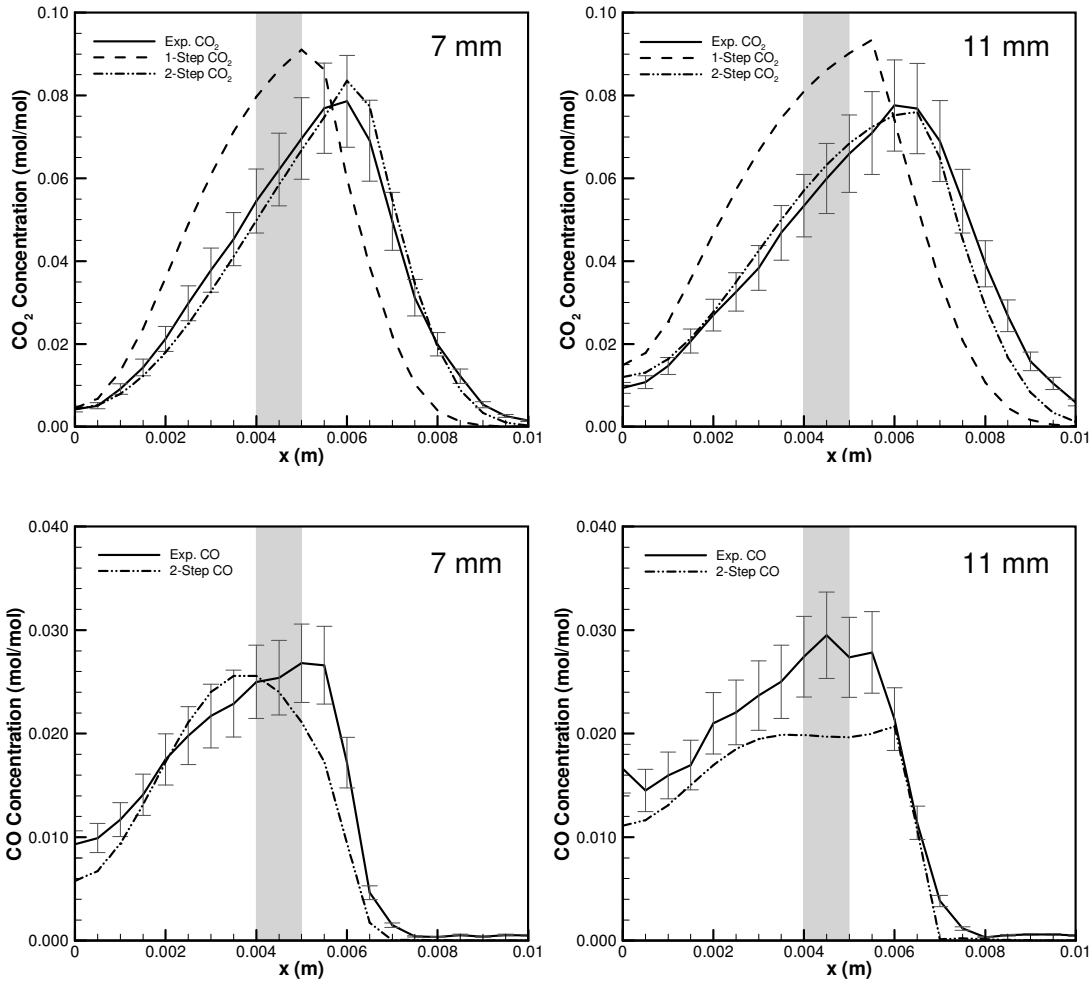

Fig. 6: Predicted and measured carbon dioxide and carbon monoxide concentrations for a methane-air slot burner (x=0 is burner centerline, shaded region is burner lip) at two elevations above the burner..

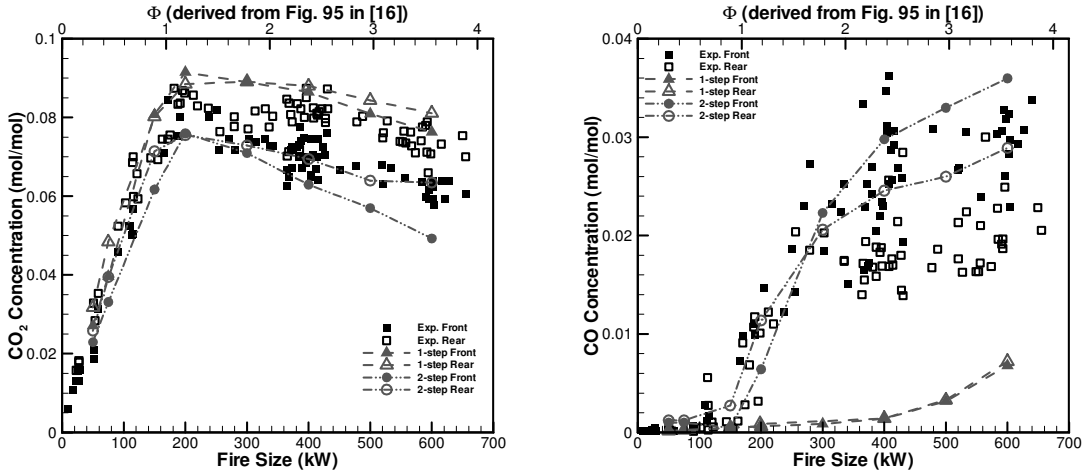

Fig. 7: CO_2 and CO predictions compared against measurements in a reduced scale enclosure (lines for predictions added as a visual aid)

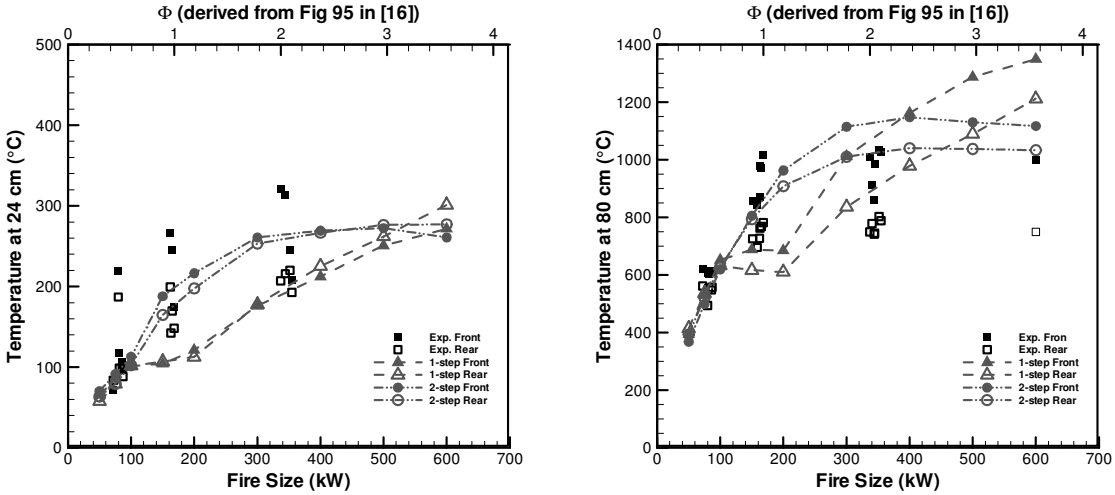

Fig. 8: Lower (left) and Upper (right predictions compared against measurements in a reduced scale enclosure (lines for predictions added as a visual aid)

Appendix F – IAFSS Symposium Paper

Validation of A CFD Fire Model Using Two Step Combustion Chemistry Using the NIST Reduced-Scale Ventilation-Limited Compartment Data

JASON FLOYD[1] and KEVIN MCGRATTAN[2]
[1]Hughes Associates, Inc.
3610 Commerce Dr., #817
Baltimore, MD 21227
[2]Building and Fire Research Laboratory
National Institute of Standards and Technology
Gaithersburg, MD

ABSTRACT

Recent testing by the Building and Fire Research Laboratory of the National Institute of Standards and Technology collected a large dataset of species, temperature, velocities, and heat fluxes for a wide range of fuels burning at varying degrees of ventilation inside a reduced scale enclosure. This dataset is extremely well documented with uncertainties well characterized, making it an excellent choice for fire model validation. Selected data from a subset of tests was used as part of a validation exercise using FDS v5. FDS v5 contains a new method of decomposing the mixture fraction coupled with a new combustion model that allows it to predict (rather than assume) CO formation in under-ventilated fires. Eleven tests were simulated and predicted vs. measured data comparisons were made for seven physical quantities distributed over twelve measurement locations. Results show the new combustion model is able to reproduce test conditions over a range of fuels and fire sizes.

KEYWORDS: CFD, validation, compartment fires, modeling

INTRODUCTION

Desired Fire Model Traits

To be broadly applicable, a computational fluid dynamics (CFD) model for fire simulation requires a number of major elements: the ability to transport multiple species of interest, a model for combustion (reactions that change one set of species to another with the release of energy, a model for radiation transport, a solid phase model for computing heat transfer into materials and the energy and mass inputs resulting from a decomposing material, and some manner of handling droplets from sprinklers/water mist systems including transport, evaporation, and solid phase interactions. Additionally, one would desire that the model do all those items well (model predictions match experiments within experimental uncertainty), be able to handle a wide range of length scales (Bunsen burner to forest fire), fuels, and materials, and be usable by a typical fire protection engineer (model complexity and computational hardware/time requirements).

The current state of fire CFD models is that any model (given an adequate grid) will do well in terms of transporting gasses and performing heat transfer into simple (i.e. non-decomposing) surfaces. This is done with varying degrees of input complexity and computational resource requirements. There are a number of approaches for radiation transport that have been used including Monte-Carlo methods, P_n methods, and various flavor of discrete ordinates methods. Each of these has its advantages and disadvantages, but generally most CFD fire models make use of some form of a discrete ordinates method. While one could argue that aspects of radiation transport, efficient generation of absorption coefficients and computing source terms on large grids, could use more development, the actual mechanics of solving for a radiative flux given those inputs is well established. That leaves combustion, decomposing solid phase, and droplets.

Transport and evaporation of droplets is key for evaluating water mist systems or simulating fuel spray fires. A key input is of course the radiant flux which serves as a mechanism for evaporating droplets as is the interaction of any diluent gasses (water vapor) with the combustion process. Ultimately, however,

much of modeling droplets becomes striking a balance between the fidelity of the physics and the resources required.

Simulating a decomposing solid phase (wood for example) is of great interest to many people; however, while progress is being made in algorithms, the ultimate success will hinge upon how well the fire-fuel feedback can be modeled. This requires in part that one make adequate predictions of the key radiating species, i.e. the combustion model must be robust.

In addition to the needs of the solid phase models, a robust combustion model is desired since gasses such as CO are of key interest to fire protection engineers, but the ability to predict them in large scale fires has been limited. Also, there is the need to predict extinction in poorly ventilated fires to evaluate risks for backdraft type events. Recognizing that improvements to the previously simple combustion model in FDS could result in across the board improvements in overall capability, a new method of tracking species and computing combustion was implemented in FDS. The remainder of this paper briefly documents the new method and a few key aspects of FDS and then validates the new version using test data from the NIST reduced scale enclosure.

Model Verification and Validation

The spectrum of model users, those who run the models to those who must approve fire protection designs based on the model runs, are always interested in how good is a model. The process of demonstrating the goodness of a model is Verification and Validation. While definitions of those differ, in general verification shows that the model was developed properly and validation shows that the model can be used for a particular application. For fire modeling, the latter typically means comparing model predictions to fire experiments. How though does one determine the model is performing adequately?

The model will never match an experiment exactly, so how much difference should be tolerated? A recent validation effort undertaken by the US Nuclear Regulatory Commission [1] has suggested that the best one can do is demonstrate that the model predictions and the measured data overlap when uncertainty is accounted for. This uncertainty includes both the measurement uncertainty associated with individual measurements but also model input uncertainties (material properties, heat release rates, dimensions, etc). This is an appropriate metric, though one that is hard to do in practice. For high fidelity models, the less one knows about what the test was, the less certain one will be of the model results. Similarly, the less certain one is of the measured data, the larger the model prediction error can be without being able to say it is incorrect.

Recent validation efforts have attempted to assess FDS's ability to model post-flashover compartments. One recent validation effort compared FDS v4 predictions of temperature with measurements made during a test series at Cardington [2]. The fires consisted of multiple wood cribs in a compartment with an effort to measure the mass loss rate of a small fraction of the wood cribs. FDS predictions of point temperatures were compared with measured data with the conclusion that FDS is unable to predict temperatures in post-flashover compartments. However, this study omitted some key aspects of the test and ignored their impact on the model uncertainty. Some key failings were: the mass loss rate data was applied as a time dependent uniform fire source rather than the spatially dependent source that existed, the fuel source was defined using a single heat of combustion (with unknown certainty) that did not make any account for the how the fuel thermal properties change over time, no assessment of the impact of uncertainties in defining the construction materials, and no assessment of the measurement uncertainty. The report ended by observing FDS predictions of average gas temperatures were low by 7 to 30 % without noting what performance could be expected given the test uncertainties.

The model validation shown in this paper, attempts to address the key components of the test uncertainty both in terms of the measured data itself and the impact the test uncertainty has on inputs and the resulting model outputs.

FIRE MODEL (FDS VERSION 5)

Fire Dynamics Simulator (FDS) version 5 was released in October 2007. A large number of changes were made to FDS from version 4. Key changes are a new method of decomposing the mixture fraction combined with a new two-step combustion model [3], a general scheme for modeling multi-layer, multi-

component reacting surfaces, a reorganization of the source code to enable easier multi-party development and code branching, the implementation of modern software QA concepts using online version control via Google Code™ open source project hosting, and online user support using Google Group™ discussion forum services. A brief overview of the mixture fraction decomposition and combustion model are provide below.

Multiple Parameter Mixture Fraction

The single parameter mixture fraction for tracking species that was used in FDS v2 – v4 has been extended into a multiple parameter mixture fraction. The use of multiple parameters allows FDS to account for extinction (two parameter approach) and CO formation and destruction (three parameter approach). The work in this paper was performed using the three parameter mixture fraction. The three mixture fraction parameters, each a conserved scalar, are

$$Z_1 = \frac{Y_\mathrm{F}}{Y_\mathrm{F}^I}, Z_2 = \frac{M_\mathrm{F}}{M_\mathrm{CO}\left(x - \left(1 - X_\mathrm{H}\right)\nu_\mathrm{S}\right)} \frac{Y_\mathrm{CO}}{Y_\mathrm{F}^I}, Z_3 = \frac{M_\mathrm{F}}{M_\mathrm{CO2}\left(x - \left(1 - X_\mathrm{H}\right)\nu_\mathrm{S}\right)} \frac{Y_\mathrm{CO2}}{Y_\mathrm{F}^I} \qquad (1)$$

In Eq. 2 and Eq. 3 M_i is the molecular weight of species i, Y_i is the mass fraction of species i, the variable x represents number of moles of carbon in the fuel, Y_F^I is the fuel mass fraction at the fuel source (i.e. dilution of the fuel stream with an inert gas is allowed), X_H is the hydrogen atom fraction in the soot, and ν_S is the fixed soot yield. Z_1 represents the mass fraction of gas that is associated with unburned fuel, Z_2 represents the mass fraction of gas that is associated with fuel that has oxidized to CO, and Z_3 represents the mass fraction of gas that is associated with fuel that has oxidized to CO_2. Full details on this new approach for tracking species can be found in [3] and [4]. This approach of decomposing Z into components is referred to as creating a mixture fraction vector [5]. The advantage of the mixture fraction is that with the three scalars, a total of seven species are tracked (N_2, O_2, fuel, CO, CO_2, H_2O, soot), which reduces both memory requirements and computational time.

Two Step Combustion

With a single parameter mixture fraction, we can only track one state of a reaction: the fully combusted state that disallows the coexistence of fuel and oxygen. Since neither fuel, nor oxygen can coexist (that would require a second parameter), heat release is computed by taken the gradient of mixture fraction across the stoichiometric surface. Physically this is computing the fuel (or oxygen) mass flux across the flame and assuming it all reacts instantaneously. This works well in general for well ventilated fires; however, it has drawbacks: complete combustion means no computations of extinction or minor product formation, numerical artifacts on coarse grids result in ringing of mixture fraction in regions of high gradients (near the stoichiometric surface) which hinders obtaining the correct heat release rate, and attempting to do flux correction on the ringing also impairs the computation of the correct total heat release rate.

The decomposed mixture fraction means one is no longer is tied to computing gradients. FDS now can track separately fuel and oxygen and the degree to which the combustion reaction has gone to completion. Note that many schemes in the combustion literature involve tracking progress variables (a fractional value of reaction completeness); however, since these variables suffer from the same numerical issues as mass fractions, on coarse grids one can still have difficulties obtaining the correct heat release rate.

Instead, the combustion routine uses directly the species mass fractions as determined by the mixture fraction parameters to determine the heat release rate in two steps: oxidation of fuel to water vapor and CO and oxidation of CO to CO_2 [6]. In the first step, if a cell contains fuel (Z_1) and oxygen with the oxygen above a temperature dependent lower limit, the fuel is converted to CO plus other products (Z_1 becomes Z_2). In the second step if a cell contains CO (Z_2) and oxygen and the temperature is high enough to support CO oxidation, then CO becomes CO_2 (Z_2 becomes Z_3). The full details on this are found in [3] and [4]. It should be noted that this approach does not allow for CO formation directly from pyrolysis as occurs in oxygenated fuels such as cellulosic materials.

REDUCED-SCALE EXPERIMENTS

In 2006, the Building and Fire Research Laboratory undertook a series of 17 fire tests involving a wide range of fuels in a reduced scale enclosure [7]. Seventeen tests involving seven different fuels (including solid, liquid, and gas) were conducted. The tests occurred in a 0.95 m wide x 1.42 m deep x 0.98 m tall compartment with a 0.48 m wide x 0.81 m tall door centered on one of the 0.95 m walls. The floor of the compartment was 0.19 m above the floor of the test facility. The compartment was lined with a ceramic fiber insulating board. The fires were centered on the floor of the compartment. Measurements included temperature, species, velocity, heat flux, and heat release rate. Measurements were processed into 64 channels of data of which 18 channels were selected for use in this paper. The first six tests partially served as shakedowns, and following them, minor changes were made to the measurement apparatus. Data from these tests was not used in this validation effort. Measurement uncertainties were generated for specific time intervals for each measurement point for each test. The reported uncertainties are solely for the measurement process (i.e. the reported uncertainty in temperature does not include a contribution due to the uncertainty in the measured fire size).

This validation study examined 18 measured quantities in 11 tests. These were: 8 gas measurements (O_2, CO_2, CO, and unburned hydrocarbons made in the front and rear of the compartment above the top of the door), 4 aspirated thermocouples (two locations in the front and rear of the compartment: the upper third and lower third of the compartment), 4 bi-directional probe velocities in the centerline of the doorway, and 2 total heat fluxes on the compartment floor (in front of and behind the burner). During each test, averages of the data were taking over time periods when the heat release rate was quasi-steady state. This process resulted in a total of 36 data points distributed over the 11 tests.

FDS MODEL

Each of the final eleven tests was modeled with FDS v5.0. A summary of the FDS modeling of the eleven tests is given in Table 1 and Table 2 provides a summary of the fuel inputs used in the FDS modeling. The chemical constituents of the natural gas supply were measured prior to testing.

Table 1. Summary of FDS Simulations of RSE Test Series

Test #	Fuel	Burner Type (dimension)	Max Size (kW)	Time (s)	Fire Specification
6.5	Natural Gas	Square burner (0.13 m x 0.13 m)	425	3400	Measured fuel flow
7	Heptane	Pool fire (0.25 m x 0.25 m)	340	5000	Hood calorimeter
8	Methanol	Pool fire (0.25 m x 0.25 m)	15	2645	Hood calorimeter
9	Ethanol	Pool fire (0.25 m x 0.25 m)	20	3540	Hood calorimeter
10	Toluene	Pool fire (0.25 m x 0.25 m)	340	6150	Hood calorimeter
11	Ethanol	Spray (into 0.20 m radius pan)	335	4800	Measured fuel flow
12	Methanol	Spray (into 0.20 m radius pan)	305	3600	Measured fuel flow
13	Polystyrene	Pellet filled pan (0.11 m radius)	15	1725	Hood calorimeter
14	Polystyrene	Pellet filled pan (0.20 m radius)	70	2340	Hood calorimeter
15	Heptane	Spray (into 0.20 m radius pan)	375	760	Measured fuel flow
16	Polystyrene	Pellet filled pan (0.30 m radius)	360	1330	Hood calorimeter

Table 2. Summary of FDS Fuel Definitions (&REAC Inputs)

Fuel	Chemistry	ΔH_c (kJ/kg)	Y_{Soot} (kg/kg)
Natural Gas	$C_{1.06}H_{4.08}N_{0.016}O_{0.015}$	48249	0.015
Heptane	C_7H_{16}	44630	0.015
Methanol	CH_3OH	19935	0.000
Ethanol	CH_3CH_2OH	28865	0.008
Toluene	C_7H_8	40589	0.170
Polystyrene	C_8H_8	25600	0.120

For each test the compartment plus a small region outside the door and above the compartment was modeled. The external region was modeled so that an open pressure boundary condition would not be present at the compartment door. The computational domain was 0.95 m x 2.44 m x 1.50 m and was gridded with a single computational mesh of 40 x 100 x 72 (288,000) cells. A grid study was performed using test 6.5 with approximately 1/2 and 2 times the number of nodes to establish that the grid was adequate. Figure 1 shows the computational domain. The burner pictured represents the pan for containing the spray fire. The spheres are locations of measurement devices used during the testing.

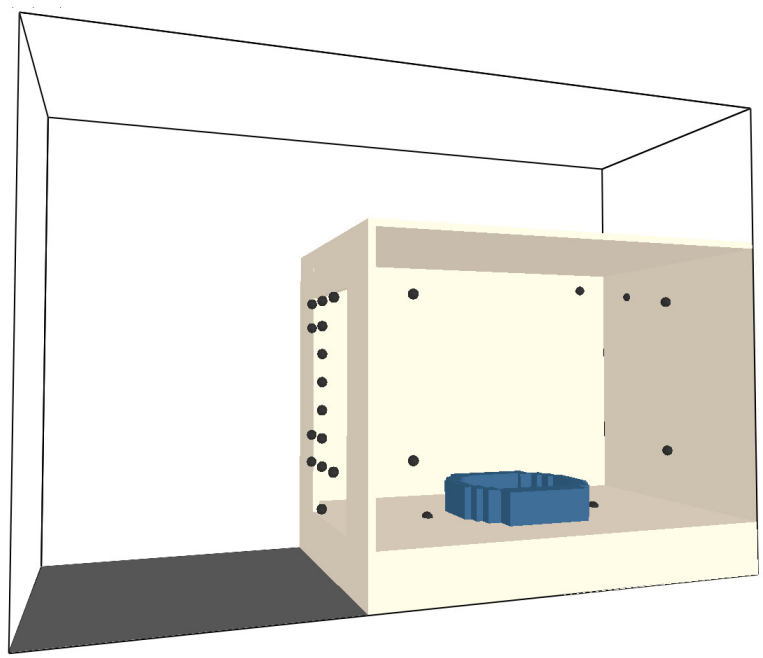

Fig. 1. View of FDS Domain for RSE Simulations

For pool fire tests, the burner was defined with a uniform, time-dependent mass flux of fuel with a temperature equal to the boiling point of the liquid. The gas fire test was similarly set though using a temperature of 100 °C to represent the slightly preheated fuel leaving the burner. Spay fire tests injected a time dependent flow of droplets assigned fuel appropriate evaporation parameters with a 250 μm average diameter through a 90° cone. The test facility floor was given thermal properties of concrete and the test compartment walls were assigned manufacturer reported properties for the ceramic boards.

In creating the inputs for each simulation, there is some uncertainty to the input data which will impact the FDS predictions being compared with the data. Uncertainties in the fuel flow rate specified in the input file will have an impact on the species production as will uncertainties in the wall thermal properties. Other input data such as fuel type and compartment geometry have little associated uncertainty. Thus, in addition to the eleven RSE tests, the maximum fire size observed in tests #6.5 (methane with low soot production) and #7 (heptane with higher soot production) was used to run a series of sensitivity calculations where

thermal conductivity of the walls was varied by 10 % and where the fire size was varied by the test determined uncertainty. Each calculation was run as quasi-steady state using a large fire and small fire. The change in the predicted quantities was then used to compute FDS uncertainties. These uncertainties were then used when plotting FDS predictions by selecting the closest corresponding uncertainty (i.e. for a large fire with a sooting fuel, the large fire heptane uncertainties were applied to the FDS results). Other uncertainties exist, such as the impact of not including the hood flow and the various flow baffles that existed around the sides of the compartment during the test.

RESULTS

Sensitivity Calculations

The sensitivity study results indicated that FDS predictions of the average velocities were not greatly affected by uncertainties in the heat release rate or wall properties with variations of 6 % or less. Similarly upper layer temperature measurements also saw little change with variations of 5 % or less. Lower layer temperatures varied more with changes up to 15 %. For the larger fire sizes, heat flux predictions varied by less than 7 %, but for the smaller fire sizes the variance was 10 % to 13 %. Gas species varied depending upon the fire size. Larger fires saw more variance in oxygen and smaller fires more variance in unburned hydrocarbons. For both this resulted from small absolute changes that were large percentages due to the low levels of either species. CO and CO_2 levels generally varied less than 10 %.

Reduced Scale Enclosure Simulations

Figures 2 through 10 plot the FDS predicted quantities (y-axis) against the measured quantities (x-axis). Horizontal error bars were taken from the NIST test report [7]. Vertical error bars were computed using the results of the sensitivity study.

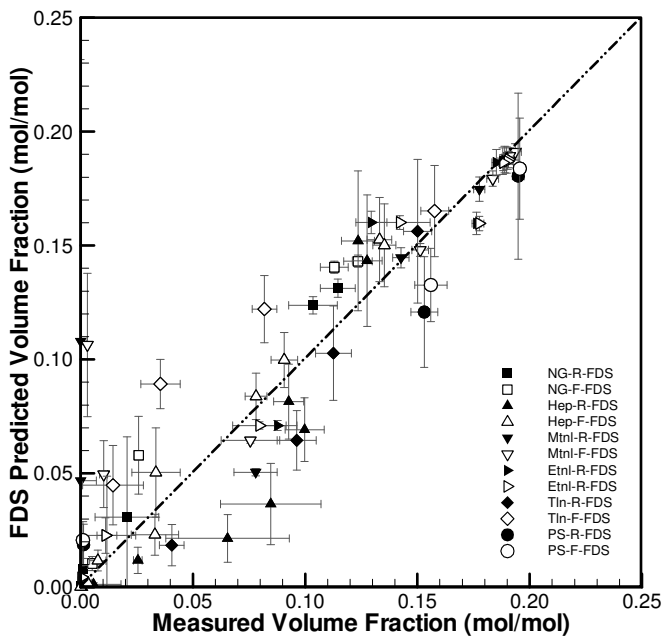

Fig. 2. FDS predicted vs. measured front and rear O_2 volume fraction

Figure 2 shows the result for the two O_2 measurement locations in the compartment. For 60 % of the dataset the predictions and measurements agree within uncertainty. For the other points there is not a clear trend either over- or under-predicting the measurements. It is observed that predictions for the large methanol spray fire (near 0,0.1), are particularly poor. A review of the simulation results indicates that the droplet evaporation algorithm was resulting in flow instabilities which resulted in the large O_2 values. This is not surprising as these issues have been documented on the GoogleCode development site.

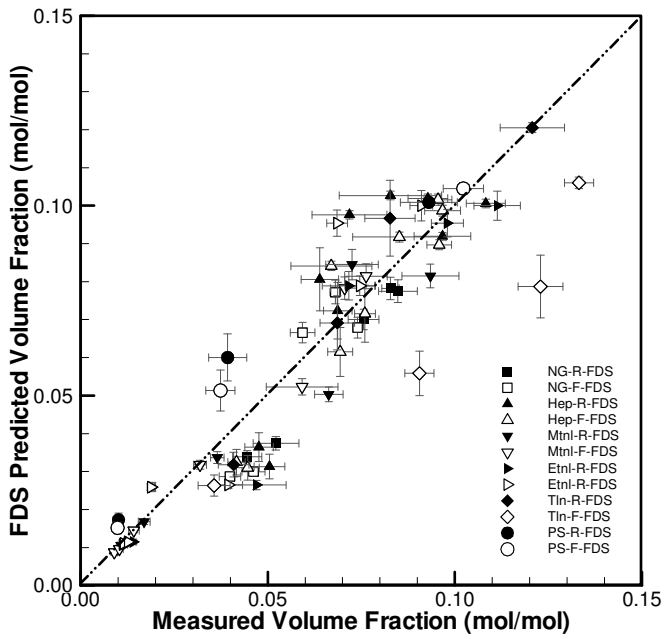

Fig. 3. FDS predicted vs. measured front and rear CO_2 volume fraction

FDS predictions of the CO_2 volume fraction, Figure 3, were within the uncertainty for 36 % of the dataset. With the exception of the rear location of the toluene data, those points that were not within the uncertainty were generally close to doing so, and if all sources of FDS uncertainty were accounted for then agreement would be likely. There is a trend towards under-prediction of the CO_2 levels. This may result from the current combustion model which treats the reaction as two separate steps and as a result may create locations where O_2 is fully consumed making CO when if parallel reactions were occurring some would be consumed by simultaneous oxidation of CO. The root mean square of the relative difference between CO_2 prediction and measurement was 19 %.

CO predictions, Figure 4, were in agreement for 40 % of the dataset. This is essentially the same performance as for CO_2. The worst predictions are for the oxygenated fuels (methanol and ethanol). These fuels can form CO without the consumption of O_2 from the air, which is a phenomena not accounted for in the current combustion model. Ignoring those data points, there is a trend towards over-prediction of CO. Given the CO_2 performance, this is expected for the same reason as for the under-prediction of CO_2.

Figure 5 shows the predicted vs. measured unburned fuel. 47 % of the data points agree for this quantity. In general, for test conditions where unburned fuel were > 1.5 %, FDS is under-predicting the values. There are two likely contributors to this. The first is the sequential reaction steps. For a given quantity of oxygen, making only CO will consume more fuel than if CO_2 is made. Secondly, FDS considers all unburned fuel to be the fuel molecule specified in the input file. Gas Chromatography of unburned fuel samples from the test indicates that the species present are primarily low molecular weight hydrocarbons. For the same mass of unburned fuel assuming it is the original fuel molecule would result in a lower volume fraction than if it were to exist as a number of smaller fuel molecules. This second contribution could be reduced by specifying a fuel molecule in the input file that maintains the stoichiometry but has a lower molecular weight. For example, C_7H_{16} (100 g/mol) could be specified as $C_{1.75}H_4$ (25 g/mol)

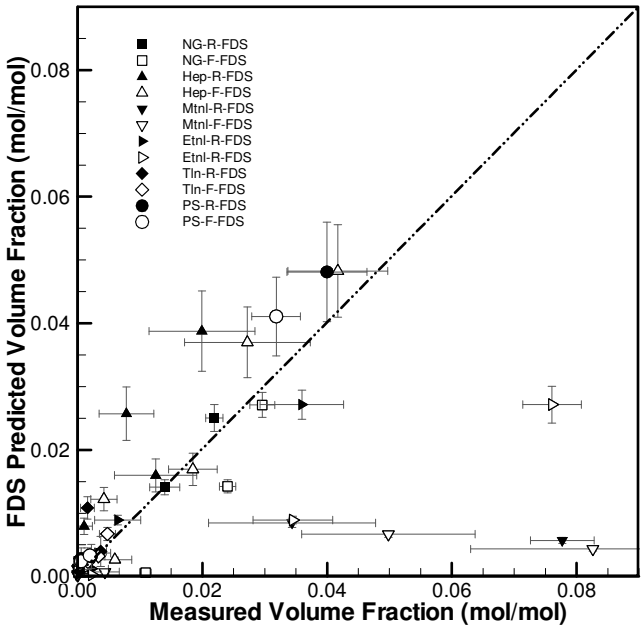

Fig. 4. FDS predicted vs. measured front and rear CO volume fraction

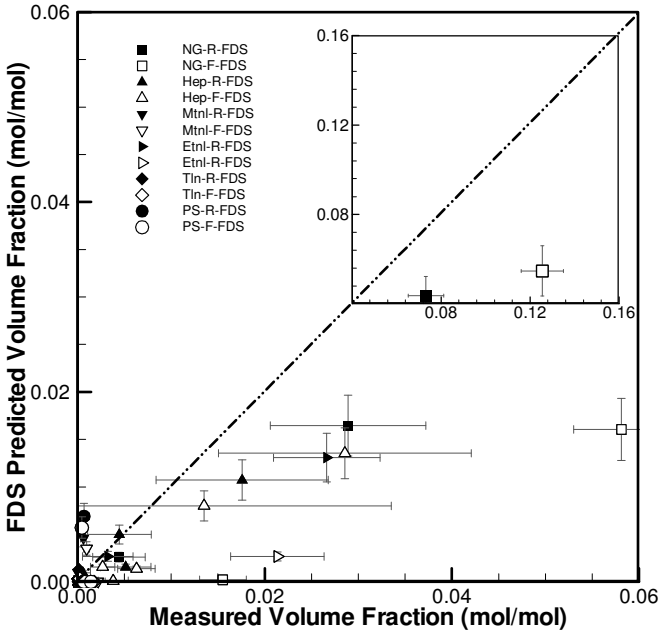

Fig. 5. FDS predicted vs. measured front and rear unburned fuel volume fraction

Figures 6 and 7 respectively show the quantities of upper and lower temperature which respectively agree within uncertainty for 28 % and 17 % of the data points. The rms relative difference for the upper measurements is only 10 % with a maximum difference of 32 % (for the previously discussed largest methanol spray fire). For the smaller fire sizes the upper temperature predictions are generally low compared to the data. This trend is not as evident for the larger fire sizes. For the lower points the rms relative difference is 18 % with a maximum difference of 75 % also for the methanol spray fire. Lower predictions are biased low in comparison to the measurements.

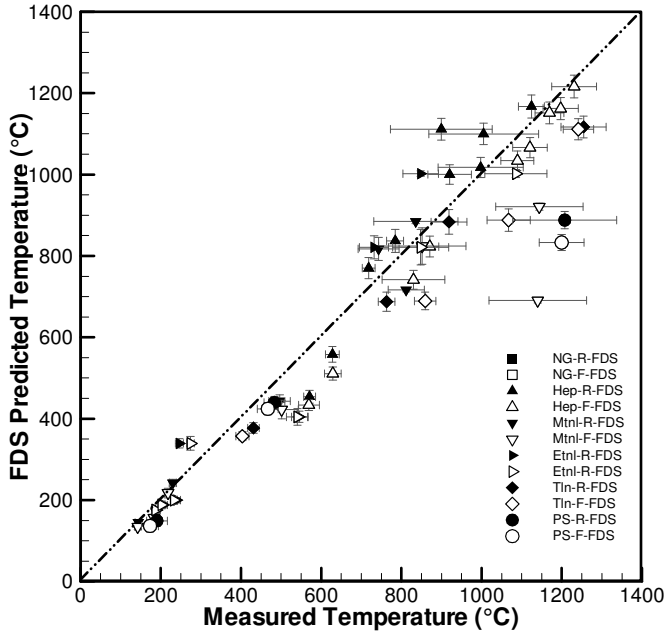

Fig. 6. FDS predicted vs. measured front and rear upper temperature

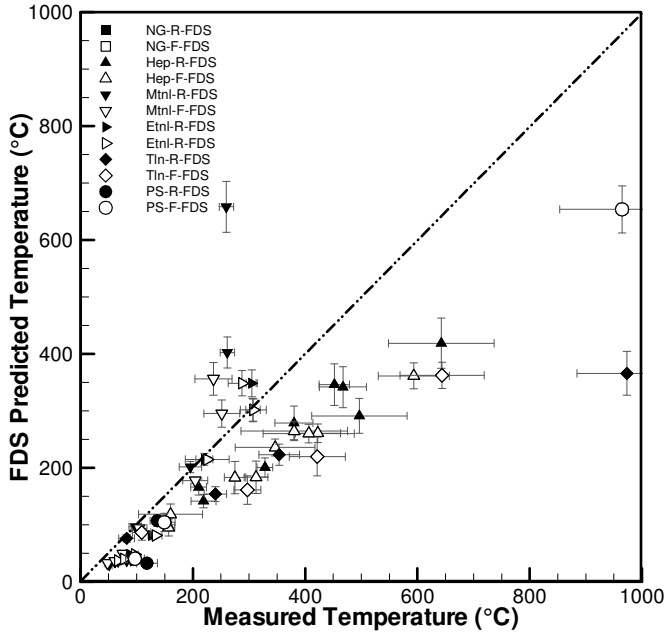

Fig. 7. FDS predicted vs. measured front and rear lower temperature

Figure 8 shows predictions vs. measurements for total heat flux to the floor. The predictions match the measurements for 44 % of the data points. For the smaller fires the predictions are generally lower than the data. Since an FDS calculation does not generally resolve flame temperatures, FDS uses a fixed radiative fraction in grid cells with heat release. For well ventilated fires (lower upper layer temperatures and a less optically thick environment) this assumption dominates the radiation source term and is a likely contributor to the under prediction. For larger fire sizes there isn't a clear trend towards either over prediction or under prediction; however, the largest relative differences are occurring when FDS over predicts the heat flux. One possible reason for this is currently the radiation model does not distinguish where the heat release

originates. The fixed radiative fraction assumption was originally developed to account for unresolved flames. In a hot upper layer with bulk oxidation of CO, this assumption is still being applied, but in this case the layer temperature should be accurate enough for generating a source term. This could be resulting in too large of a radiative source term in the upper layer. Overall the rms difference in the heat flux prediction was 41 %.

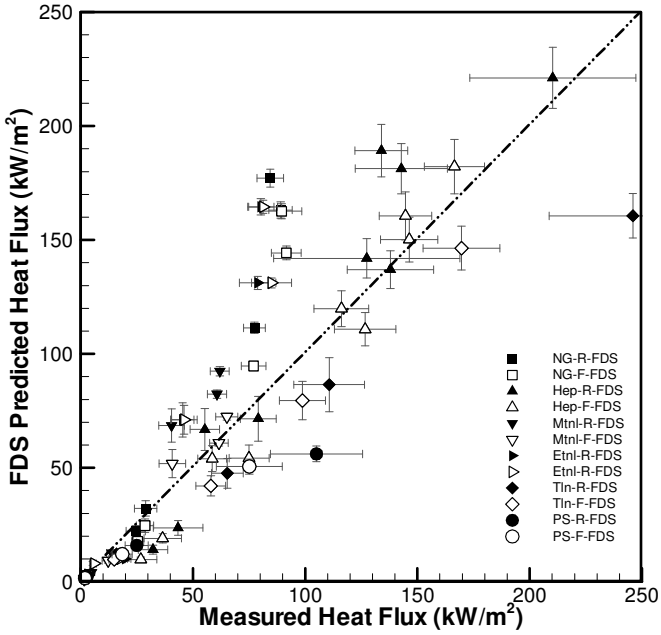

Fig. 8. FDS predicted vs. measured front and rear floor total heat flux

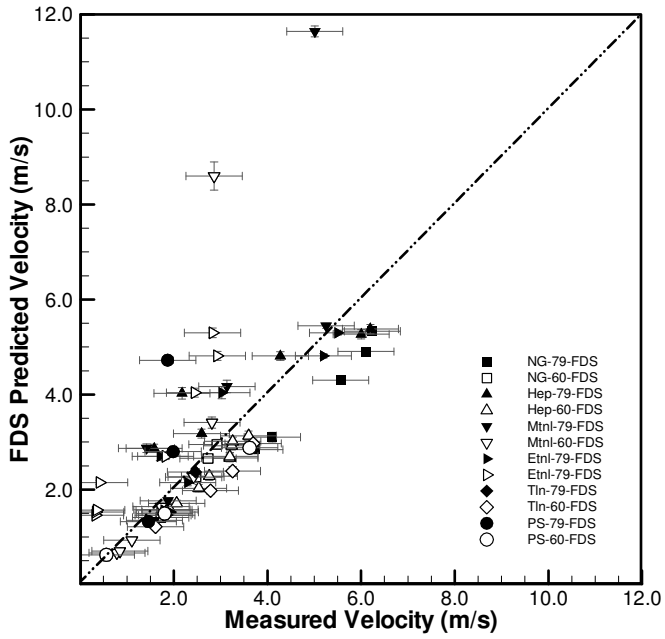

Fig. 9. FDS predicted vs. measured doorway centerline velocities at 0.79 m and 0.60 m

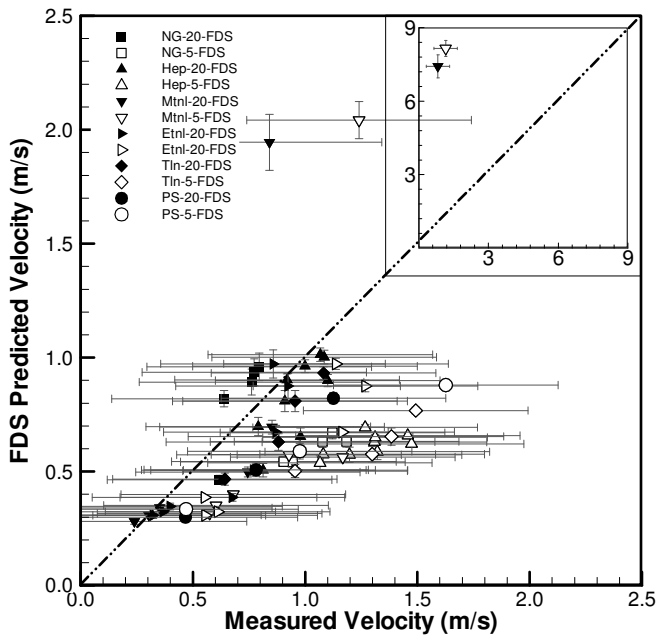

Fig. 10. FDS predicted vs. measured doorway centerline velocities at 0.20 m and 0.05 m

Figures 9 and 10 show predicted vs. measured velocities in the upper and lower portion of the doorway to the compartment. FDS predicted within uncertainty 61 % of the time in the upper doorway and 72 % of the time in the lower doorway. It is noted that measurement uncertainties were fairly large for these quantities. As with other quantities the worst outliers resulted from the methanol spray fire. This is an indication that further development of the droplet routines is needed. In the lower door, FDS generally under predicted the measured values. In the upper doorway there were more data points where the FDS predictions were lower than the data; however, among data points where predictions lay outside the uncertainties there were more over predictions. After removing the methanol outliers, the rms differences were 44 % for the upper locations and 31 % for the lower locations. However, it is noted that the data uncertainty averaged 36 % for the upper and 64 % for the lower.

CONCLUSIONS

FDS v5 was used to simulate 11 of the 17 reduced scale enclosure tests documented in [7]. A sensitivity analysis was performed for two of the major contributors to the model input uncertainty. This analysis revealed the velocity predictions and upper layer temperature predictions were not particularly sensitive to the heat release and material property uncertainties. Most other quantities had uncertainties ranging up to 15 %. The exception was gas concentrations when the predicted value was low (<< 1 %) in which case uncertainties were large (> 100 %); however, in these cases the relative difference was low.

With the exception of the alcohol tests FDS correctly predicted the trends in various gas species and matched the measurements within uncertainty for approximately half the data set. It can be seen that the current implementation of the two-step combustion model is over predicting CO, under predicting CO_2, and under predicting unburned fuel. The assumption that the first step is infinitely fast combined with performing the two steps sequentially rather than allowing for some simultaneous reaction is a likely contributor to this.

With the exception of the largest fire size of the methanol spray fires, velocities were well predicted by FDS. However, the measured data for velocity (especially in the lower layer) has fairly large uncertainties. Relative differences between FDS predictions and the measurements were on the order of the measurement uncertainty.

Temperature predictions by FDS did not match the data within uncertainty as well as other parameters. However, in the upper layer while only 28 % of the predictions were within uncertainty the average relative

difference was only 10 %. In terms of predicted heat flux, the relative differences in temperature prediction did not translate to the heat flux as FDS predictions vs. measurements matched within uncertainty for over 40 % of the dataset. The pattern of relative differences in the heat flux predictions suggest that the radiative source term for layers with oxidizing CO may need to be revisited.

The new two step combustion model has been shown capable of reproducing the conditions within the reduced scale enclosure over a range of fuels and fire sizes. While, additional work in the underlying mechanics of implementing the model is required, the overall approach (which adds little in terms of a computational burden) is a success.

ACKNOWLEDGEMENTS

This work was funded by the United States Department of Commerce, National Institute of Standards and Technology, Building and Fire Research Laboratory through the Fire Grants Program.

REFERENCES

[1] Salley, M., "Verification & Validation of Selected Fire Models for Nuclear Power Plant Applications," US Nuclear Regulatory Commission Report NUREG-1824, 2007.

[2] Pope, N.D., Bailey, C.G., (2006) Quantitative Comparison of FDS and Parametric Fire Curves with Post-Flashover Compartment Fire Test Data, Fire Safety Journal 41: 99-110. http://dx.doi.org/10.1016/j.firesaf.2005.11.002

[3] Floyd, J.E. and McGrattan, K.B., "Multiple Parameter Mixture Fraction With Two-Step Combustion Chemistry for Large Eddy Simulation", *Proceedings of Interflam 2007*, 2007, pp 907-918.

[4] McGrattan, K ., Hostikka, S., Floyd, J., Baum, H., and Rehm, R., "Fire Dynamics Simulator (Version 5): Technical Reference Guide", National Institute of Standards and Technology Report NIST SP 1018-5, Gaithersburg, MD, 2007.3

[5] Fox, R. *Computational Models for Turbulent Reacting Flows*, Cambridge University Press, Cambridge UK, 2003.

[6] Westbrook, C. and Dryer, F. (1981), Simplified Reaction Mechanisms for the Oxidation of Hydrocarbon Fuels in Flames, Combustion Science and Technology 27:31-43. http://dx.doi.org/10.1080/00102208108946970

[7] Bundy, M., et al., "Measurements of Heat and Combustion Products in Reduced-Scale Ventilation-Limited Compartment Fires," National Institute of Standards and Technology Report NIST TN 1483, Gaithersburg, MD, 2007.